Zoological Journal of the Linnean Society, 2021, **191**, 772–822. With 22 figures.

A new species group from the *Daphnia curvirostris* species complex (Cladocera: Anomopoda) from the eastern Palaearctic: taxonomy, phylogeny and phylogeography

ALEXEY A. KOTOV[1*], PETR G. GARIBIAN[1], EUGENIYA I. BEKKER[1], DEREK J. TAYLOR[2] and DMITRY P. KARABANOV[1,3]

[1]*A. N. Severtsov Institute of Ecology and Evolution of Russian Academy of Sciences, Leninsky Prospect 33, Moscow 119071, Russia*
[2]*Department of Biological Sciences, The State University of New York at Buffalo, 109 Cooke Hall Buffalo, NY 14260, USA*
[3]*I. D. Papanin Institute for Biology of Inland Waters of Russian Academy of Sciences, Borok Yaroslavl Area, 152742, Russia*

Received 3 August 2019; revised 25 March 2020; accepted for publication 6 April 2020

The eastern Palaearctic is a centre of diversity for freshwater cladocerans (Crustacea), but little is known about the evolution and taxonomy of this diversity. *Daphnia curvirostris* is a Holarctic species complex that has most of its diversity in the eastern Palaearctic. We examined the phylogeography, rates of evolution and taxonomic status for each clade of the *D. curvirostris* complex using morphological and genetic evidence from four genes. The cybertaxonomical and morphological evidence supported an eastern Palaearctic clade, with at least four species (described here as the ***Daphnia korovchinskyi* sp. nov.** group) having diagnostic morphological characters. We also detected convergent morphological characters in the *D. curvirostris* complex that provided information about species boundaries. Two of the new species (***Daphnia koreana* sp. nov.** and ***Daphnia ishidai* sp. nov.**) are known from single ponds and are threatened by human activity. Divergence time estimates suggested an ancient origin (12–28 Mya) for the *D. korovchinskyi* group, but these estimates are complicated by the small number of calibration points.

ADDITIONAL KEYWORDS: biogeography – genetics – invasive species – morphology – phylogeny – systematics.

INTRODUCTION

Wallace (1876) founded biogeography based on regionalism detected in well-studied groups, such as higher plants, mammals and advanced insects, but to 19th century naturalists, freshwater invertebrates appeared to have few geographical boundaries over vast distances. Darwin (1882) detected hidden dispersal abilities in freshwater invertebrates (aerial plankton and hitchhiking) and proposed that frequent long-distance dispersal and mixing prevented regionalism. However, detailed taxonomic revisions and biogeographical studies in the past few decades have revealed that the biogeography of freshwater invertebrates is more complex than mere 'cosmopolitanism'.

The water fleas (Crustacea: Branchiopoda: Cladocera) are among the most important models for the study of freshwater biodiversity. Major advances in the taxonomy of Cladocera occurred at the end of the 20th and the beginning of the 21st centuries (Frey, 1991; Korovchinsky, 2004; Smirnov, 1992a, 1996; Van Damme *et al.*, 2011). These morphology-based revisions resulted in a total replacement of the concept of cosmopolitanism (Baas Becking, 1934; Brehm, 1955; Darwin, 1882), with regionalism and continental

*Corresponding author. E-mail: alexey-a-kotov@yandex.ru
[Version of record, published online 17 June 2020; http://zoobank.org/ urn:lsid:zoobank.org:act:35E53D06-8D20-4440-9227-69F52DE11D56]

endemism being more frequent (Brooks, 1957; Frey, 1982, 1987). Vast and key biogeographical regions, such as the Palaearctic, remain poorly studied, but biogeographical studies of Palaearctic cladocerans in the molecular era are beginning to appear (Bekker *et al.*, 2016; Kotov *et al.*, 2016; Xu *et al.*, 2009, 2011).

Forró *et al.* (2008) evaluated the number of cladoceran taxa in each global biogeographical zone and concluded that the most diverse region is the Palaearctic. They attributed this diversity pattern, in part, to a historical sampling artefact arising from weak sampling of the tropics and thorough sampling of the western Palaearctic (Korovchinsky, 1996). The observed large number of cladoceran taxa is also a reflection of the vastness of the Palaearctic and its diversity of habitat. Moreover, the Palaearctic has had a complicated recent geological and climatic history, including a strong influence of Pleistocene glaciation cycles (Hewitt, 2000). The number of endemic taxa was also found to be maximal in the Palaearctic (Forró *et al.*, 2008), but this increased endemism was attributed to the presence of species flocks in Lake Baikal and the Caspian Sea (Dumont, 2000; Cristescu & Hebert, 2002).

There are other significant zones of endemism in the Palaearctic. Korovchinsky (2006), referring to the 'ejected relict' hypothesis (see detailed review by Eskov, 1984), concluded that the 'concentration of endemics in the warm temperate–subtropical zone of both hemispheres' is characteristic of cladoceran zoogeography. Such endemism is well known in the Mediterranean region (Alonso, 1991), but recently, another important zone of cladoceran endemism has been detected in the eastern Palaearctic, including north-eastern China, Japan, Korea and the Russian Far East. Interestingly, the Far East (including the Amur Basin) has long been proposed as a centre of endemism for freshwater fish (Berg, 1962; Nikolsky, 1956), but surprisingly few cladoceran endemics are known from the Far East. However, cladocerans of China and Korea are still poorly studied despite the large number of recent faunistic papers (Chen, 1991; Tian, 2004), regional books (Chiang & Du, 1979; Yoon, 2010), checklists (Ji *et al.*, 2015; Xiang *et al.*, 2015) and detailed morphologically based studies that have been published recently (Kotov *et al.*, 2012; Jeong *et al.*, 2014). Initial genetic studies of Cladocera have also begun, but the research has been limited to the genus *Daphnia* (Wei *et al.*, 2015; Kotov & Taylor, 2019; Ma *et al.*, 2019), with few exceptions (Liu *et al.*, 2018; Ni *et al.*, 2019).

Poppe & Richard (1890) published the first paper on the cladocerans of Japan. Ishikawa (1895a, b, 1896a, b, c) followed by describing three species of *Daphnia* and two species of *Moina* from Tokyo and nearby sites. Later, Uéno (1927, 1934, 1937, 1972) made a long and influential series of contributions to Japanese cladocerology. Tanaka (1994, 1996, 1997) provided descriptions of many Japanese cladocerans, including *Daphnia* (Tanaka & Tominaga, 1986), but avoided describing any new species. Until recently, Japan seemed to be a relatively well-studied region, with few endemics and a typical Palaearctic fauna (Uéno, 1934; Korovchinsky, 2013) (Ishikawa's *Daphnia* taxa were not accepted; see Benzie, 2005). In the 2000s, the molecular genetic study of *Daphnia* began to change the notion that Japan lacked regional cladoceran products (Ishida & Taylor, 2007a, b). The genetic study of other cladocerans beyond *Daphnia* in Japan has also been conducted recently (Lakatos *et al.*, 2015).

The accumulation of evidence for the existence of a specific faunistic complex of Cladocera in the Russian Far East was probably initiated by the description of *Diaphanosoma dubium* Manujlova, 1964, which was found in several water bodies of Primorie (Manujlova, 1964). When *Eurycercus macracanthus* Frey, 1973 was discovered, it appeared to be endemic to the Amur River basin (Frey, 1973), but subsequently, it was found to be distributed widely across northern Eurasia (Bekker *et al.*, 2012). A few more taxa from the Amur River basin studies were later discovered (Smirnov, 1992b; Korovchinsky, 2000). When a unique programme of Russian cladocerologists was formed in the 2000s, there was an increase in regional diversity (Korovchinsky, 2009, 2010; Sinev *et al.*, 2009; Smirnov & Sheveleva, 2010; Kotov *et al.*, 2011a, b).

The application of molecular genetic methods opened a new stage in the history of cladoceran systematics. East Asia is now recognized as a centre of diversity for cladoceran species groups (Ishida & Taylor, 2007a, b), a pattern that has been found among cladoceran families and orders (Belyaeva & Taylor, 2009; Kotov *et al.*, 2009, 2016; Xu *et al.*, 2009, 2011; Millette *et al.*, 2011).

The most studied genus of Cladocera (especially among molecular biologists) is the genus *Daphnia* O.F. Müller, 1785 (Anomopoda: Daphniidae; see the review by Benzie, 2005). The species delimitation in *Daphnia* is notoriously problematic (Benzie, 2005; Kotov, 2015), and these problems are only resolved in part by genetic methods (Petrusek *et al.*, 2008; Zuykova *et al.*, 2018b). Recent progress has been made on east Asian *Daphnia* in a series of investigations (Ishida *et al.*, 2006, 2011; Kotov *et al.*, 2006; Ishida & Taylor, 2007a, b; Popova *et al.*, 2016; Kotov & Taylor, 2019). Two new species from the *Daphnia curvirostris* Eylmann, 1887 species group were described, namely *Daphnia tanakai* Ishida, Kotov & Taylor, 2006, from the mountains of Japan, and *Daphnia sinevi* Kotov, Ishida & Taylor, 2006, from the Far East of Russia (Ishida *et al.*, 2006; Kotov *et al.*, 2006). Kotov & Taylor (2019) provided a trans-Holarctic phylogeographical study of the *D. curvirostris* complex based on nuclear (*HSP90*) and mitochondrial (*ND2*) DNA sequence data. They found 12 phylogroups (potential biological species) organized into five main

clades for the *D. curvirostris* complex. Among them, nine phylogroups (subclades) and three main clades are endemic to East Asia: (1) *D. tanakai*; (2) the *D. sinevi* species group (three subclades); and (3) a newly described species group represented by four related phylogroups with clear geographical differentiation.

A universal 'objective' method for the delimitation of species is an aim of taxonomy. The conflicts between molecular and morphological phylogenetic studies are well known (Hillis, 1987; Wiens, 2004; Dabert *et al.*, 2010), but phylogenetic incongruence can also arise among molecular loci (Hailer *et al.*, 2012). Such conflicts may be resolved, in part, by adding more loci (for example, translated and non-translated), applying different approaches to molecular taxonomy and by co-analysing the results from different types of analyses (Nei & Kumar, 2000). We follow such a combined approach in our study, and we use methods of both 'traditional' taxonomy and cybertaxonomy (see de Carvalho *et al.*, 2007; de Carvalho & Ebach, 2009; Kotov & Gololobova, 2016).

We here assess the status of independent species for each phylogroup of the eastern Palaearctic *D. curvirostris* complex based on morphological analysis and sequence data from two additional genes (*COI* and *12S*) and combined trees based on four genes (including newly obtained sequences of *ND2* and *HSP90*). We use this larger dataset to assess the global phylogeography of the group.

Abbreviations for the collections

AAK, personal collection of A. A. Kotov, Moscow, Russia; MGU, Zoological Museum of Moscow State University, Moscow, Russia; NIBRIV, Invertebrate collection of the National Institute of Biological Resources (NIBR), Inchon, Republic of Korea.

MATERIAL AND METHODS

Sampling and morphological studies

This contribution continues our series of papers combining both DNA sequences and detailed morphological descriptions of the daphniids (Ishida *et al.*, 2006; Kotov *et al.*, 2006). These works resulted in the creation of databases with preliminary morphology-based identification at the level of species or species group (Fig. 1).

Samples were collected using a Juday-type or an Apstein-type (100 µm mesh size) plankton net and were immediately fixed in 96% ethanol. Sampling was supplemented with material obtained from colleagues who might have used different nets for collecting their samples. For morphological examination, animals were selected from alcohol-preserved samples under a dissecting microscope, placed on slides (in a drop of glycerol) and studied under a high-power optical microscope *in toto*. Then, ten adult and two juvenile females, five adult (if present) and five juvenile males (if present) from each population were dissected for analysis of morphological details, including the appendage structure. A system of numeration of setae on thoracic limbs was applied as in previous papers (Ishida *et al.*, 2006).

DNA extraction, amplification and sequencing

For genetic studies, *D. curvirostris*-like taxa (Fig. 1; Supporting Information, Appendix S1) were initially selected from our samples; each specimen was identified accurately by morphological characters up to at least the species-group level (Ishida *et al.*, 2006; Kotov *et al.*, 2006). Genomic DNA was extracted from single adult females using the Wizard Genomic DNA Purification Kit (Promega Corp., Madison, WI, USA). Four markers were investigated: (1) the 5′-fragment of the first subunit of mitochondrial cytochrome oxidase (*COI*), a protein-coding marker having a relatively high mutation rate and interspecific variability for an effective taxon differentiation that is widely used in routine DNA barcoding (Hebert *et al.*, 2003); (2) the 5′-fragment of the mitochondrial *12S* ribosomal RNA (rRNA) gene (*12S*), with a structure demonstrating an alternation of highly conservative duplexes and variable loops and potentially having a strong potential for DNA barcoding (Yang *et al.*, 2014); (3) the second subunit of the mitochondrial NADH dehydrogenase gene (*ND2*), a locus with confirmed significance for the delimitation of taxa within the *D. curvirostris* group (Kotov *et al.*, 2006; Juracka *et al.*, 2010; Kotov & Taylor, 2019); for this gene we added new sequences (including new populations) to the dataset of Kotov & Taylor (2019); and (4) a fragment of the nuclear gene encoding heat shock protein 90 (*HSP90*) containing three protein-encoding exons and two introns. This locus was also used effectively in previous phylogenetic reconstructions of *Daphnia* (Kotov *et al.*, 2006; Kotov & Taylor, 2019); we added new sequences to the dataset of Kotov & Taylor (2019), including new populations.

Primers for amplification are listed in Table 1. Owing to the variability of the *COI* flanking regions in *Daphnia* (Bekker *et al.*, 2018), we used different sets of primers: two pairs of universal degenerate primers and specific primers designed for the *D. curvirostris* group. For partially degraded samples, we used the internal primers for a conservative portion of the *COI* fragment: a combination of F+iR and iF+R primers gives two PCR products of ~350 bp length each, with an overlap zone of ~70 bp. The assembly results in a contig of the *COI* fragment of 650–720 bp in size (depending on the primer set). These internal primers

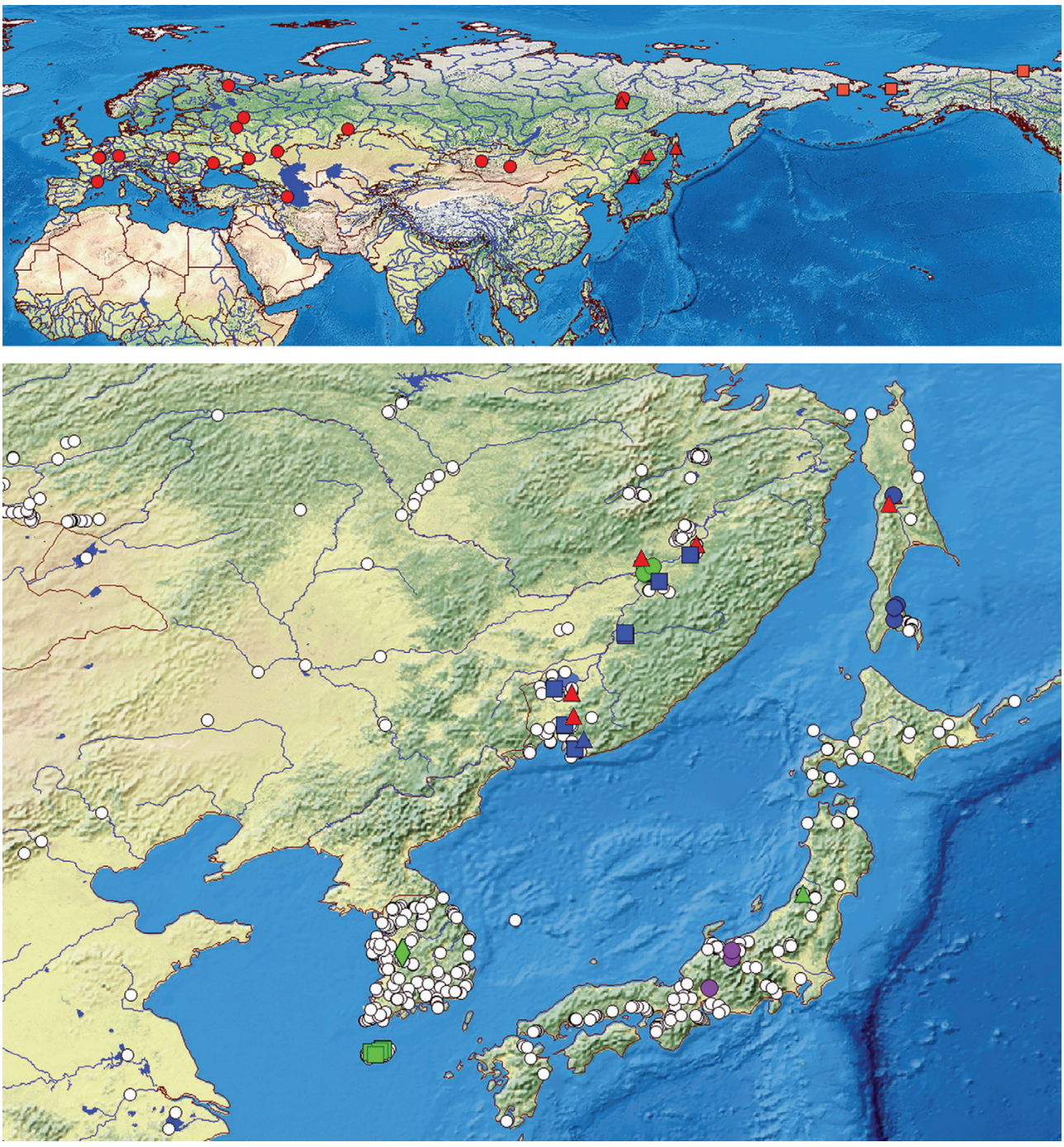

Figure 1. Distribution of the phylogroups of the *Daphnia curvirostris* complex in the Holarctic. Top panel, studied populations of the *D. curvirostric* species group (subclades A–C). Bottom panel, populations belonging to all species groups in the Far East of Eurasia. Shapes of different colours correspond to different phylogroups (see the results of phylogenetic analysis). Open circles indicate localities from where any taxa of *Daphnia* were detected by morphological methods by our team. Visualization of the localities was made in DIVA-GIS7.5.0 (https://www.diva-gis.org) using free spatial GIS data from http://www.naturalearthdata.com as the layers. Note that this is updated in comparison to the dataset of Kotov & Taylor (2019).

were tested for different species of the *D. curvirostris* group; they demonstrated both a high amplification success rate and a strong specificity for the *COI* locus. Likewise, internal primers were designed for the *12S* rDNA locus amplification (for pairs F+iR and iF+R) for a highly conservative portion. The overlap of the

Table 1. Primers and annealing temperatures used to amplify mitochondrial and nuclear fragments used in this study

Gene	Primer	Sequence 5′–3′	Temperature (°C)	Reference
COI	Dcurv_COI-F	TTCATATTTGGAATCTGGTCA	47	This paper
	Dcurv_COI-R	ATAGATGYTGRTATAAAATTG	47	This paper
	Dcurv_COI-iF	TTCTMCCHCCTGCHCTYACA	52	This paper
	Dcurv_COI-iR	GGRTAVACTGTYCAYCCAGT	52	This paper
	Daph-COI-F_M13	tgtaaaacgacggccagttAYCAATCATAAGGACYATTGGRAC	52	Xu *et al.* (2014), with modification
	Daph-COI-R_M13	caggaaacagctatgactaKGTGATWCCNACHGCTCAKAC	52	Xu *et al.* (2014), with modificatiom
	jgLCO1490_M13	tgtaaaacgacggccagttNTCNACNAAYCAYAARGAYATTGG	48	Geller *et al.* (2013), with change
	jgHCO2198_M13	caggaaacagctatgactaNACYTCNGGRTGNCCRAARAAYCA	48	Geller *et al.* (2013), with modification
12S	12S-F	ATGCACTTTCCAGTACATCTAC	50	Colbourne & Hebert (1996)
	12S-R	AAATCGTGCCAGCCGTCGC	50	Colbourne & Hebert (1996)
	Dcurv_12S_iF	GTAATCTGRCAACGGCGGTA	48	This paper
	Dcurv_12S_iR	TAGAGGAGCTTGYCCTRTAA	48	This paper
ND2	MetF2	TGGGTTCATGCCCCATTTATAG	48	Ishida *et al.* (2006)
	TrpR	GAAGGTTTTTAGTTTAGTTAACTTAAAATTCT	48	Ishida *et al.* (2006)
HSP90	HSP90-F	TTACGAGTCCAGATGGGCTT	52	Kotov *et al.* (2006)
	HSP90-R	ATCCGTTATGAATCCCTGACTGA	52	Kotov *et al.* (2006)
Sequence	M13-F	tgtaaaacgacggccagtt	60	Messing (1983), with modification
Sequence	M13-R	caggaaacagctatgacta	60	Messing (1983), with modification

Lower case indicates M13 tailing and sequencing primers.

two fragments was ~80 bp, permitting a contig length of ~600 bp. Locus *ND2* (930 bp) and *HSP90* (~800 bp) were amplified using specific Cladocera primers (Kotov & Taylor, 2019).

Polymerase chain reactions (PCRs) were carried out in a total volume of 20 μL, consisting of 2 μL of genomic DNA solution, 1 μL of each primer (10 mM), 6 μL of double-distilled H_2O and 10 μL of ready-to-use PCR Master Mix 2X solution (Promega Corp., Madison, WI, USA). The PCR products were visualized in a 1.5% agarose gel stained with ethidium bromide and purified by QIAquick Spin Columns (Qiagen Inc., Valencia, CA, USA) according to the manufacturer's protocol. The PCR program included a preheating of 3 min at 94 °C; 40 cycles (initial denaturation of 30 s at 94 °C, annealing of 40 s at a specific temperature and an extension of 80 s at 72 °C) and a final extension of 5 min at 72 °C (Table 1).

Each PCR product was sequenced bidirectionally on the ABI 3730 DNA Analyzer (Applied Biosystems) using the ABI PRISM BigDye Terminator v.3.1 kit at the Syntol Co., Moscow. Initial analysis of the chromatograms, formation of contigs and their subsequent editing was done with the Sanger Reads Editor in the Unipro uGENE v.1.30 package (Okonechnikov *et al.*, 2012). The authenticity of the sequences was verified by BLAST comparisons with published cladoceran sequences in mBLAST (Boratyn *et al.*, 2013). The sequences from this study were submitted to the National Center for Biotechnology Information (NCBI) GenBank database (accession numbers MN184897–MN184987 and MN202473–MN202501). Additional information (DNA sequences, alignments, phylogenetic trees and images) used in this study were deposited in the open repository Open Science Framework (http://osf.io/k9uxf/).

Population analysis, alignment and phylogenetic analysis

To reduce the influence of population structure on our results, we subdivided all of the specimens a priori into large population groups (clades) according to the phylogeny of Kotov & Taylor (2019). We also used the clade abbreviations and colours/shapes of symbols on the maps and trees from that publication.

The most powerful tests of neutrality are based on haplotype frequencies, but the results of such analyses are affected by the level of genetic recombination (Ramírez-Soriano *et al.*, 2008). As a result, we performed the Genetic Algorithm for Recombination Detection test for recombination (Kosakovsky Pond *et al.*, 2006) for all loci. These tests were applied using default settings: (1) separately for each clade; and (2) for the set of all clades on the web server Datamonkey 2.0 (Weaver *et al.*, 2018). We applied the F_S test (Fu,

1997) and R_2 statistics (Ramos-Onsins & Rozas, 2002) to confirm neutrality and describe demographic processes (Ramírez-Soriano *et al.*, 2008; Garrigan *et al.*, 2010). Nucleotide diversity analysis (Nei & Kumar, 2000), neutrality tests, mismatch analyses, coalescent simulations and statistics associated with population growth and divergence were carried out using DnaSP v.6.12 (Rozas *et al.*, 2017). Also, a test for a positive selection according to the mixed effects model of evolution (MEME; Murrell *et al.*, 2012) was performed for coding loci on the web server Datamonkey 2.0 (Weaver *et al.*, 2018). Again, default parameter settings were used for MEME.

Alignment was carried out using the MAFFT v.7 algorithm (Katoh & Standley, 2016) based on the server of the Computational Biology Research Center, Japan (http://mafft.cbrc.jp). For more accurate alignments, sequences of *D. curvirostris* from NCBI GenBank [EF375872 (*COI*), JQ861680 (*12S*) and DQ132619 (*ND2*)] were used as references at the initial stages of the alignment. For determination of the exon–intron boundaries of the *HSP90* locus, we used the sequence DQ845255 and fully translated sequence of this locus of *Daphnia pulex* (Linnaeus, 1758), KC845247, after splicing. Each locus was aligned independently. For *HSP90*, the two introns were aligned independently, whereas all exons were assembled to a single contig for alignment. For protein-coding genes (*COI*, *ND2* and exon of *HSP90*), we used the 'Translation Align' option with the FFT-NS-i strategy. For alignment of the ribosomal *12S* locus, we used the Q-INS-i strategy, which takes into consideration the secondary structure. Non-coding fragments (*HSP90* introns) were aligned using the FFT-NS-2 strategy. Linking sequences and their partitioning for subsequent analyses were made in SequenceMatrix v.1.8 (Vaidya *et al.*, 2011).

The best-fitting models of the nucleotide substitutions for each locus and for linked data were selected using ModelFinder v.1.6 (Kalyaanamoorthy *et al.*, 2017) at the Center for Integrative Bioinformatics Vienna Webportal, Austria (http://www.iqtree.org; Trifinopoulos *et al.*, 2016) based on minimal values of the Bayesian information criteria (BIC) and the log-likelihood of the tree. The BIC model parameters were almost identical to those obtained using the corrected Akaike information criterion (AICc). Given that there are differing approaches for modelling the evolutionary process, including substitution models (Arenas, 2015; Barley & Thomson, 2016), we used the simplest models, as recommended by Nei & Kumar (2000).

Phylogenetic reconstruction using the data from all genes was realized with the 'star' coalescent model in BEAST2 (Heled & Drummond, 2010) and the approach of Chernomor *et al.* (2016) for maximum likelihood (ML) phylogenies. Phylogenetic reconstructions based on the ML and Bayesian inference (BI) methods were made for each gene separately (including nuclear), for the full set of mitochondrial genes and for all 'unlinked' genetic data.

Sequences from the present study and previously obtained sequences, i.e. from Kotov & Taylor (2019), were combined in the phylogenetic analysis (Supporting information, Appendix S1). For ML analysis, we used the IQ-TREE v.1.6.9 algorithm (Nguyen *et al.*, 2015), using the Webportal CIBIV, Austria. Each set of sequences was analysed based on the best model found automatically by the W-IQ-TREE (Trifinopoulos *et al.*, 2016). To estimate the branch support values, we used UFbootstrap (Minh *et al.*, 2013) and posterior probabilities (PPs) from the Bayesian analysis in BEAST v.2.5.1 (Bouckaert *et al.*, 2014). For BI analysis, we identified all of the parameters of the substitution model using the Bayesian information criterion (BIC) from BEAUti v.2.5.1 (Drummond *et al.*, 2012). In each analysis, we conducted four independent runs of Markov chain Monte Carlo (MCMC; 100 million generations, with selection of one generation every 10 000 generations), with effectiveness control in R We There Yet (RWTY) for R (Warren *et al.*, 2017). A consensus tree based on the maximum clade credibility (MCC) was obtained in TreeAnnotator v.2.5.1 (Drummond *et al.*, 2012), with half increased burn-in rate determined in RWTY (but ≥ 20%). Given that the main clades for BI and ML were congruent, we present the BI trees, with branch support for key nodes.

Separate mitogenome and nuclear trees were estimated in *BEAST2 to reveal the conflicts between nuclear and mitochondrial genomes (Fisher-Reid & Wiens, 2011). For the visualization of possible cases of clade mixing and/or hybridization, we used a tanglegram (Scornavacca *et al.*, 2011) for mitochondrial and phylogenetic networks and a galled network (a generalization of galled trees) of three mitochondrial and three nuclear loci according to the algorithm of Huson *et al.* (2009). We ignored one-third of the possible connections in the reconstruction with DendroScope v.3.5 (Huson & Scornavacca, 2012).

Cybertaxonomic species delimitation based on DNA data

Several approaches to the automatic species delimitation were applied here.

1. To estimate the number of operational taxonomic units, the aligned sequences were subjected to the Objective Clustering at 3% threshold in SpeciesIdentifier/TaxonDNA v.1.8 (Meier *et al.*, 2006), based on the sequence divergence threshold (Hebert *et al.*, 2003).

2. The Automatic Barcode Gap Discovery (ABGD) analysis (Puillandre *et al.*, 2012), searching for the 'barcode gaps' (Hebert *et al.*, 2004), was carried out at the Atelier de BioInformatique web server, France (http://wwwabi.snv.jussieu.fr/public/abgd/abgdweb.html), with values of Pmin = 0.001, Pmax = 0.1, Steps = 100, X = 10, Nb = 25 and 'simple' *p*-distances, most appropriate for the DNA barcoding (Collins *et al.*, 2012).
3. The general mixed Yule-coalescent (GMYC) model was made to assign analysed individuals to the species according to ultrametric time trees derived from single-locus data (Pons *et al.*, 2006). We used the Bayesian GMYC model in the 'bGMYC' package (Reid & Carstens, 2012) for R v.3.6 x64 (http://www.r-project.org) to discover species in the MCMC trees based on a concatenated matrix for each locus. Given that bGMYC is prone to over-split trees containing identical alleles (i.e. zero-length branches) into species (Reid & Carstens, 2012), we dropped any zero-length tips from the MCMC tree before the analyses, then ran 'bGMYC' using the multiple-threshold models in the 'bGMYC' package using sequences of *Daphnia laevis* Birge, 1879 as outgroups. Sorting, rerooting of the trees and outgroup deletion was done in R according to the script of Sweet *et al.* (2018). Ultrametric trees for each locus were evaluated in BEAST2 using substitution models, as for the phylogenetic analysis above, a strict clock model and a Yule process. We sampled 12 million MCMC generations, with retention of one tree every 10 000 generations and a 20% burn-in parameter. We used TRACER v.1.7 (Rambaut *et al.*, 2018) to evaluate convergence of parameters [based on an effective sample size (ESS) > 400]. For the bGMYC analysis, we randomly selected 100 ultrametric trees from the 1000 trees after burn-in from BEAST2. For each of the 100 trees selected, the analyses consisted of 250 000 generations with a burn-in of 25 000. We set the threshold parameter priors, t1 and t2, to 2 and 100, respectively, and the starting parameter value was set at 100. The results were accepted as statistically significant at a modified $P > 0.99$ level. This *P*-value should significantly reduce the likelihood of excessive 'fragmentation' in the designation of taxonomic structure.
4. Single gene trees were analysed applying the Bayesian implementations of the PTP algorithm, Bayesian implementation of the Poisson Tree Processes model (bPTP) (Zhang *et al.*, 2013) at the web server of Heidelberg Institute for Theoretical Studies, Germany (http://species.h-its.org/). This method does not require an ultrametric input tree to delineate entities corresponding to the phylogenetic species concept. Thus, we used ML phylogenetic trees as input data. Parameters of bPTP were MCMC 500 000, thinning 200, burn-in 0.25 and *p* 0.05. Removing the outgroup in initial runs did not affect delimitation results. Consequently, we did not use this option.
5. The combined species tree estimation and species delimitation analysis, as available with STACEY (Species Tree And Classification Estimation, Yarely; Jones, 2017), was done in BEAST2. We assumed a birth–death speciation tree prior while using a collapse height of 0.001 and estimated collapse weight with an initial value of 0.5 using a beta prior [1–1] around [0–1]; following suggestions for prior choice in species tree analysis using *BEAST2, Jeffrey's prior was used for growth rate and population scaling factor; the relative death was estimated using a beta prior [1–1] around [0–1], like Vitecek *et al.* (2017). We used ploidy settings as ½. Genealogical relationships were estimated by STACEY with four independent generations (50 million generations of MCMC, sampling of every 10 000 generations) after incorporating the suggestions from an initial run. STACEY log files, as stated above, were examined with TRACER v.1.7 to evaluate whether parameters reach a convergence based on ESS > 200. Supports for the tree topologies estimated by STACEY were examined by constructing a maximum clade credibility tree using the TreeAnnotator v.1.8 (part of the BEAST2 package) after discarding the first one-third of all estimated trees. Species delimitations based on the trees estimated by STACEY were assessed with the Java application speciesDA (http://www.indriid.com/software.html), using the same burn-in, a collapse height of one-tenth of the average branch and default similarity cut-off.
6. Multilocus species delimitation using Bayesian model comparison (Rannala & Yang, 2003; Degnan & Rosenberg, 2009) was implemented in the 'tr2' packet (Fujisawa *et al.*, 2016) for PYTHON v.3.7 (http://www.python.org) using the 'blind' variant of the analysis, without any preliminary species delimitation. We used the information on sequences and ML trees for all studied loci with full datasets (> 60%); the consensus multilocus tree from *BEAST2 was used as a guide tree for STACEY.

PHYLOGEOGRAPHICAL RECONSTRUCTIONS

For a preliminary testing of the phylogeographical models, we analysed aligned sequences of the 658 bp *COI* fragment (for which there is the largest number of studied populations, with additional data in GenBank, and which is frequently described as 'a genetic standard') in BioGeoBEARS (Matzke, 2013), with an integrated 64x package 'R' v.3.5.1 in RASP v.4b (Yu *et al.*, 2015). Program limitations allowed us to take

into the analysis 57 sequences from nine phylogenetic lineages of the *D. curvirostris* group from 12 large geographical regions. The program used four possible distribution ranges and regarded each population as an independent clade (without a priori taxonomic subdivision). Six biogeographical models [standard dispersion–vicariance models and those with a correction to the speciation events (+J)] were evaluated according to the AICc (Matzke, 2014) in BioGeoBEARS. Phylogenetic reconstruction for the input data was done in BEAST2, running four independent MCMC chains of 100 million generations, with the retention of one tree each 10 000 generations. For RASP files, 100 trees were randomly selected from the BEAST2 set through the script in the R package (Sweet *et al.*, 2018); a condensed tree was obtained, with 50% burn-in. A model of dispersal–extinction–cladogenesis (DEC) was selected according to the minimal value of the AICc. We rejected approximate models (DEC+J and S-DEC; Yu *et al.*, 2015), because their use increased the AICc values.

We used the RASP v.4b module of the Bayesian inference for discrete areas, BayArea (Landis *et al.*, 2013), as an alternative and accurate stochastic approach for the description of the evolution of distribution range as a continuous process (Yu *et al.*, 2015). We used the same input files and localities as in DEC, performing 10 million MCMC generations, selecting a tree each 10 000 generations, with a burn-in of 20% of the first generations. Four independent runs of BayArea were made to increase the ESS; the results of runs were combined and visualized through the 'Combine result' tool in RASP.

A haplotype network was constructed in popART v.1.7 with the integer neighbor-joining network algorithm (Leigh *et al.*, 2015) and minimal reticulation tolerance.

To test the applicability of our data to molecular clock analyses, we used a maximum likelihood test in MEGA-X (Kumar *et al.*, 2018), with locus-specific substitution models. Models were also partitioned by codon position for the protein-coding loci. *Daphnia laevis* was used as an outgroup. The use of nuclear loci (with exon–intron structures as in *HSP90*) obviously makes the molecular clock calibration more complicated and increases the uncertainty (Belyaeva & Taylor, 2009; Schwentner *et al.*, 2013). We therefore used the mitochondrial genes (both protein-coding and ribosomal ones) for clock-like analyses.

In our biogeographical reconstructions, we initially used the rate of accumulation of mutations in the *COI* locus for calibration. We determined a rate of nucleotide substitutions between groups of populations and within them (Nei & Kumar, 2000) and calculated 'clear' non-corrected intergroup *p*-distances in MEGA-X (Kumar *et al.*, 2018). Translation of these distances to the divergence time was made based on the substitution rate in the *COI* locus of: (1) 0.8–1.4%/Myr ('fast clock'; Knowlton & Weigt, 1998; Schwentner *et al.*, 2013); and (2) 0.11%/Myr for the genus *Daphnia* ('slow clock'; Kotov & Taylor, 2011).

The age of the *D. curvirostris s.l.* lineage differentiation was then estimated using a relaxed molecular clock approach, with an uncorrelated lognormal distribution of branch rates (Drummond *et al.*, 2006) in BEAST v.1.10.4 (Suchard *et al.*, 2018). This approach allowed us to take into consideration the substitution rates for each branch and each locus. Relaxed molecular clocks were used because strict clock-like models were rejected in MEGA-X for all data. A Yule process was used (Gernhard, 2008). Calibration points were taken from previous publications (Kotov & Taylor, 2011; Schwentner *et al.*, 2013) with 15% standard deviation. Input files for BEAST were composed in BEAUti, part of the BEAST package. All analyses were made using nucleotide substitution models from previous phylogenetic reconstructions (see above). Four independent runs for 10 million generations were performed; one tree was selected each 10 000 generations. Input files were composed in LogCombiner and then converted to tree files in the TreeAnnotator program of BEAST v.1.10.4 (Suchard *et al.*, 2018). TRACER v.1.7.1 was used to confirm run convergence and to examine the ESS for each parameter. Trees were visualized in FigTree v.1.4.4 (http://tree.bio.ed.ac.uk/software/figtree/). Minimal speciation time was estimated in the 'splits' packet for R v.3.5.2 (Fujisawa & Barraclough, 2013). A calibration tree from BEAST v.1.10.4. was used as the input ultrametric tree.

RESULTS

TAXONOMIC ACCOUNT AND MORPHOLOGICAL DESCRIPTIONS

We present the taxonomic account first, in order to have the names of previously undescribed taxa available for our subsequent results and discussion. We found diagnostic morphological characters for four aforementioned closely related species forming the *Daphnia korovchinskyi* species group.

ORDER ANOMOPODA SARS, 1865

SUBORDER ARADOPODA KOTOV, 2013

FAMILY DAPHNIIDAE STRAUS, 1820

GENUS *DAPHNIA* O.F. MÜLLER, 1785

SUBGENUS *DAPHNIA* (*DAPHNIA*) O.F. MÜLLER, 1785

DAPHNIA (*DAPHNIA*) *CURVIROSTRIS* SPECIES COMPLEX

***DAPHNIA* (*DAPHNIA*) *KOROVCHINSKYI* SP. NOV.**

(FIGS 2–4)

LSID: urn:lsid:zoobank.org:act:ED643231-29A8-40E9-8E7C-890ED9E94FC0

Daphnia sp. nov., clade I in Kotov & Taylor, 2019: figs 1, 2.

Etymology: This species is dedicated to N. M. Korovchinsky, renowned Russian cladocerologist, who participated in collection of samples in Khabarovsk Territory, including the type specimens.

Type locality: Puddle 2 in a rut (48.40289°N, 134.8769°E), Island of Bol'shoy Ussuriysky in the Amur River, Khabarovsk Territory, Russia. The type series was collected on 1 September 2007 by A. A. Kotov and N. M. Korovchinsky.

Holotype: A parthenogenetic female, MGU ML172. Label of the holotype: '*Daphnia korovchinskyi* sp.nov., 1 parth. ♀ from a puddle at Island of Island of Bol'shoy Ussuriysky, Khabarovsk Territory, Russia, HOLOTYPE'.

Paratypes: Twelve females, MGU ML173. Eleven females, MGU ML174. The rest of specimens, AAK M-0625. Twenty females from a pond (48.62314°N, 135.1366°E) near Vinogradovka village, near a road to Khohlatskaja Protoka of the Amur River, Khabarovsk Territory, collected on 2 September 2007 by A. A. Kotov and N. M. Korovchinsky, AAK M-0630.

Short diagnosis: Parthenogenetic female. Body subovoid, caudal spine short. Head relatively large, with a low anterior crest, head posterior margin with a strong, arched projection, a deep incision between antenna I and labrum base. Rostrum relatively short (as a result, tips of longest aesthetascs reach its tip); rostrum tip slightly bent posteriorly and subdividing into two lobes by a 'line' of prerostral fold, with posterior lobe always smaller than anterior one. Spinules occupy less than half of dorsal and ventral valve margin. In posteroventral portion of valve, on inner face of valve, there are fine setae with setules between them. First abdominal process almost straight, directed anteriorly; second process short, bent distally; third process as a massive mound on the segment. Postabdomen with a smooth postanal angle. Postabdominal claw with first pecten consisting of stout, thin teeth; second pecten consisting of seven to ten large teeth; third pecten consisting of numerous, fine setules. Body of antenna I completely reduced; antennular seta arising immediately from head surface; aesthetascs protruding posteroventrally, and their tips do not reach tip of rostrum. Limb I with relatively long setae 3; limb II with an anterior seta 1 about two-thirds length of other setae, bilaterally setulated distally and 11–12 setae of filter plate of gnathobase; limb III with seta 2 of exopod longer than seta 4, bearing short setules; seta 3 on inner distal portion of limb rudimentary; limb V with projected inner distal portion.

Juvenile female I with a single necktooth. Ephippial female. Male unknown.

Size: ≤ 1.71 mm.

Full description

Adult parthenogenetic female: Body subovoid in lateral view, maximum height in middle of valves (Fig. 2A). Dorsal margin usually convex; a depression between head and rest of body absent. Posterodorsal angle with a relatively short caudal spine; ventral margin regularly convex. Head relatively large, with a low anterior crest and a relatively short rostrum, its tip slightly bent posteriorly; in lateral view, rostrum tip subdividing into two lobes by a 'line' of prerostral fold, with posterior lobe always smaller than anterior one (Fig. 2B–E); posterior margin of head with a strong, heavily reticulated projection separated from base of labrum by a deep depression; ventral margin of head slightly concave. Compound eye large, lying ventral to middle body axis and out of the anteriormost extremity of head; ocellus minute. Labrum as a fleshy main body and a large, setulated distal labral plate (Fig. 2C). Carapace subovoid; spinules present on caudal spine and occupying less than half dorsal and ventral valve margin (Fig. 2A). In posteroventral portion of valve, on inner face of valve, there are fine setae with series of setules between them (Fig. 1F, H, I); near caudal spine, frequently there are only setules, but any setae absent (Fig. 2G, I, K, L).

Abdomen consisting of four segments. The first (basal-most) abdominal process is almost straight, directed anteriorly; the second (middle) process shorter, bent distally; the third (distal-most) process as a massive mound on the segment; on all processes there are rare, fine setules; the fourth segment lacks a process (Fig. 2M). Postabdomen elongated, tapering distally, with ventral margin straight or slightly concave, lacking setules. Preanal margin long, concave; preanal angle smooth; postanal angle not expressed. Paired spines on postanal and anal portion, with their size continuously increasing distally. Postabdominal seta as long as preanal margin, its distal segment shorter than basal one. Postabdominal claw long, regularly bent, with a pointed tip (Fig. 2N, O). On outer side, three successive pectens along the dorsal (concave) margin: the first (proximal) pecten consisting of stout, thin teeth; the second (medial) pecten consisting of five to ten large teeth; the third pecten composed of numerous, fine setules, not reaching the tip of claw. Fine denticles

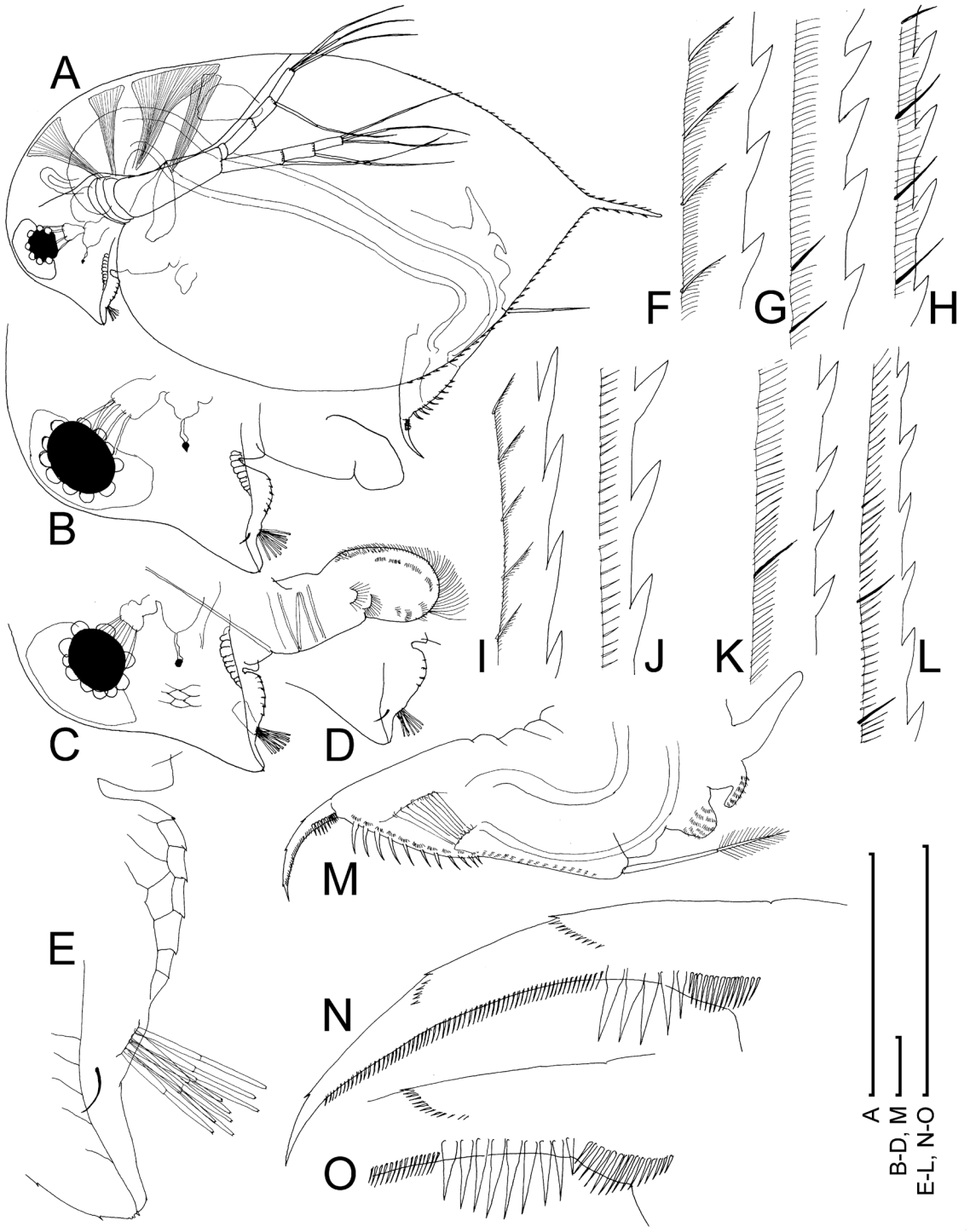

Figure 2. ***Daphnia korovchinskyi***, large parthenogenetic female from a rut puddle, Island of Bol'shoy Ussuriysky on the Amur River, Khabarovsk Territory, Russia. A, lateral view. B, C, head. D, E, rostrum and antenna I. F, G, armature of posteroventral and posterior margin of valve in a female. H, posteroventral margin in second female. I, J, posteroventral and posterior margin of valve in a third female. K, L, posteroventral and posterior margin of valve in a fourth female. M, postabdomen and abdomen. N, O, postabdominal claw and its proximal portion. Scale bars denote 1 mm for A and 0.1 mm for B–O.

at distal end of medial pecten, in middle of third pecten and distal portion on claw ventral (convex) margin.

Antenna I with a completely reduced body, nine aesthetascs (of different length) and antennular seta arising immediately from the surface of the head; aesthetascs protruding posteroventrally, and their tips do not reach tip of rostrum (Fig. 2E). Antenna II (Fig. 3A) with a narrow coxal part possessing two short sensory setae of different length. Basal segment elongated, with a minute distal spine at its anterior face (Fig. 3B), but a relatively long distal sensory seta with pointed tip on its posterior face (Fig. 4C). Antennal branches elongated, four-segmented exopod slightly shorter than three-segmented endopod, all with series of minute denticles. Antennal formula: setae 0-0-1-3/1-1-3. Each swimming seta with basal and distal segments bilaterally setulated; a chitinous insertion within distal segment near joint with basal segment (Fig. 3D–G). Spines on apical segments rudimentary; spine on the second segment of exopod rudimentary (Fig. 3B).

Limb I without an accessory seta; outer distal lobe (Fig. 4A: ODL) with a long seta unilaterally armed distally with short setules and a short, thin, naked seta (Fig. 4B); inner distal lobe (Fig. 4A: IDL), or endite 4, with a single, long anterior seta (1), bearing short setules distally (Fig. 4C). Endite 3 with a long anterior seta (Fig. 4A: 2), armed with minute setules (Fig. 4D) and two posterior setae (Fig. 4A: a and b). Endite 2 with a short anterior seta (Fig. 4A: 3), armed with minute setules (Fig. 4E) and two posterior setae (Fig. 4A: c and d). Endite 1 with a small anterior seta (Fig. 4A: 4), armed with minute setules (Fig. 4F) and four posterior setae (Fig. 4A: e–h). Two ejector hooks of different length. Limb II with an ovoid epipodite; distal portion as a large lobe bearing two soft, setulated setae (Fig. 4G); four endites supplied in toto by five setae, among them, a stiff, anterior seta (Fig. 4G: 1), about two-thirds the length of other setae on distal-most endite, bilaterally setulated distally (Fig. 4H). Gnathobase with two clear rows of setae: four anterior setae (Fig. 4I: 1–4) and 11–12 posterior setae of gnathobasic 'filter plate' (Fig. 4I: a–l), seta 4 longer than half of seta c or d or e. Limb III with a subglobular epipodite and a flat exopodite bearing four distal (Fig. 3J: 1–4) and two lateral (5 and 6) setae; seta 2 longest, with short setules distally. Inner distal portion of limb with four endites: endite 4 with a single, long anterior seta (Fig. 3K: 1) and a posterior (a) seta; endite 3 with a single anterior seta (2) and a single posterior (b) seta of similar size; endite 2 with a rudimentary anterior seta (3) and two posterior setae (c and d); endite 1 with a large anterior seta, bilaterally armed with relatively long setules (4) and four posterior (e–h) setae. The rest of limb inner distal portion as a single large lobe, modified gnathobase, bearing numerous filtering setae and a single, relatively long anterior seta armed with short setules (Fig. 4K: 1) in its distal corner. Limb IV with a large, setulated pre-epipodite, ovoid epipodite and wide, flat exopodite, with protruding and setulated inner distal angle and bearing four distal (Fig. 4L: 1–4) and two lateral (5 and 6) setae. Inner distal portion of this limb with completely fused endites, distally with two setae of unclear homology (Fig. 4M); the most part of limb inner margin is a gnathobase filter plate consisting of numerous filtering setae. Limb V with a small, setulated pre-epipodite, subovoid epipodite, triangular exopodite supplied with two short distal setae (Fig. 4N: 1 and 2) and a large lateral seta (3). Inner limb portion as an ovoid flat lobe, with setulated inner margin and a single, large seta.

Juvenile female: Body subrectangular, with straight posterior margin and longer caudal spine; spinules cover closest to caudal spine part of dorsal margin and less than half of ventral margin, with no spinules at posterior margin. Head with a straight ventral margin; rostrum short; dorsal margin convex, with a single necktooth; dorsal organ in posterior portion of head, with a slight depression posterior to it (Fig. 3H). Postabdominal claw with the second pecten consisting of teeth more numerous and smaller in size when compared with the teeth of adults (Fig. 3I).

Ephippial female, male: Unknown.

Size: Parthenogenetic females 0.83–1.71 mm.

Taxonomic comments: No *D. curvirostris*-like taxa have been described previously from the Far East of Russia (with the exception of *D. sinevi*). *Daphnia sinevi* differs from *D. korovchinskyi* in a series of characters. Notably, *D. sinevi* lacks the full reduction of antenna I body found in *D. korovchinskyi*. The validity of *D. korovchinskyi* is supported by the absence of descriptions for similar taxa.

Distribution: *Daphnia korovchinskyi* is known from only two localities in the Amur River valley near Khabarovsk, Russia. Both localities are small, shallow, temporary water bodies. It appears to have a restricted geographical range.

DAPHNIA (*DAPHNIA*) *ISHIDAI* SP. NOV.

(FIGS 5–8)

LSID: urn:lsid:zoobank.org:act:D8304465-FB1D-4365-9B2F-7C10D2130F0A

Daphnia sp. from Ootori-Ike of Kotov *et al.*, 2006: 1070–1071, table 1, fig. 2.

Daphnia sp. (Japan) of Juracka *et al.*, 2010: fig. 9.

Daphnia sp. nov., clade J of Kotov & Taylor, 2019: figs 1, 2.

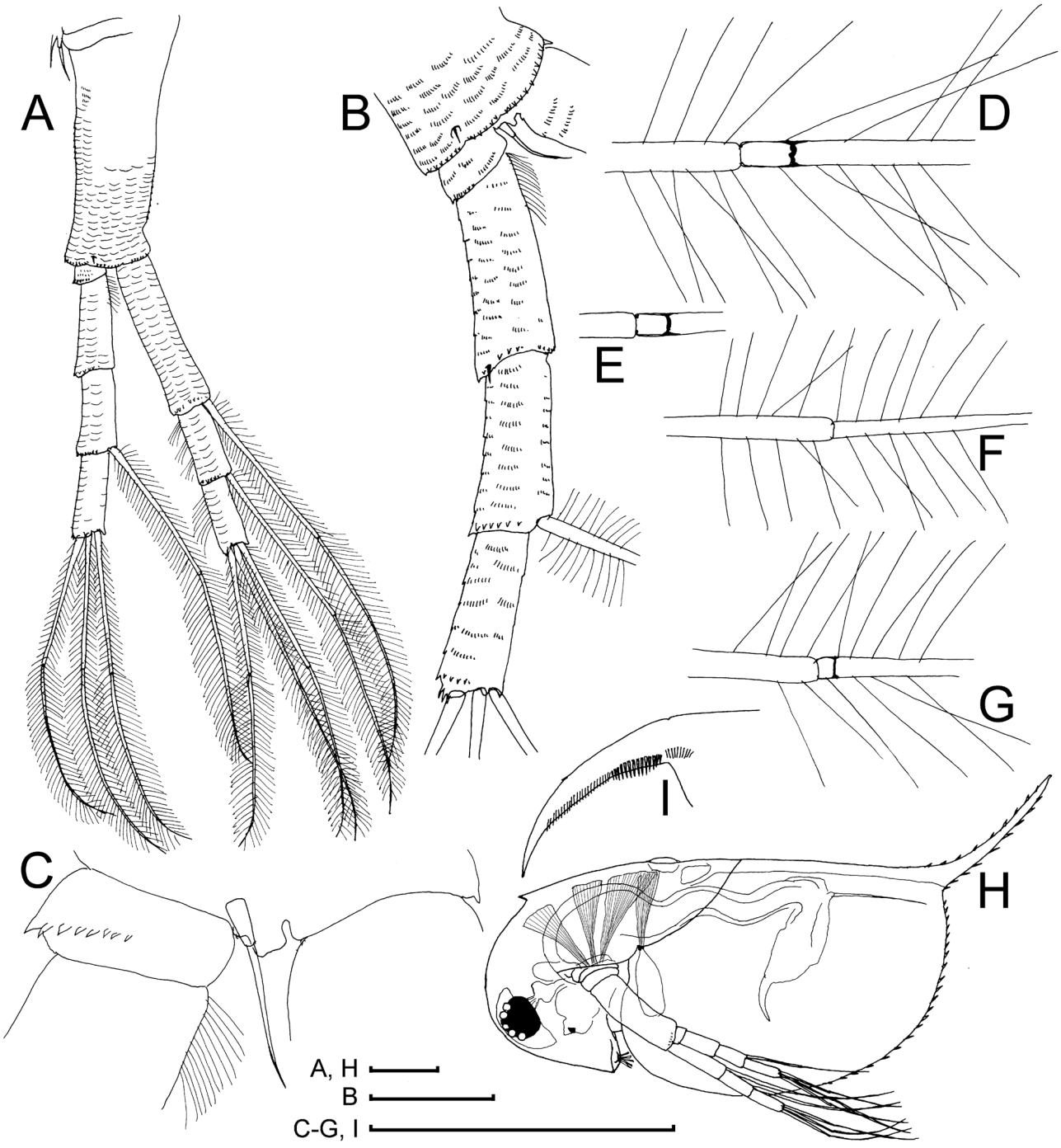

Figure 3. ***Daphnia korovchinskyi***, large parthenogenetic (A–G) and juvenile (H, I) females from a rut puddle, Island of Bol'shoy Ussuriysky on the Amur River, Khabarovsk Territory, Russia. A, B, antena II, anterior view. C, distal portion of its distal segment and proximal segment of its exopod, posterior view. D–G, apical setae of different individuals. H, juvenile of instar I, lateral view. I, its postabdominal claw. Scale bars denote 0.1 mm.

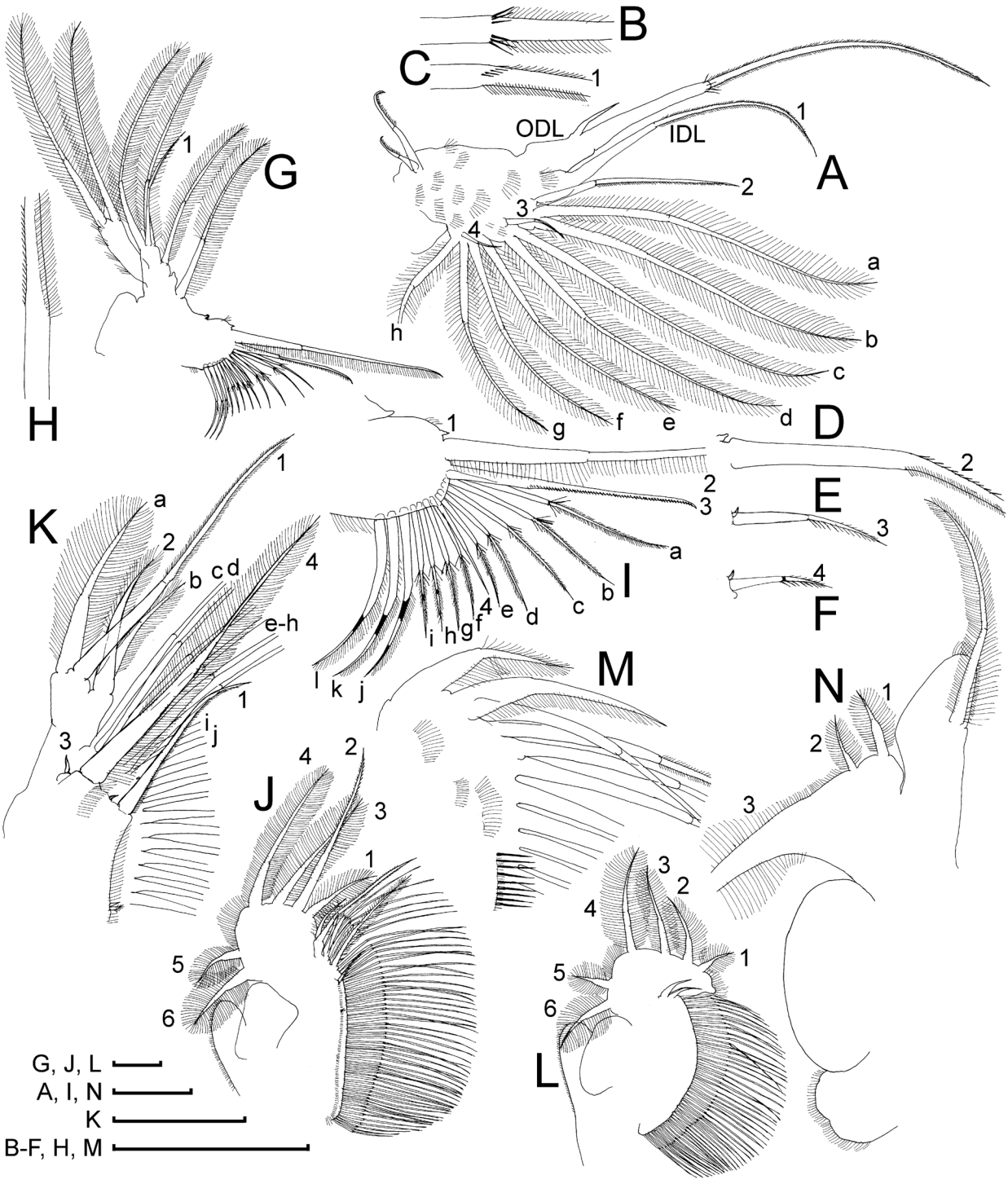

Figure 4. ***Daphnia korovchinskyi***, thoracic limbs of a large parthenogenetic female from a rut puddle, Island of Bol'shoy Ussuriysky on the Amur River, Khabarovsk Territory, Russia. A, limb I. B, armature of its largest outer distal lobe seta. C, armature of its inner distal lobe seta. D–F, anterior setae 4, 3 and 2 on inner limb face. G, limb II. H, armature of its anterior seta 1. I, gnathobase II. J, K, limb III and its inner distal portion. L, M, limb IV and its inner distal portion. N, limb V. Scale bars denote 0.1 mm.

Etymology: This species is dedicated to Dr Seiji Ishida, who contributed to the study of *D. curvirostris*-like species and other cladocerans in Japan (see Ishida *et al.*, 2006; Kotov *et al.*, 2006) and collected the type series of this species.

Type locality: Lake Otori Ike (38.3658°N, 139.8302°E, 963 m a.s.l.), Yamagata Prefecture, North part of Honshu Island, Japan. The type series was collected on 10 October 2005 by S. Ishida.

Holotype: A parthenogenetic female, MGU Ml177. Label of the holotype: '*Daphnia ishidai* sp. nov., 1 parth. ♀, Lake Otori ike, Honshu Osland, Japan, HOLOTYPE'.

Paratypes: Fifteen parthenogenetic females, MGU Ml178. Five juvenile males, MGU Ml179. Ten parthenogenetic females, MGU Ml180.

Short diagnosis: Parthenogenetic female. Body subovoid; caudal spine short. Head relatively small, lacking an anterior crest, its posterior margin with a regularly arched projection; no deep incision between antenna I and labrum base. Rostrum relatively short (as a result, tips of longest aesthetascs reach its tip); rostrum tip slightly bent anteriorly and subdividing into two lobes by a 'line' of prerostral fold, with posterior lobe always larger than anterior one. Spinules present only on caudal spine and dorsal margin immediately near caudal spine. In posterior portion of valve, on inner face of valve, only a row of minute setules, but any setae absent. First abdominal process almost straight, directed anteriorly; second process short, bent distally; third process as a massive mound on the segment. Postabdomen with a smooth postanal angle. Postabdominal claw with three pectens of relatively rough denticles, among which denticles in third (distal) row are only somewhat shorter than the rest. Body of antenna I completely reduced; antennular sensory seta not found; aesthetascs protruding posteroventrally, and their tips reach tip of rostrum. Limbs I with relatively long setae 2 and 3; limb II with a relatively short anterior seta 1, bearing fine setules and 10–11 setae of filter plate of gnathobase; limb III with seta 2 of exopod III bearing medium-sized setules; seta 2 on exopodite III longer than seta 4; seta 3 on inner distal portion of moderate size; limb V with projected inner distal portion.

Juvenile female and male of first instar without a neck tooth.

Ephippial female with straight dorsal margin of valves; ephippium with two resting eggs, axes of which are perpendicular to its dorsal margin; egg chambers not separated from each other; posterodorsal portion of valves with caudal spine incorporated into ephippium.

Adult male with dorsal margin of valves almost straight, not elevated above head; depression between head and valves shallow; head with a well-developed rostrum, without a supra-occular depression. No setae and even setules on inner face of posterior margin. Abdomen with first and second processes as rounded mounds. Postabdomen with maximum height in its middle; postanal angle projected. Gonopore opens subdistally, without a genital papilla. Postabdominal claw as in female. Antenna I with notably small antennular seta, located far from distal end of antenna I body; male seta (flagellum) long, bisegmented; its distal segment naked, with a hooked tip. Limb I with ODL bearing a rudimentary seta and a large seta supplied with minute setules distally; on endite 3 both setae 2 and 2′ are relatively long. Limb II distal-most endite with a short, hook-like anterior seta 1, with setulated distal segment, along one side its basal-most setules are markedly robust.

Size: Female ≤ 1.19 mm; adult male ≤ 0.91 mm.

Full description

Adult parthenogenetic female: Body subovoid in lateral view; maximum height in middle of valves (Fig. 5A). Dorsal margin of valves slightly elevated above head, slightly and regularly convex; a depression between head and rest of body almost smoothed. Posterodorsal angle with a short caudal spine; ventral margin convex. Head relatively large, lacking an anterior crest, with a short rostrum, its tip slightly bent anteriorly; in lateral view, the tip subdividing into two lobes by a 'line' of prerostral fold, with posterior lobe always larger than anterior one (Fig. 5B–D); posterior margin of head with a regularly arched projection, no deep incision between antenna I and labrum base; ventral margin of head slightly concave. No crest or helmet on head; compound eye large; ocellus small and located far from base of antenna I. Labrum with a fleshy main body and a large, setulated distal labral plate (Fig. 5C). Carapace subovoid, with the spinules present only on caudal spine; sometimes one or two spinules located at posterior-most portion of dorsal margin. In posterior portion of valve, on inner face of valve, only a row of minute setules, but any setae absent (Fig. 5F).

Abdomen relatively short, consisting of four segments. The first (basal-most) abdominal process thick, almost straight, directed anteriorly; the second (middle) process short, bent distally; the third (distal-most) process as a massive mound on the segment; on all processes there are rare, fine setules. The fourth segment lacks a process (Fig. 5G, I). Postabdomen elongated, tapering distally, with ventral margin straight or slightly concave and lacking setules. Preanal margin long, almost straight or slightly convex,

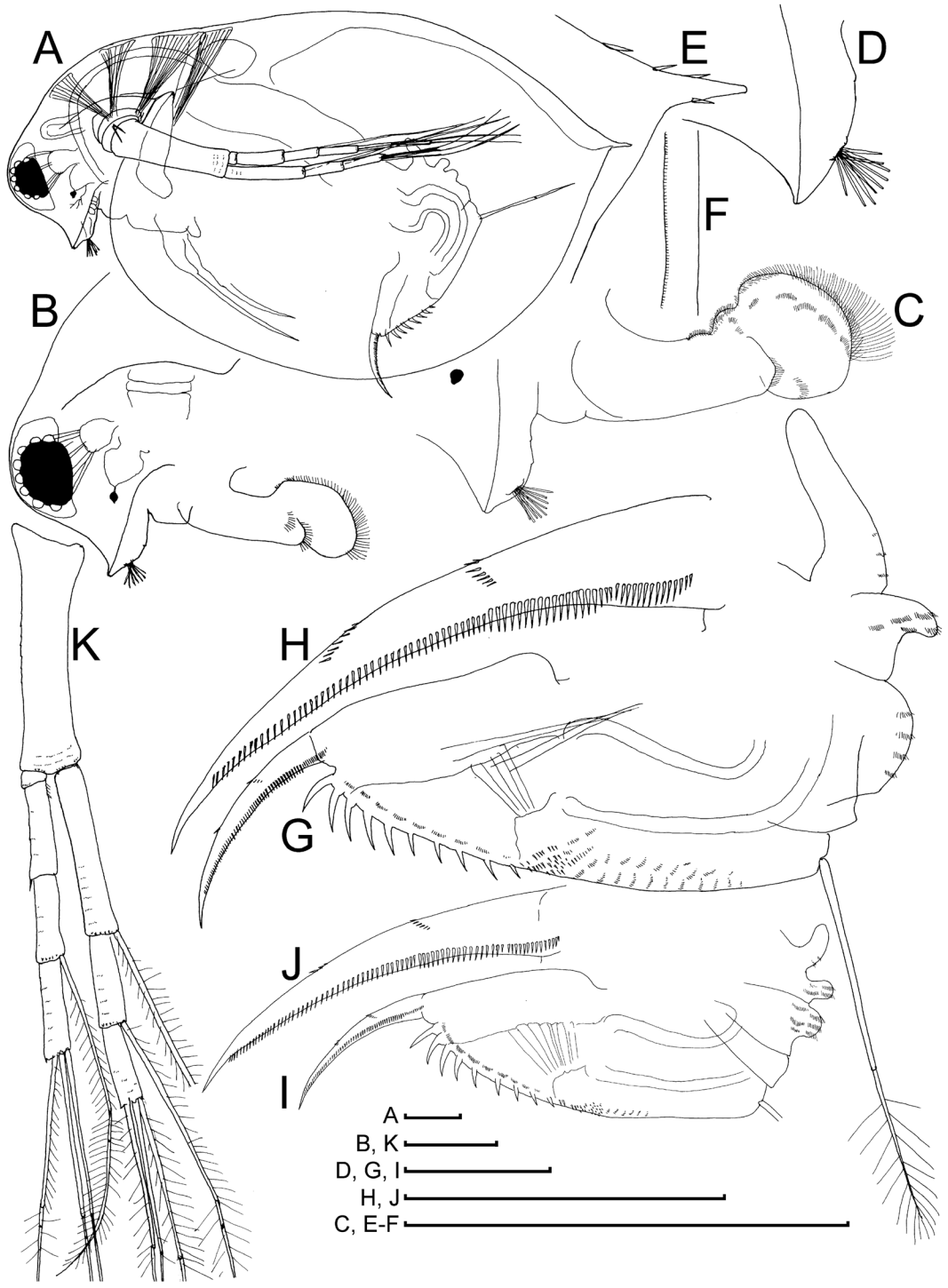

Figure 5. ***Daphnia ishidai***, parthenogenetic female from Otori ike, Honshu Island, Japan. A, large female, lateral view. B, head. C, rostrum, antenna I and labrum. D, posterior head margin. E, caudal spine. F, armature of posterodorsal margin of valve. G, H, postabdomen of large female and its claw. I, J, postabdomen of smaller adult female and its claw. K, antenna II. Scale bars denote 0.1 mm.

with series of minute setules. Preanal and postanal angles not expressed. Paired spines on postanal and anal portion, with their size continuously increasing distally. Postabdominal seta longer than preanal margin, with its distal segment shorter than the basal one. Postabdominal claw long, regularly bent, with a

pointed tip (Fig. 5H). On outer side, three successive pectens along the dorsal margin: the first (proximal) pecten consisting of stout, relatively short teeth; the second (medial) pecten consisting of 15–20 somewhat larger teeth; the third pecten consisting of numerous, rough denticles of size less than two times smaller than those in the second pecten, not reaching the tip of claw. Fine denticles at middle of ventral margin and at distal end of medial pecten. In smaller adult females, abdominal processes shorter (Fig. 5I), and difference in size between denticles in second and other pectens (Fig. 5J) on postabdominal claws smaller than in adult.

Antenna I with completely reduced body; nine aesthetascs (of different length) arising immediately from head surface, but an antennular sensory seta is not found (Fig. 5C, D). Antenna II (Fig. 5A, K) with coxal part possessing two short sensory setae of different length. Basal segment elongated, with no distal spine at its anterior face, but a relatively long distal sensory seta with pointed tip on its posterior face (Fig. 6A). Antennal branches elongated, with four-segmented exopod slightly shorter than three-segmented endopod, all with series of minute denticles. Antennal formula: setae 0-0-1-3/1-1-3. Each swimming seta with basal and distal segments bilaterally setulated; a chitinous insertion within distal segment near joint with basal segment (Fig. 6B). Spines on apical segments rudimentary, and spine on the second segment of exopod rudimentary (Fig. 5K).

Limb I without an accessory seta; outer distal lobe (Fig. 6C: ODL) with a long seta unilaterally armed distally with short setules and a short, thin seta bilaterally setulated distally (Fig. 6D); inner distal lobe (Fig. 6C: IDL) or endite 4, with a single, long anterior seta (1), bearing short setules distally (Fig. 6E). Endite 3 with a long anterior seta (2), armed with minute setules (Fig. 6F) and two posterior setae (a and b). Endite 2 with a short and thin anterior seta (3), armed with minute setules (Fig. 6G) and two posterior setae (c and d). Endite 1 with a small anterior seta (4), armed with minute setules (Fig. 6H) and four posterior setae (e–h). Two ejector hooks of different length. Limb II with an ovoid epipodite; distal portion as a large lobe bearing two soft, setulated seta. Four endites supplied *in toto* by five setae, among them, a stiff, anterior seta (Fig. 6I: 1), about half to two-thirds the length of other setae on distal-most endite, unilaterally setulated by fine setules distally (Fig. 6J). Gnathobase with two clear rows of setae: four anterior setae (Fig. 6K: 1–4) and ten or 11 posterior setae of gnathobasic 'filter plate' (Fig. 6I: a–k), with seta 4 longer than half of seta c or d. Limb III with a subglobular epipodite and a flat exopodite bearing four distal (Fig. 6M: 1–4) and two lateral (5 and 6) setae; seta 2 longer than seta 4, with relatively long setules distally. Inner distal portion of limb with four endites: endite 4 with a single anterior seta (Fig. 6N: 1) and a posterior (a) seta; endite 3 with a single anterior seta (2) and a single posterior (b) seta; endite 2 with an anterior seta (3) of moderate size and two posterior setae (c and d); endite 1 with a large anterior seta (4) and four posterior setae (e–h). The rest of limb inner distal portion as a singular large lobe, modified gnathobase, bearing numerous filtering setae and a single, relatively long anterior seta (Fig. 6N: 1) in its distal corner. Limb IV with a setulated pre-epipodite, ovoid epipodite and wide, flat exopodite, with protruding and setulating inner distal angle and bearing four distal (Fig. 6O: 1–4) and two lateral (5 and 6) setae. Inner distal portion of this limb with completely fused endites, distally with two setae of unclear homology (Fig. 6O); the greater part of the limb inner margin is a gnathobase filter plate consisting of numerous filtering setae. Limb V with a setulated pre-epipodite, subovoid epipodite, triangular exopodite supplied with two small distal setae (Fig. 6R, S: 1 and 2) and a large lateral seta (3). Inner limb portion as an ovoid flat lobe, with setulated inner margin and a single, large seta.

Juvenile female I: Body more elongated, with straight posterior margin and longer caudal spine; spinules cover closest to caudal spine part of dorsal margin and about half of ventral margin (Fig. 7A); no setules at posterior margin. Head with slightly convex ventral margin; rostrum short; dorsal organ in posterior portion of head, with a slight depression posteriorly to it.

Ephippial female: Dorsal margin of valves straight (Fig. 7I); dorsal wall of carapace additionally chitinized, forming a dorsal plate that bears fine spinules along its length (Fig. 7J). Ephippium with two resting eggs, axes of which perpendicular to its dorsal margin; egg chambers not separated from each other; most of ephippium also darkly pigmented and covered with sculpturing of polygonal cells; posterodorsal portion of valves with caudal spine incorporated into ephippium.

Juvenile male I (Fig. 7B): Similar to female I, but with a short, massive antenna I, bearing terminal aesthetascs and sensory seta (Fig. 7C).

Male of prereproductive instar (Fig. 7D): With a subovoid body; dorsal margin of valves almost straight, not elevated above head; rudimentary depression between head and valves; posterodorsal angle with a short caudal spine. Head with a well-developed, rounded rostrum. Anterior-most extremity occupied with optic vesicle, with no supra-occular depression posterior to it. Eye large; ocellus small. Valve with anteroventral angle not prominent; small denticles at ventral margin, but no setae. No setules at posterior margin.

Abdomen with a process on second (from distal end) segment. Postabdomen shape and armature in general as in female, but postanal angle projected

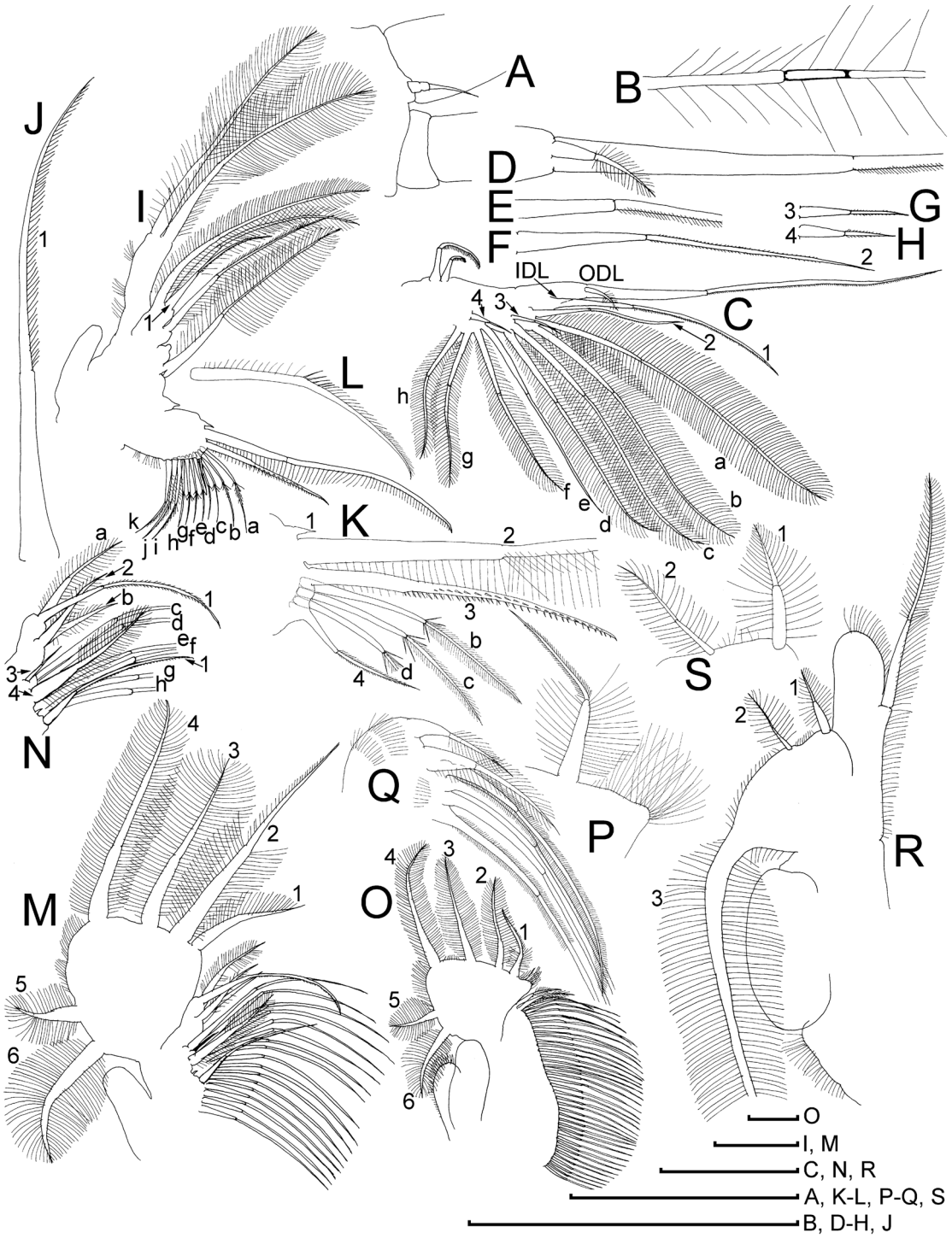

Figure 6. ***Daphnia ishidai***, head and thoracic appendages of parthenogenetic female from Otori ike, Honshu Island, Japan. A, distal sensory seta on proximal segment of antenna II. B, apical swimming seta. C, limb I. D, setae on its outer distal lobe. E, seta on inner distal lobe. F–H, setae 2, 3 and 4. I, limb II. J, stiff anterior seta 1 on its inner distal portion. K, gnatobase II. L, proximalmost seta of gnathobase filter plate. M, limb III; proximal third not shown. N, inner distal portion of limb III. O, limb IV. P, inner corner of its exopodite. Q, inner distal portion. R, S, limb V and distal portion of exopodite. Scale bars denote 0.1 mm.

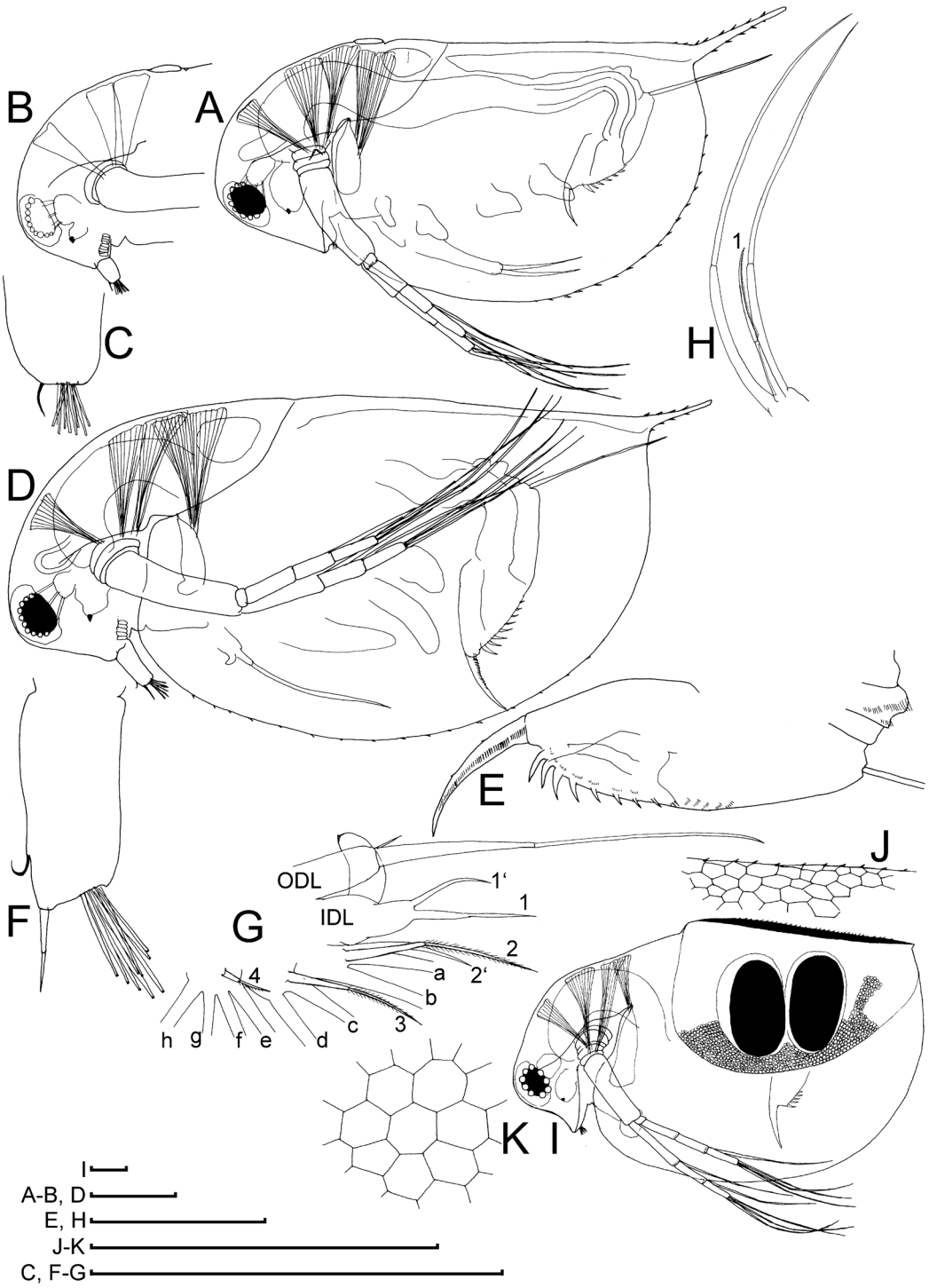

Figure 7. ***Daphnia ishidai*** from Otori ike, Honshu Island, Japan. A, juvenile female of instar I. B, C, juvenile male of instar I and its antenna I. D, pre-adult, male. E, its postabdomen. F, antenna I. G, limb I. H, inner distal portion of limb II. I, ephippial female. J, dorsal portion of ephippium. K, reticulation on ephippium. Scale bars denote 0.1 mm.

(Fig. 7E). Position of gonopore unclear. Spinules in second pecten on postabdomen subequal in size to other setules. Postabdominal claws with three pectens of relatively rough setules, among which setules in third (distal) row only somewhat shorter than the rest.

Antenna I short, without setules; antennular sensory seta thin, short (Fig. 7F); aesthetascs of different length,

but longer than antenna I maximum diameter. Male seta short, bisegmented, and located on top of a conical, distal (postaesthetasc) process, its tip naked.

Limb I with ODL large, bearing a rudimentary seta and a large seta (Fig. 7G) without setules distally; IDL with a bent copulatory hook and two setae of different size (1 and 1′); in contrast to female, endite 3 with four setae (additional seta of unclear homology marked as 2′), seta 3 larger than in female. Limb II with distal-most endite bearing anterior seta 1, setulated distally, with length about one-third the length of other setae (Fig. 7H: 1).

Adult male: Body low; dorsal margin of valves almost straight, not elevated above head; depression between head and valves shallow; posterodorsal angle distinct, with a short caudal spine (Fig. 8A). Head with a moderate rostrum; region of antenna I joint with a special depression (Fig. 8B, C); posterior margin slightly convex. No supra-occular depression; eye large; ocellus small. Valve with anteroventral angle distinctly prominent ventrally; whole ventral margin with numerous setae, located submarginally (on inner face of valve) in anterior and posterior portions of valve (Fig. 8E). No setae and even setules on inner face of posterior margin (Fig. 8F).

Abdomen with reduced processes; only a small mound present on first segment (counting from basal end); process on second segment small (Fig. 8G, H). Postabdomen with maximum height in its middle; postanal angle well expressed. Gonopore opens subdistally, without a genital papilla. On outer surface of postabdominal claws, all three pectens consist of thin setules (Fig. 8I).

Antenna I long, almost straight (Fig. 8B, C); antennular seta small (length about half diameter of antenna I), located far from distal end of antenna I body; aesthetascs of different length; among them, largest aesthetasc 1.5 times longer than antenna I maximum diameter. Male seta (flagellum) on top of a conical, distal (postaesthetasc) process. This seta long, bisegmented; its distal segment naked, with a hooked tip (Fig. 8J).

Limb I: ODL large, cylindrical (Fig. 8K: ODL), bearing a rudimentary seta and a large seta supplied with minute setules distally (Fig. 8L); IDL with a bent copulatory hook and two setae of different size (Fig. 8K: 1 and 1′); in contrast to female, endite 3 with four setae (additional seta marked as 2′), both setae 2 and 2′ relatively long; seta 3 remarkably larger than in female; seta 4 somewhat larger than in female. Limb II: distal-most endite with a short, hook-like anterior seta 1, with setulated distal segment, along one side; basal-most setules are notably robust (Fig. 8N, O).

Size: Holotype 0.91 mm; parthenogenetic females 0.58–1.19 mm (N = 50); ephippial females 0.98–1.10 mm (N = 5); juvenile males 0.56–0.82 mm (N = 10); adult male 0.91 mm (N = 1).

Comments: The population from Otori-Ike was previously determined by us to be *D.* cf. *morsei* Ishikawa, 1895 based exclusively on female characters (Kotov *et al.*, 2006). Our subsequent finding of adult males demonstrated that the species from Otori-Ike is new to science. No *D. curvirostris*-like species was described from Japan or any other nearby regions except for *D. tanakai* and *D. sinevi*, differences from which are given in the key.

Three species were described by Ishikawa from Japan: *Daphnia morsei* Ishikawa, 1895, *Daphnia whitmani* Ishikawa, 1895 and *Daphnia mitsukuri* Ishikawa, 1896 (Ishikawa, 1895a, b, 1896a). The last of these is obviously a member of the *Daphnia obtusa* Kurz, 1875 group, taking into consideration a series of setae on the valve ventral margin (Ishikawa, 1896a: plate 11, fig. 1). Unfortunately, the type localities of Ishikawa's species are not likely to exist today, and the author's descriptions and illustrations are not detailed enough to formulate an accurate diagnosis of these taxa (Ishida *et al.*, 2006). At the same time, Kotov & Taylor (2010) found two *Daphnia* lineages that were morphologically similar to *D. morsei* and/or *D. whitmani* at a single locality in Japan. But now it is obvious that the aforementioned lineages belong to the *D. pulex* group (Kotov & Taylor, 2010).

In contrast, *D. ishidai* obviously belongs to the *D. curvirostris* group, which is a part of the *Daphnia longispina* (O.F. Müller, 1776) complex. *Daphnia ishidai* differs from *D. tanakai*, another Japanese *D. curvirostris*-like taxon, in having a long distal sensory seta on the basal segment of antenna II in the female and a well-developed rostrum in the male and differs from *D. sinevi* having a regularly curved posterior margin of the head, with completely reduced body of antenna I and straight dorsal margin of ephippium. Among all well-described species of *Daphnia* (from any group), *D. ishidai* is unique in having completely reduced setae and particularly small setules at the inner side of the posterior valve margin.

For identification of the daphniid taxa in Japan, it is important that both *D. morsei* and *D. whitmani* were found in small ponds or pools. They also have a characteristically large size (≤ 4 mm including caudal spine in *D. morsei*) and a dorsal and ventral margin covered with spinules. In contrast to *D. ishidai*, the adult males of *D. morsei* have a rudimentary rostrum and a concave preanal margin of the postabdomen, whereas the adult males of *D. whitmani* have a long sensory seta on antenna I, reaching the base of the male seta (flagellum). No other habitually similar forms were described from Japan or nearby regions (with the exceptions of *D. tanakai* and *D. sinevi*).

Distribution: The taxon is known only from a single lake in Honshu Island, Japan, although many, if not most, lakes of Japan were sampled by S. Ishida and other Japanese hydrobiologists (Ishida *et al.*, 2011;

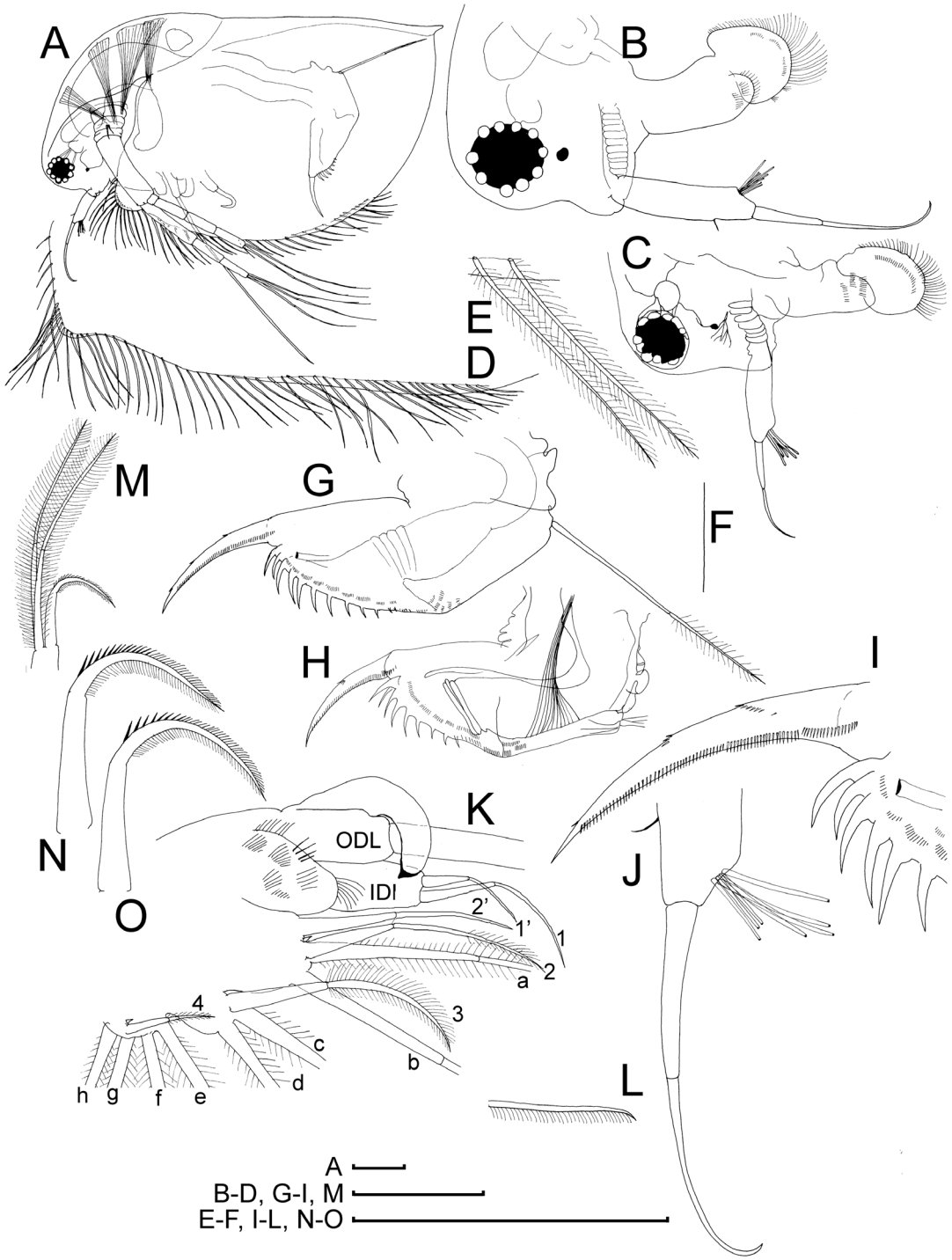

Figure 8. ***Daphnia ishidai***, adult male from Otori ike, Honshu Island, Japan. A, general view. B, C, head, lateral view. D, ventral margin of valve. E, setae at posterior portion of ventral margin. F, posterior margin of valve. G, H, postabdomen. I, its distal portion. J, distal portion of antenna I. K, limb I with outer distal lobe (ODL) and inner distal lobe (IDL) marked. L, distal portion of seta of its outer distal lobe. M, inner distal portion of limb II. N, O, stiff seta of inner distal portion of limb II. Scale bars denote 0.1 mm.

So *et al.*, 2015; Tokishita *et al.*, 2017). Apparently, this is a micro-endemic species, possibly inhabiting only a single mountain lake in Japan.

DAPHNIA KOREANA SP. NOV.

(FIGS 9–13)

LSID: urn:lsid:zoobank.org:act:6ABA6D42-8CC6-4342-A7A5-2EC0F4732A43

Daphnia sinevi Kotov, Ishida & Taylor in Jeong *et al.*, 2014: 219.

Daphnia sp. nov., clade L in Kotov & Taylor, 2019: figs 1, 2.

Etymology: The taxon is named for Korea, where this species was found; originally from Korean 고려, *Koryŏ*.

Type locality: A pond in Deok Seong (wetland) (36.51391°N, 127. 2669°E), Chuncheongnam-do, South Korea. The type series was collected on 17 September 2011 by H. G. Jeong and A. A. Kotov.

Holotype: An adult male, NIBRIV0000835125.

Allotype: A parthenogenetic female, NIBRIV0000835126.

Paratypes: Twenty parthenogenetic females, NIBRIV0000835127. Twenty adult males, NIBR NIBRIV0000835128. Twenty parthenogenetic females, NIBRIV0000835129. Ten parthenogenetic females, MGU Ml181. The rest of the females and males, AAK M-2098.

Other material excluded from type series (other date of collection): Many parthenogenetic females from type locality collected on 4 April 2012 by H. G. Jeong, A. A. Kotov, M. A. Gololobova and M. A. Kotova.

Short diagnosis: Parthenogenetic female. Body subovoid; caudal spine of moderate length (Fig. 9A). Head relatively large, with a low anterior crest; head posterior margin with a strong, arched projection, with a deep incision between antenna I and labrum base (Fig. 9B–D). Rostrum relatively short (as a result, tips of longest aesthetascs almost reach its tip); rostrum tip slightly bent posteriorly and subdividing into two lobes by a 'line' of prerostral fold, with posterior lobe always larger than anterior one. Spinules occupy less than half of dorsal and ventral valve margin. In posteroventral portion of valve, on inner face of valve, there are fine setae with setules between them (Fig. 9E–I); no setules near caudal spine base (Fig. 9J, K). First abdominal process almost straight, directed anteriorly (Fig. 9L); second process short, bent distally; third process as a massive mound on the segment. Postabdomen with a smooth postanal angle. Postabdominal claw with first pecten: first (proximal-most) consisting of relatively short, rough teeth; second pecten consisting of seven or eight large teeth; third pecten consisting of numerous, fine setules (Fig. 9L–N). Body of antenna I completely reduced; antennular seta arising immediately from head surface; aesthetascs protruding posteroventrally, with their tips almost reaching tip of rostrum (Fig. 9D). Antenna as in previous species (Fig. 10A–E). Limb I with a relatively long seta 3 (Fig. 11A); limb II with an anterior seta 1 about two-thirds of the length of other setae, bilaterally setulated distally and 11–12 setae of filter plate of gnathobase (Fig. 11D); limb III with seta 2 of exopod longer than seta 4, bearing short setules (Fig. 11C); seta 3 on inner distal portion of limb of a moderate size (Fig. 11D, E); limb IV (Fig. 11F) as in previous species; limb V (Fig. 11G) as in previous species.

Juvenile female I (Fig. 10G, H) with a single necktooth.

Ephippial female with straight dorsal margin of valves; ephippium with two resting eggs, axes of which are perpendicular to its dorsal margin; egg chambers not separated from each other; posterodorsal portion of valves with caudal spine incorporated into ephippium (Fig. 10I, J).

Adult male with dorsal margin of valves straight, not elevated above head; depression between head and valves shallow (Fig. 12A); head with a well-developed rostrum (Fig. 12B, C), without a supra-occular depression. Setulation of ventral margin and denticles on valves as in previous species (Fig. 12D–J). Both setae and series of setules on inner face of posterior margin (Fig. 12G). Abdomen first and second processes with smooth mounds; postabdomen with maximum height in its middle; postanal angle not expressed (Fig. 12K, L). Gonopore opens subdistally, without a genital papilla. Postabdominal claw as in female (Fig. 12M-N). Antenna I with a small antennular seta, located far from distal end of antenna I body; male seta (flagellum) long, with its distal segment naked, slightly bent (Fig. 12K). Limb I with ODL bearing a rudimentary seta and a large seta (Fig. 13A) supplied with minute setules distally (Fig. 13B); copulatory hook thick, with a tooth at tip (Fig. 13C, D). Limb II distal-most endite with a short, hook-like anterior seta 1, with setulated distal segment (Fig. 13E, F). Juvenile male (Fig. 13G–I) with a necktooth.

Size: Female 0.8–2.04 mm; male 0.8–1.21 mm.

Distribution: The species was found in only a single pond in South Korea, although samples from 438 localities were investigated. Unfortunately, the type locality has since been destroyed owing to urbanization

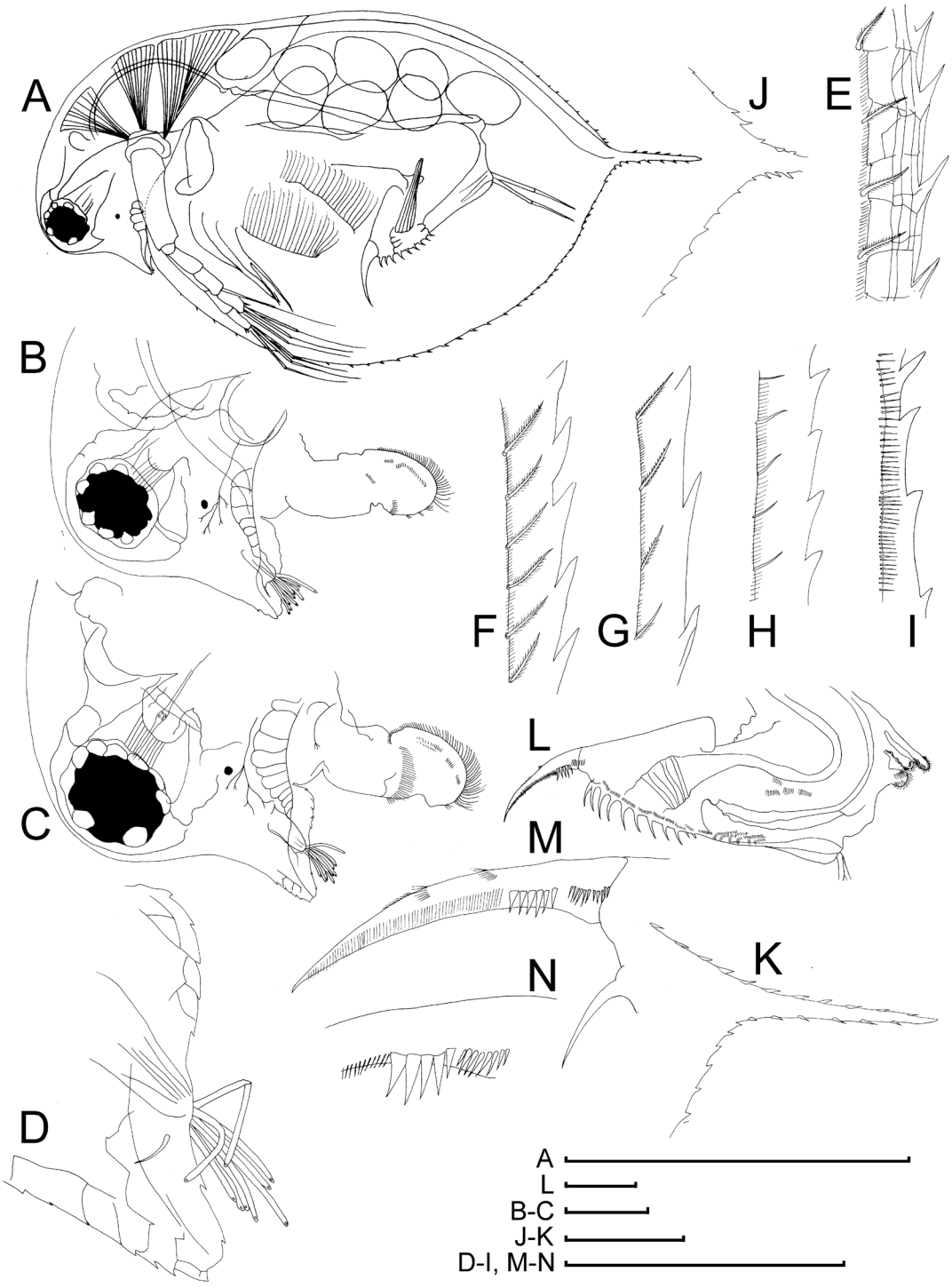

Figure 9. ***Daphnia koreana***, parthenogenetic female from a pond in Deok Seong wetland, Chuncheongnam-do, South Korea. A, large female, lateral view. B, C, head. D, rostrum and antenna I. E–I, armature of posterodorsal margin of valve. J, K, base of caudal spine. L, abdomen and postabdomen of large female. M, N, its claw. Scale bars denote 1 mm for A and 0.1 mm for B–N.

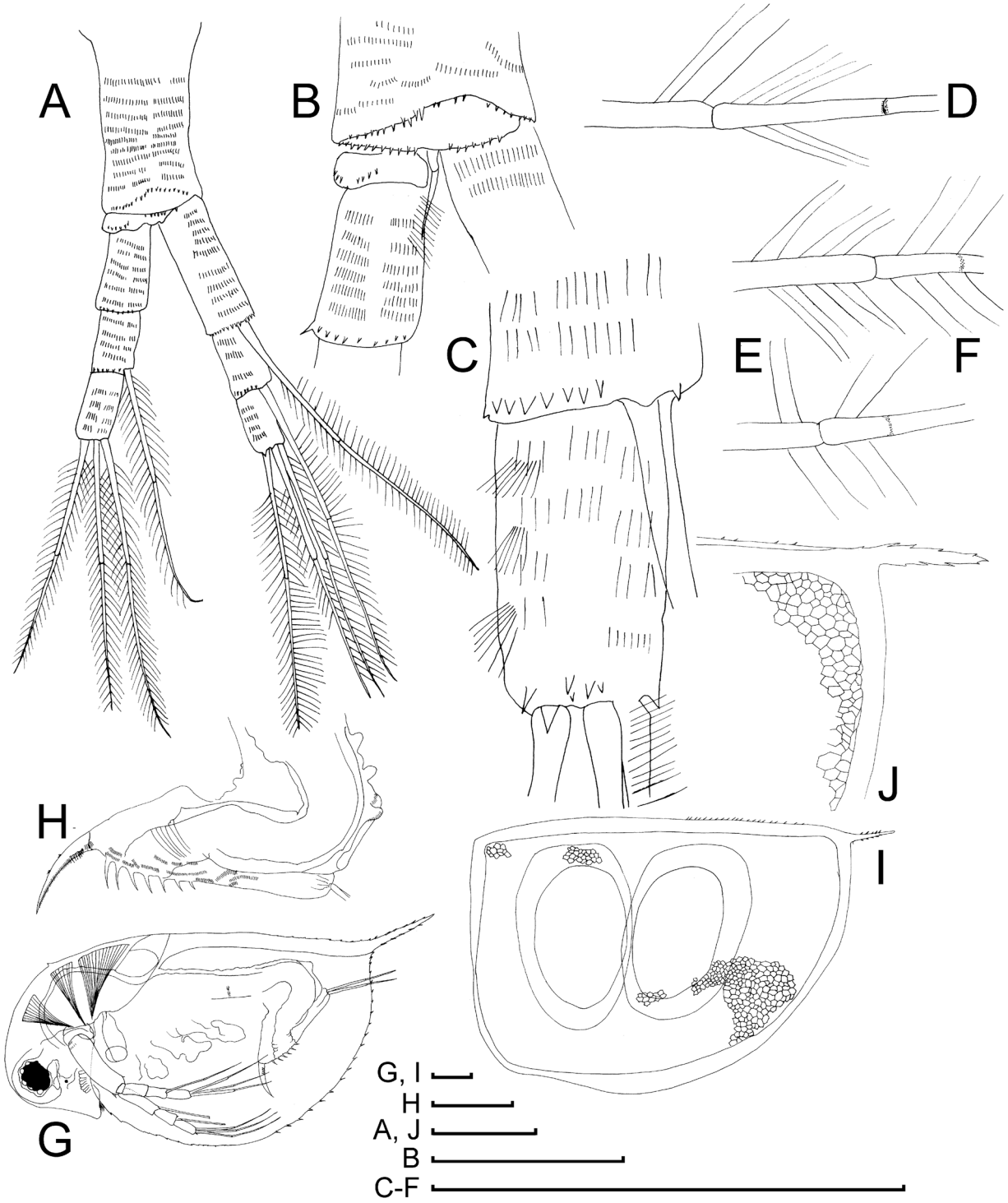

Figure 10. ***Daphnia koreana***, females from a pond in Deok Seong wetland, Chuncheongnam-do, South Korea. A, antenna II of large adult parthenogenetic female. B, distal portion of its basal segment. C, apical segment of antenna II endopod. D–F, apical swimming setae. G, juvenile female. H, its postabdomen. I, ephippium. J, its posterior portion. Scale bars denote 0.1 mm.

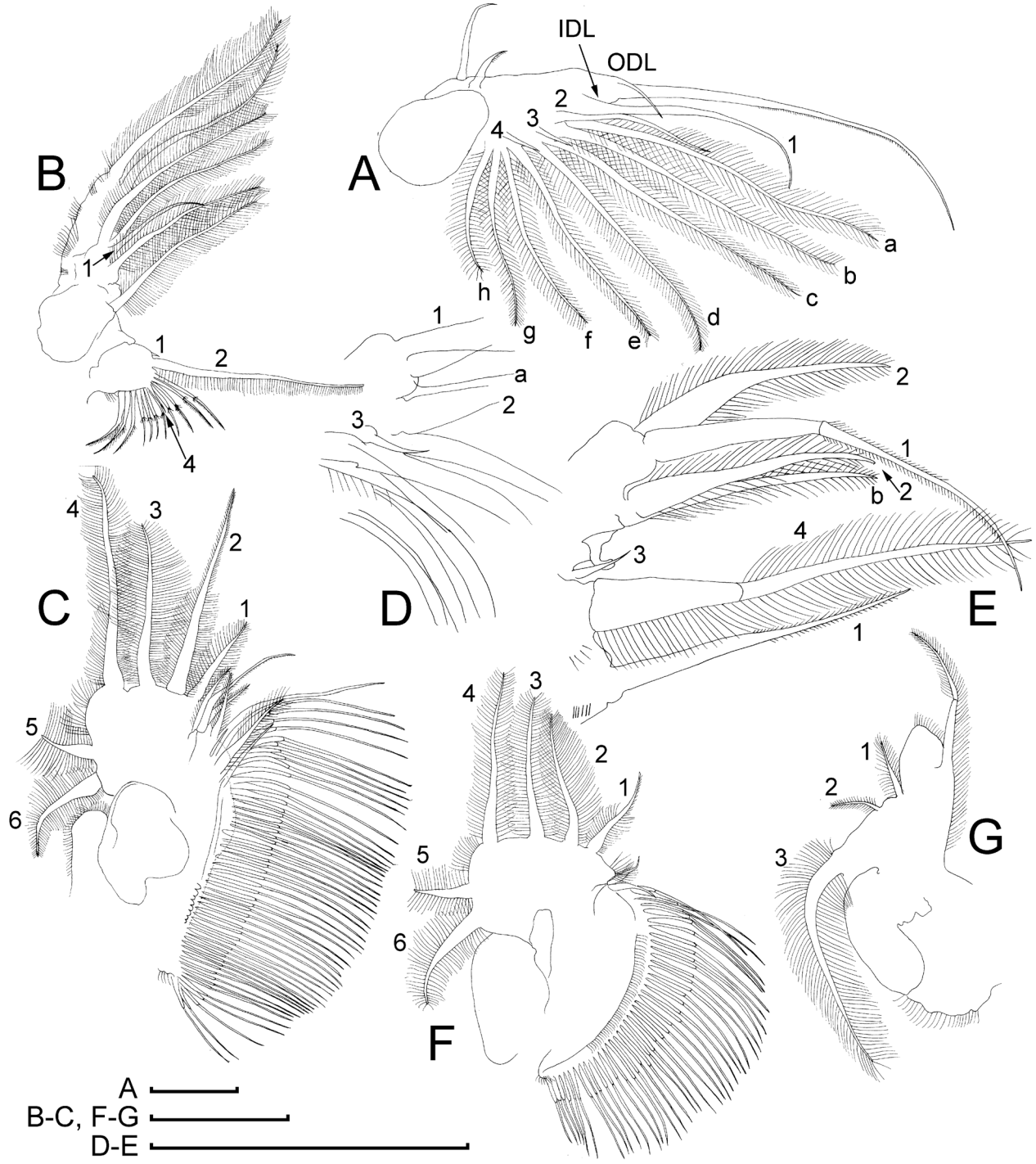

Figure 11. ***Daphnia koreana***, thoracic limbs of parthenogenetic female from a pond in Deok Seong wetland, Chuncheongnam-do, South Korea. A, limb I. B, limb II. C, limb III. D, E, its inner distal portion. F, limb IV. G, limb V. Scale bars denote 0.1 mm.

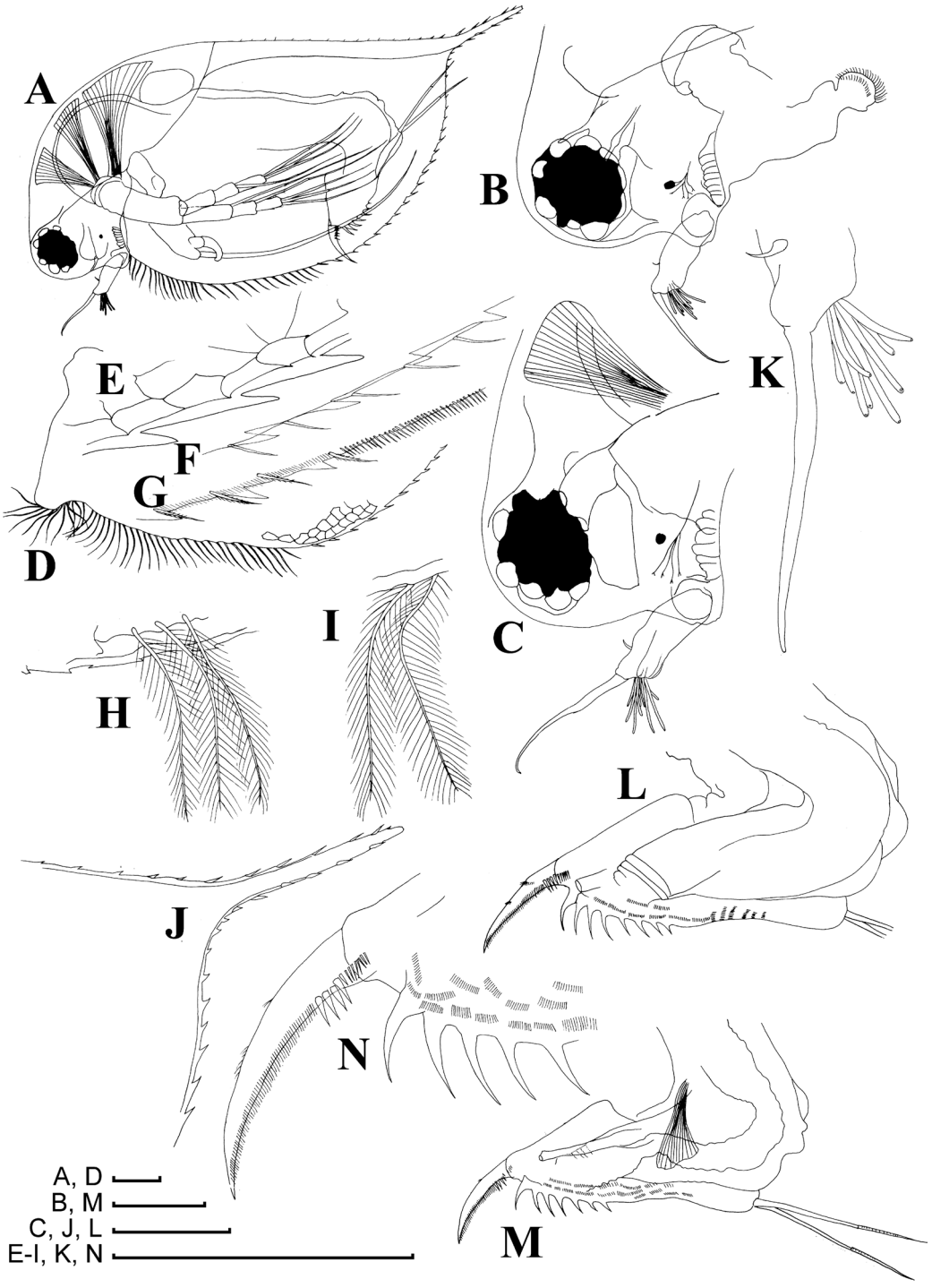

Figure 12. ***Daphnia koreana***, adult male from a pond in Deok Seong wetland, Chuncheongnam-do, South Korea. A, lateral view. B, C, head. D, armature of ventral margin. E–G, armature of posteroventral and posterior margin. H, I, setae at ventral margin. J, base of caudal spine. K, antenna I. L, M, postabdomen and abdomen. N, postabdominal claw. Scale bars denote 0.1 mm.

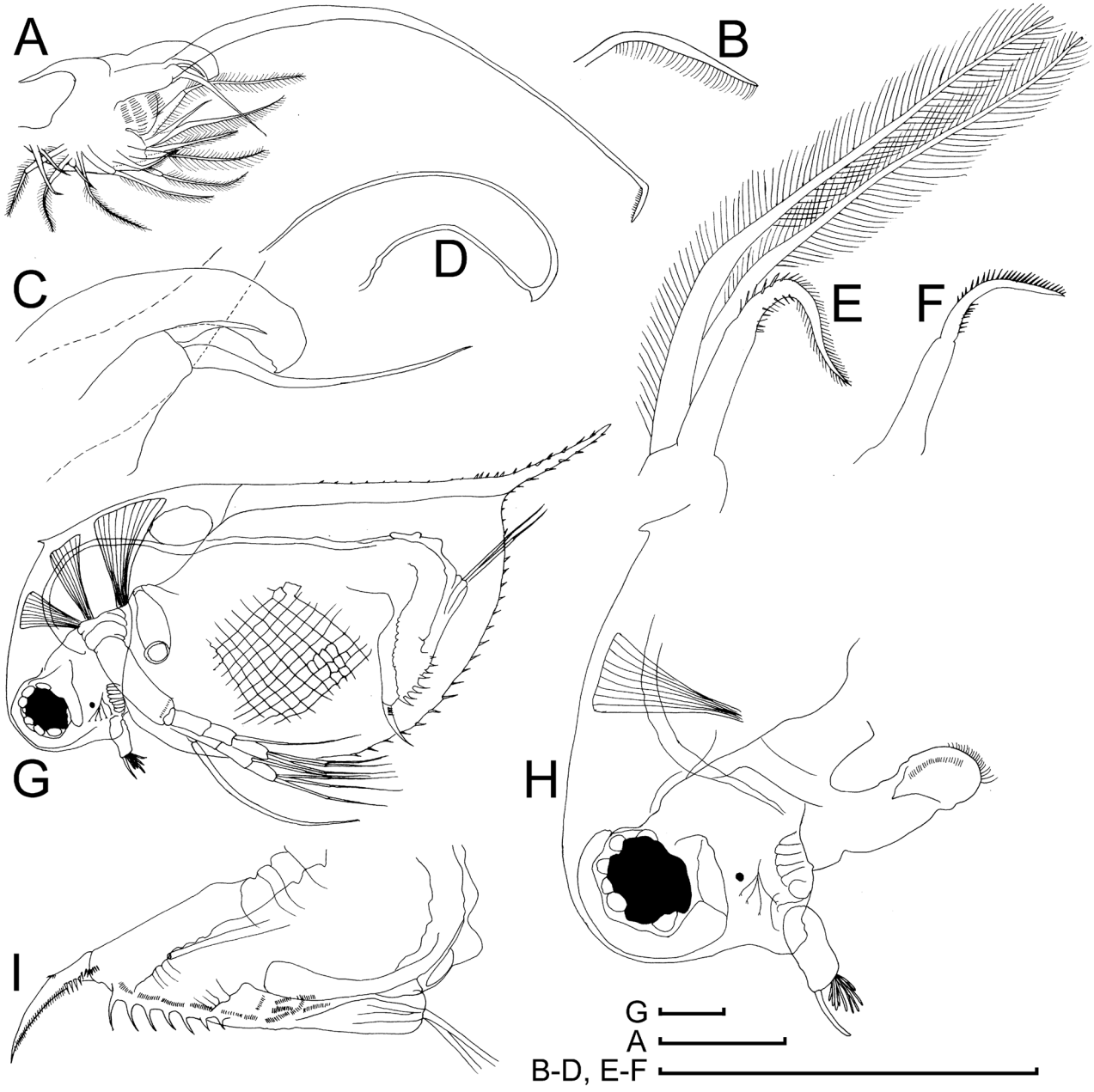

Figure 13. ***Daphnia koreana***, adult (A–F) and juvenile (G–I) male from a pond in Deok Seong wetland, Chuncheongnam-do, South Korea. A, limb I of adult male. B, distal portion of its outer distal lobe seta. C, D, copulatory hook. E, F, stiff seta on inner distal portion of limb II. G, juvenile male, lateral view. H, head. I, postabdomen and abdomen. Scale bars denote 0.1 mm.

in this region. Therefore, this taxon is threatened with extinction (if not already extinct).

DAPHNIA JEJUANA SP. NOV.

(FIGS 14–18)

LSID: urn:lsid:zoobank.org:act:35E53D06-8D20-4440-9227-69F52DE11D56

Daphnia sp. nov., clade K of Kotov & Taylor, 2019: figs 1, 2.

Etymology: The taxon is named after its type locality, Jeju Island (Republic of Korea), from Korean제주**도**, *Jeju-do*.

Type locality: DoSun-cheon pool 1 (33.30593°N, 126.4672°N), Jeju-do, South Korea. The type series was collected on 28 November 2012 by A. A. Kotov and H. G. Jeong.

Holotype: An adult male, NIBRIV0000835132.

Allotype: A parthenogenetic female, NIBRIV 0000835133.

Paratypes: Twenty adult males, NIBRIV0000835135. Twenty parthenogenetic females, NIBRIV0000835134. Ten parthenogenetic females, MGU Ml182. Five adult males, MGU Ml183. Many males, ephippial and parthenogenetic females, AAK M-2556 and AAK M-2557.

Material excluded from type series: many ephippial and parthogenetic females from pond near Dream Forest (33.48783°N, 126.6946°E), collected on 13 February 2012 by H. G. Jeong, AAK M-2353 and AAK M-2355; 20 females from the same locality, NIBRIV0000835130; many males, ephippial and parthenogenetic females from pond near Hallasan (33.43225°N, 126.5983°N), collected on 28 November 2012 by A. A. Kotov and H. G. Jeong, AAK M-2552; 20 females from the same locality, NIBRIV0000835131; many parthenogenetic females from pond in Dream forest (33.48719°N, 126.7031°E), collected on 28 November 2012 by A. A. Kotov and H. G. Jeong, AAK M-2553; many males, ephippial and parthenogenetic females from DoSun-cheon pool 2 (33.30595°N, 126.4658°E), collected on 28 November 2012 by A. A. Kotov and H. G. Jeong, AAK M-3280 and AAK M-3281; a few parthenogenetic females from Billbae pond (33.40374°N, 126.351°E), collected on 28 November 2012 by A. A. Kotov and H. G. Jeong, AAK M-3289; and 20 females from the same locality, NIBRIV0000835136.

Short diagnosis: Parthenogenetic female. Body subovoid; caudal spine of moderate length (Fig. 14A). Head relatively large, with a low anterior crest; head posterior margin with a strong, arched projection; a deep incision between antenna I and labrum base (Fig. 14B–E). Rostrum relatively short (as a result, tips of longest aesthetascs almost reach its tip); rostrum tip slightly bent posteriorly and subdividing into two lobes by a 'line' of prerostral fold, with posterior lobe always larger than anterior one. Spinules occupy less than half of dorsal and ventral valve margin. In posteroventral portion of valve, on inner face of valve, there are fine setae with setules between them (Fig. 14F–K); no setules near caudal spine base (Fig. 14L). First abdominal process almost straight, directed posteriorly (Fig. 14M); second process short, bent distally; third process as a massive mound on the segment. In juveniles, abdominal segments rudimentary (Fig. 14N). Postabdomen with a projected postanal angle (Fig. 14M, N). Postabdominal claw with first pecten: first (proximal-most) consisting of relatively long, thin teeth; second pecten consisting of six to eight large teeth; third pecten consisting of numerous, fine setules (Fig. 14O, P). Body of antenna I completely reduced; antennular seta arising immediately from head surface; aesthetascs protruding posteroventrally, and their tips reach tip of rostrum (Fig. 14E). Antenna as in previous species (Fig. 15A–G). Maxilla I as in previous species (Fig. 16A). Limb I with a relatively long seta 3 (Fig. 15B); limb II with an anterior seta 1 about two-thirds of the length of other setae, bilaterally setulated distally and numerous setae of filter plate of gnathobase (Fig. 16C); limb III with seta 2 of exopod shorther than seta 4, bearing short setules (Fig. 16D); seta 3 on inner distal portion of limb of a moderate size (Fig. 16E); limb IV (Fig. 16F) as in previous species, limb V (Fig. 16G) as in previous species.

Ephippial female with straight dorsal margin of valves; ephippium with two resting eggs, axes of which are perpendicular to its dorsal margin; egg chambers not separated from each other; posterodorsal portion of valves with caudal spine incorporated into ephippium (Fig. 15H, I).

Adult male with dorsal margin of valves straight, not elevated above head; depression between head and valves present (Fig. 17A); head with a well-developed rostrum (Fig. 17B–D), without a supra-occular depression. Setulation of ventral margin and denticles on valves as in previous species (Fig. 17E–I). Only setae on inner face of posterior margin (Fig. 17H, I). Abdomen first and second processes as smooth mounds; postabdomen with maximum height in its middle; postanal angle projected (Fig. 17K, L). Gonopore opens subdistally, without a genital papilla. Postabdominal claw as in female (Fig. 17M). Antenna I with a small antennular seta, located far from distal end of antenna I body; male seta (flagellum) long, with its distal segment naked, slightly bent (Fig. 17B–D, 18A, B). Limb I with ODL bearing a rudimentary seta and a large seta (Fig. 18C) supplied with minute setules distally (Fig. 18D); copulatory hook thin, with a tooth at tip (Fig. 18E, F). Limb II distal-most endite with a short, hook-like anterior seta 1, with setulated distal segment (Fig. 18G).

Size: Female 1–2.27 mm; male 0.85–1.31 mm.

Distribution: *Daphnia jejuana* is endemic to Jeju Island, where it is common in ponds and pools. It has never been detected in large lakes or in co-existence with other *Daphnia* species (e.g. *D.* cf. *obtusa* Kurz, 1874 and *Daphnia sinensis* Gu, Xu, Li, Dumont & Han, 2013) in small water bodies of Jeju Island.

GENETIC ACCOUNT

The GARD test detected no evidence for recombination between phylogenetic lineages of *D. curvirostris* (the results have been deposited to the Open Science Framework, http://osf.io/k9uxf/). Consequently, we

KEY TO *DAPHNIA CURVIROSTRIS*-LIKE TAXA IN FAR EAST ASIA

1. Rostrum of female notably long (as a result, tips of aesthetascs are located far from rostrum tip); sensory seta on male antenna I reaches tip of post-aesthetasc projection ..... *D. curvirostris* group
   Female rostrum short (as a result, tips of longest aesthetascs reach or almost reach its tip); sensory seta on male antenna I does not reach tip of post-aesthetasc projection 2
2. In females, a remainder of the body of antenna I as a low projection ..... *D. sinevi* group
   Body of antenna I completely reduced 3
3. In female, the rostrum not subdivided into two lobes by a 'line' of prerostral fold; posterior margin of valve not incorporated into ephippium; male without a rostrum ..... *D. tanakai*
   In female, the rostrum subdivided into two lobes by a 'line' of prerostral fold; additional characters unknown for *D. korovchiskyi*, but characteristic of other taxa: posterior margin of valve incorporated into ephippium; male with well-developed rostrum 4
4. Female head remarkably small; rostrum tip slightly bent anteriorly; prominence on posterior head margin shallow, with no deep incision between it and labrum; no setae at posteroventral valve margin; postabdominal claw armed with three pectens of relatively rough setules, among which setules in third (distal) row are only somewhat shorter than the rest ..... *D. ishidai*
   Female head relatively large; rostrum tip slightly bent posteriorly, prominence on posterior head margin strong and arched, with a deep incision between it and labrum; setae alternated with series of setules at posteroventral valve margin; postabdominal claw with first pecten of long and thin setules, second pected with strong teeth, third pecten of numerous thin setules 5
5. Female distal-most abdominal projection directed anteriorly; seta 2 on exopodite III longer than seta 4; seta 3 on inner distal portion of limb III rudimentary … *D. korovchinskyi*
   Female distal-most abdominal projection directed posteriorly; seta 2 on exopodite III shorter than seta 4 or subequal in length to it; seta 3 on inner distal portion of limb III short, but not rudimentary 6
6. Postabdomen both in females and males with a projected postanal angle; setules in first pecten of postabdominal claw thin; in male, first (proximal-most) abdominal process projected ..... *D. jejuana*
   Postabdomen both in females and males with smooth postanal angle; setules in first pecten of postabdominal claw rough; in male, first (proximal-most) abdominal process smooth ..... *D. koreana*

ignored recombination in subsequent analyses (F_S test and R_2 statistics). The MEME analyses indicated significant episodic positive selection at the *ND2* locus, position 3 (isoleucine–leucine substitution) and at the *COI* locus, position 3 (alanine–valine substitution) (results have been deposited to Open Science Framework, http://osf.io/k9uxf/). It is known that substitutions in the active centres of the molecules, specially for non-homologue amino acids, are more important for phylogenetic reconstructions (Echave *et al.*, 2016). In our cases, in *COI* we observed a substitution of the homologues and in *ND2* a substitution of isomers; such events do not change the molecule conformation, and the chance of a competitive advantage of such variants is low. Moreover, the topology of the ML trees of *COI* and *ND2* did not change after the exclusion of the nucleotides in the third position from the alignment. We therefore ignored the influence of selection in subsequent analyses.

Our coalescent simulation in DnaSP v.6 with ten replications for all loci demonstrated that the most probable demographic model of the *D. curvirostris* group was the 'Population split or admixture' (results have been deposited to Open Science Framework, http://osf.io/k9uxf/), in agreement with the conclusion of Kotov & Taylor (2019). This demographic structure had to be taken into consideration in all subsequent analyses.

Substitution models for all loci are represented in Table 2. All selected models demonstrated convergence according to the BIC and AICc, providing additional evidence for model fit (Posada & Buckley, 2004). For the protein-coding loci, the second codon position is usually more conservative (Perlwitz *et al.*, 1988). We also tested more complicated (mixed) models with different base substitution rates for different codon positions in protein-coding genes. We did not find any significant differences in the topology of the trees using mixed models (ML) and unlinked data with separation of the codon position (BI).

Phylogenetic results based on different genes gave similar results. The phylogeny based on each gene separately and on its combinations revealed five main clades (1–5), whereas the number of well-recognized subclades (A–L) was somewhat different in different analyses:

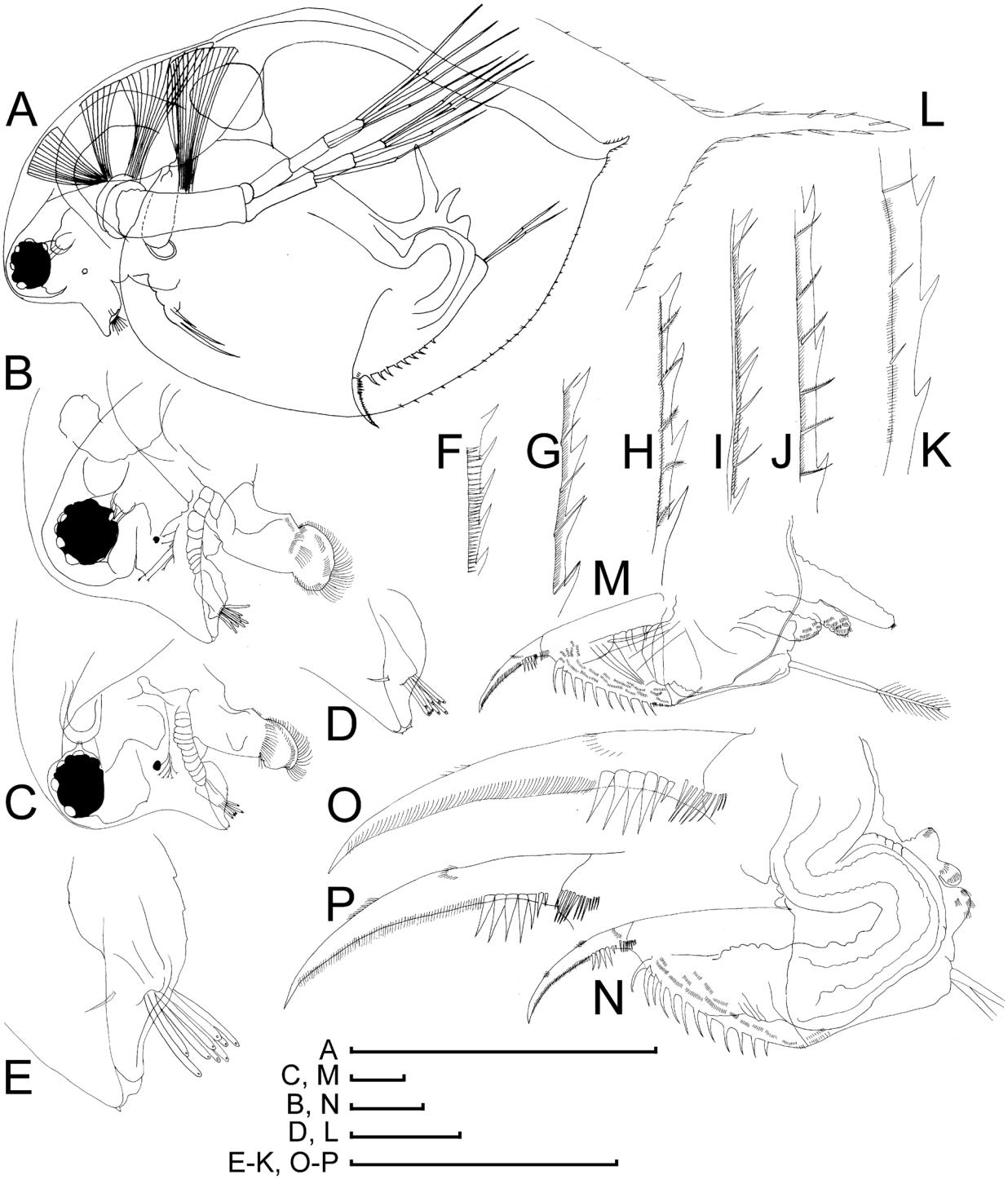

Figure 14. ***Daphnia jejuana***, parthenogenetic female from DoSun-cheon pool 1, Jeju-do, South Korea. A, large parthenogenetic female, lateral view. B, C, head. D, E, rostrum. F–K, armature of posteroventral margin. L, base of caudal spine. M, N, abdomen and postabdomen. O, P, postabdominal claw. Scale bars denote 1 mm for A and 0.1 mm for B–P.

1. The *Daphnia curvirostris* group is indicated by red symbols in Figures 1, 19 and 20. Subclade 'A' (*D. curvirostris s.s.*) has a broad distribution in the Northern Palaearctic (Fig. 1), from Europe to Yakutia. The Mexican population also belongs here, supporting a Palaearctic origin hypothesis. No additional populations are added here in comparison to Kotov & Taylor (2019), but new genes are added.

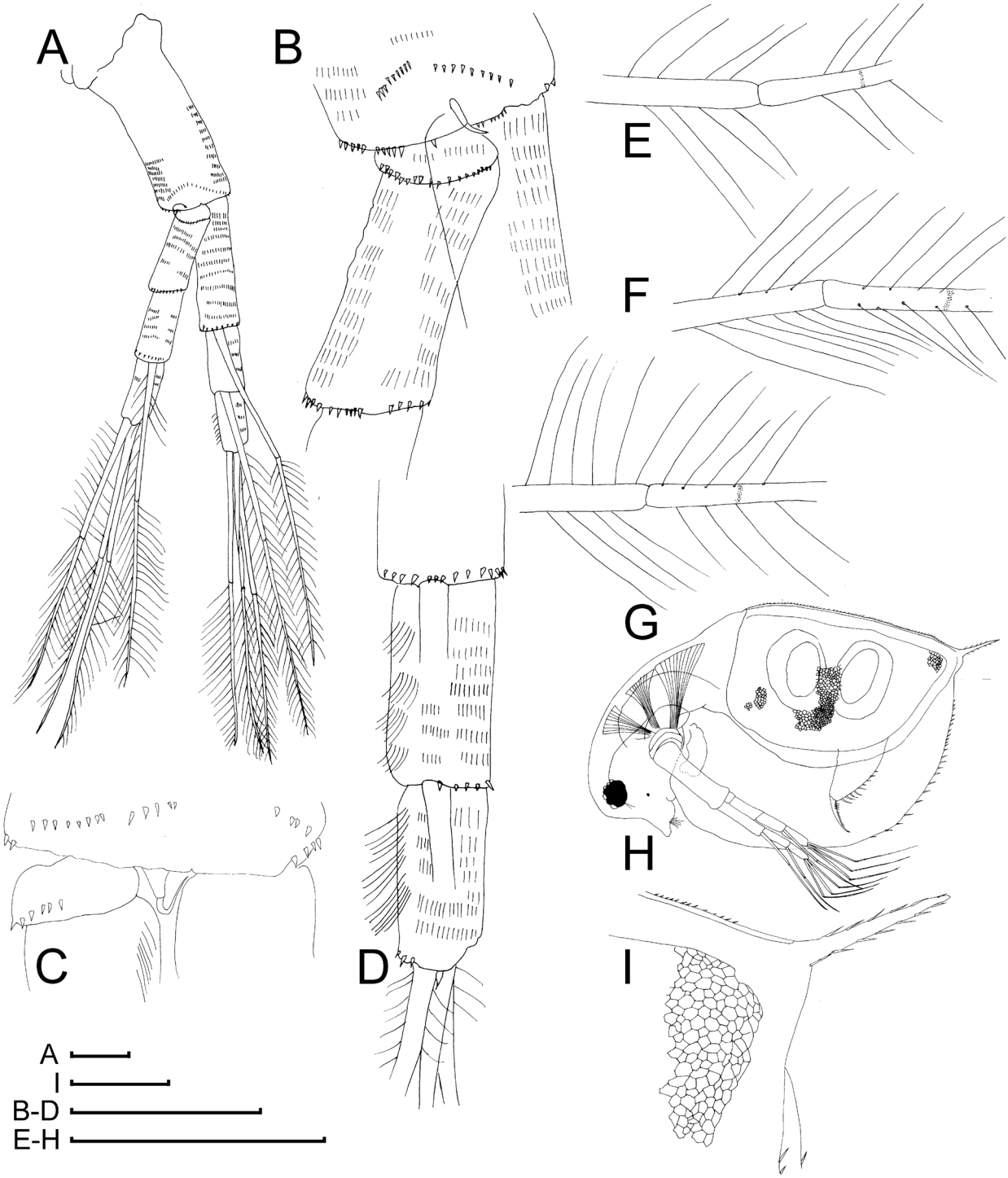

Figure 15. ***Daphnia jejuana***, female from DoSun-cheon pool 1, Jeju-do, South Korea. A, antenna II of large parthenogenetic female. B, C, distal portion of its basal segment, anterior and posterior view. D, apical segment of antennal endopod. E–G, apical swimming setae. H, ephippial female. I, posterior portion of ephippium. Scale bars denote 0.1 mm.

Subclade 'B' is present in Yakutia, Khabarovsk Territory, Primorsky Territory and Sakhalin Island. Subclade 'C' is present in north-western Alaska, Northwest Territories of Canada and Chukotka Peninsula; its trans-Beringian status is an important original conclusion.

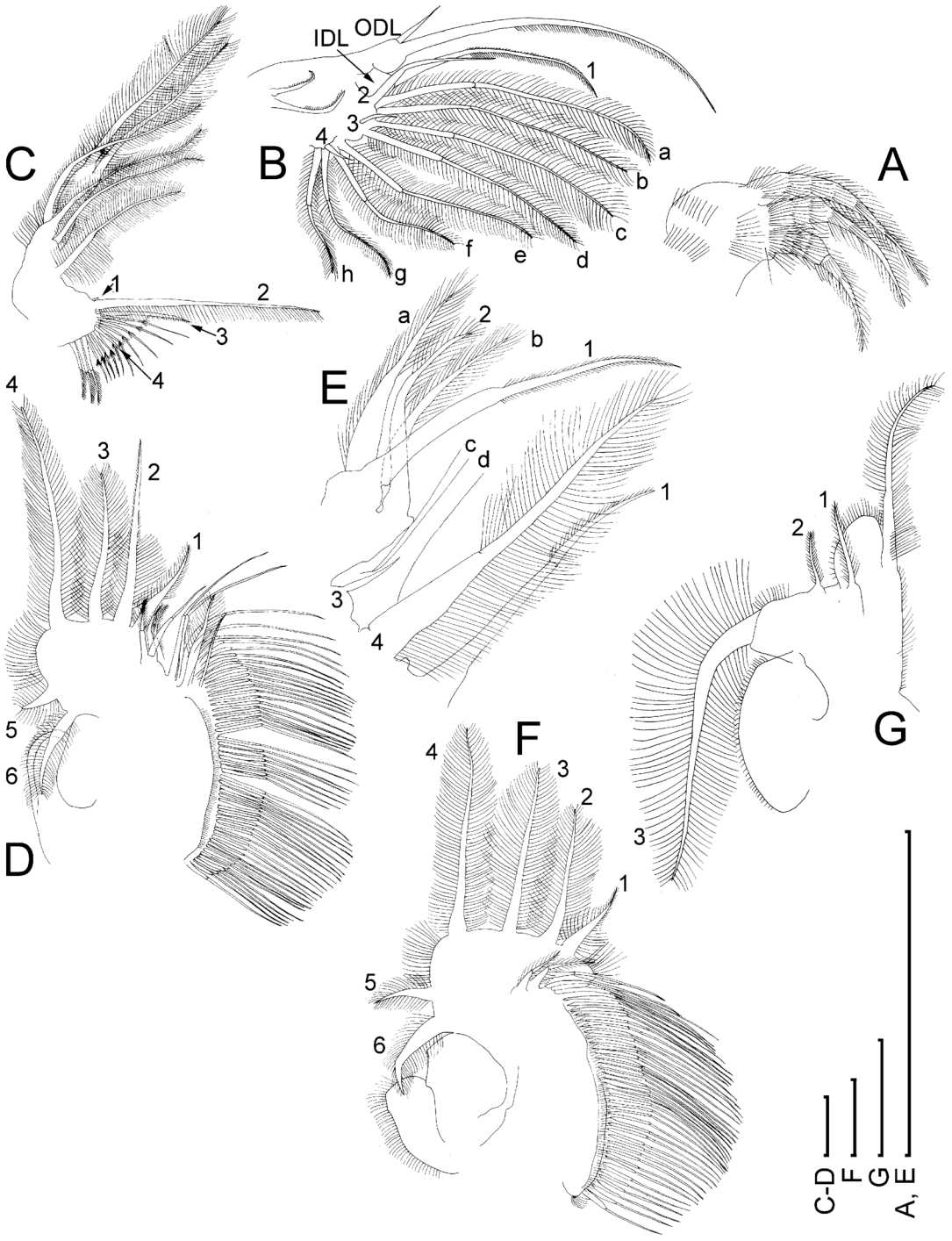

Figure 16. ***Daphnia jejuana***, head and thoracic limbs of large parthenogenetic female from DoSun-cheon pool 1, Jeju-do, South Korea. A, maxilla I. B, limb I. Abbreviations: IDL, innder distal lobe; ODL, outer distal lobe. C, limb II. D, limb III. E, its inner distal portion. F, limb IV. G, limb V. Scale bars denote 0.1 mm.

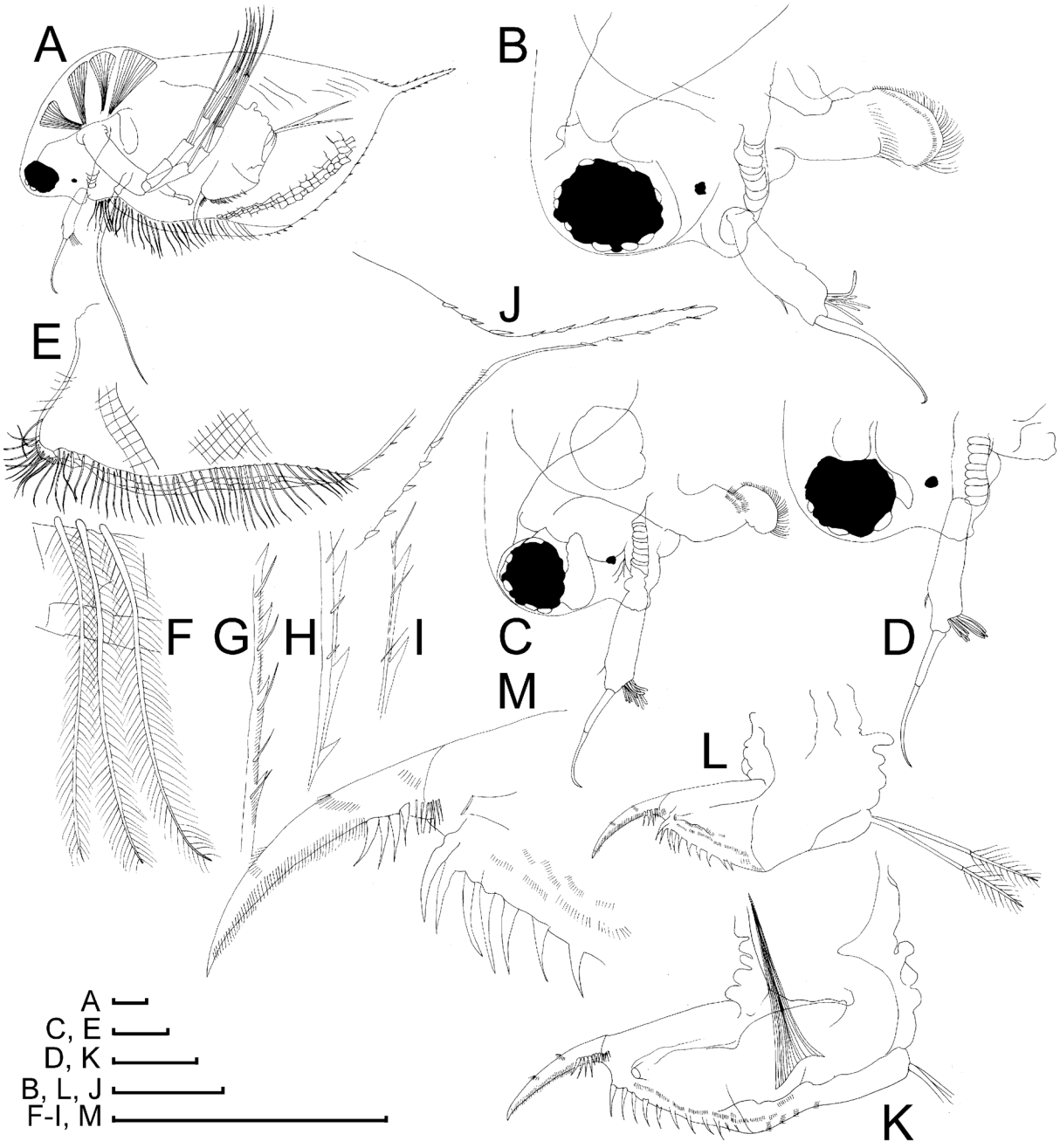

Figure 17. ***Daphnia jejuana***, adult male from DoSun-cheon pool 1, Jeju-do, South Korea. A, lateral view. B–D, head. E, armature of ventral margin. F, setae at ventral margin. G–I, armature of posteroventral margin. J, base of caudal spine. K, L, abdomen and postabdomen. M, postabdominal claw. Scale bars denote 0.1 mm.

2. *Daphnia hrbaceki* Juračka, Kořínek & Petrusek, 2010 is marked by a black circle in Figures 19 and 20. The single internal subclade 'D' is found in a pool in Central Europe.
3. *Daphnia tanakai*, indicated by a purple circle in Figures 1, 19 and 20, is a Far Eastern endemic. It is represented by a single subclade 'E' found in a few lakes in the mountains of Japan.
4. The *D. sinevi* group, indicated by blue symbols in Figures 1, 19 and 20, is restricted to the continental Far East of Russia and Sakhalin Island. Subclade 'F' is an endemic to Sakhalin Island where it is common; subclade 'G' is found in a single population in Primorsky Territory; and subclade 'H' (*D. sinevi s.s.*) is the most common species in small water bodies located in the continental Far East of Russia.

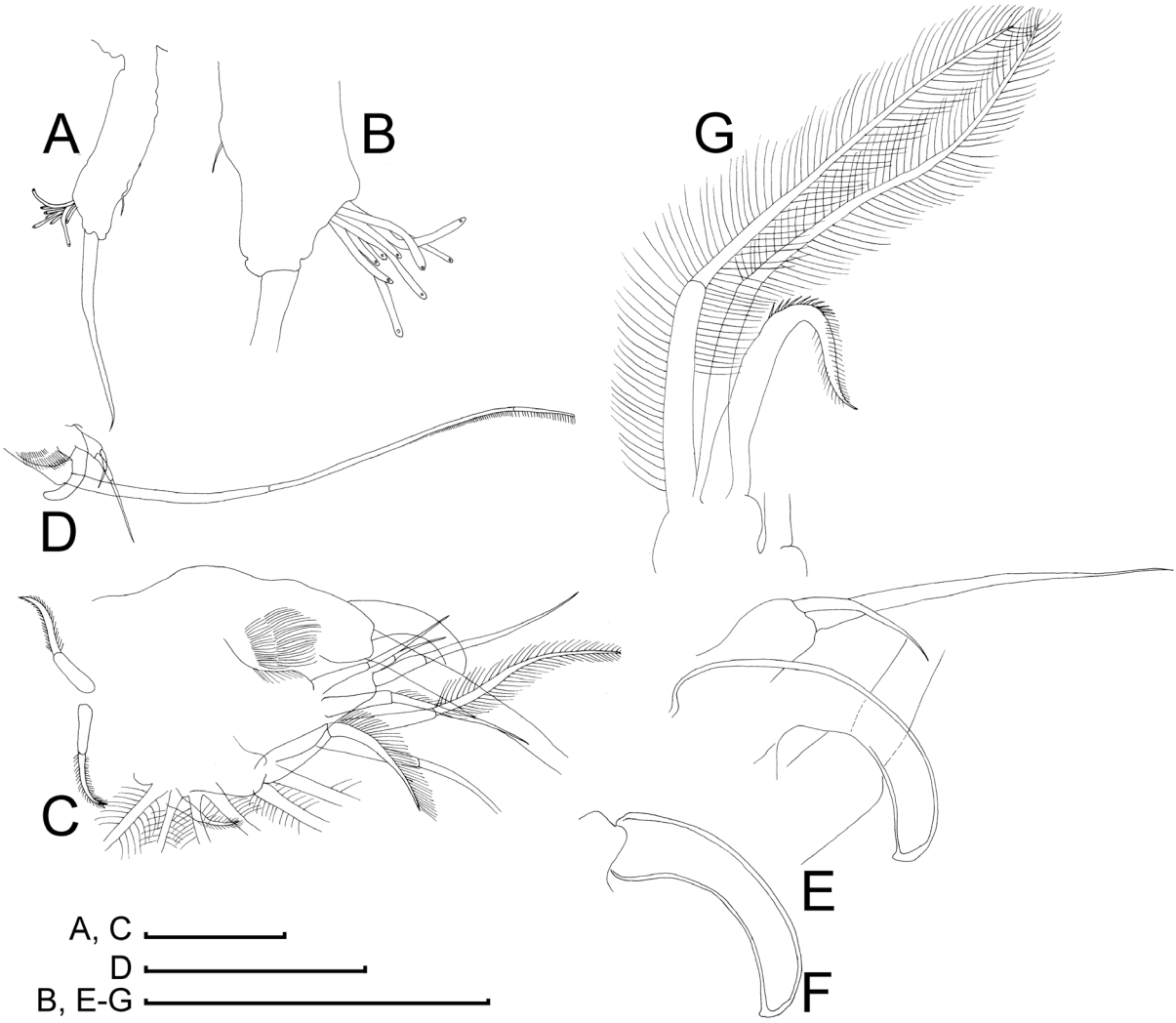

Figure 18. ***Daphnia jejuana***, head and thoracic limbs of adult male from DoSun-cheon pool 1, Jeju-do, South Korea. A, antenna I. B, its distal portion. C, corm of limb I. D, its distal portion. E, F, copulatory hook. G, inner distal portion of limb II. Scale bars denote 0.1 mm.

5. The *D. korovchinskyi* group, indicated by green symbols in Figures 1, 19 and 20, is endemic to the Far East of Eurasia, but has four subregional subclades. Subclade 'I' is found in two localities in Khabarovsk Territory; subclade 'J' is found in a single lake in Japan; subclade 'K' is found in a single locality in continental Korea; and subclade 'L' is found in many localities on Jeju Island (South Korea), where it is common and represents the only species of the *curvirostris* complex.

Figure 20 represents the tree based on the only specimens for which we had all four genes sequenced. As can be seen, selection of operational taxonomic units depended on the applied algorithm and the locus analysed. A minimal number of phylogenetic lineages could be selected based on a formal approach based on genetic distances (SI3%) and ABGD, whereas bGMYC and bPTP suggested a more complicated taxonomic structure of the species complex. Finally, multilocus reconstructions based on STACEY and tr2 methods also supported the existence of five main clades and four subclades within the *D. korovchinskyi* group (only tr2 did not support separation of the subclades I and J within the *D. korovchinskyi* group).

The tanglegram for mitochondrial and nuclear phylogenetic networks (Supporting Information, Fig. S1) demonstrated that the general topology of two trees was identical from the root until the terminal branches. A single ambiguity concerned the position of clade J in comparison to other related clades from Japan and continental Far East.

Table 2. Models of nucleotide substitutions

Locus	Position	Best model BIC	Best model AICc	Mixed model	Log-likelihood of the tree (BIC)
12S	–	TN+F+G4{0.1305}	TN+G4	–	–1630.7
COI	First	TNe{5.1842,89.2465}+FQ+I{0.5791}	TNe+I	MGK+F3X4+G4{3.3718}	–3096.0 (position)
	Second	F81 + F	F81		–3091.4 (mix)
	Third	TIM{8.4219,0.4778,4.3265}+F{0.3119,0.1647,0.1244,0.3987}+G4{4.8278}	TIM+G4		
ND2	First	HKY{35.0331}+F{0.2773,0.2271,0.1885,0.3069}+G4{0.3858}	HKY+G4	MGK+F3X4+G4{2.64581}	–5052.1 (position)
	Second	TN{15.8596,2.0746}+F{0.1534,0.2136,0.1461,0.4868}+G4{0.1639}	TN+G4		–5145.4 (mix)
	Third	TN{16.8838,9.0409}+F{0.3251,0.2133,0.1491,0.3124}+G4{2.1692}	TN+G4		
HSP90	First	HKY{9.7536}+F{0.3193,0.1161,0.4373,0.1272}+I{0.9455}	HKY+I	SCHN05+G4{1.2752}	–1459.6 (position)
(exon)	Second	F81+F	F81		–1501.1 (mix)
	Third	TNe{8.4902,16.2299}+FQ+G4{1.0856}	TNe+G4		
Intron 1	–	F81+F+I{0.3412}	F81+I	–	–305.7
Intron 2	–	TIM2+F	TIM2	–	–396.9

Abbreviations: AICc, corrected Akaike information criterion; BIC, Bayesian information criterion. Base substitution rates: F81, equal rates but unequal base frequencies (Felsenstein, 1981); HKY, unequal transition/transversion rates and unequal base frequencies (Hasegawa *et al.*, 1985); TIM, transversion model with variable base frequencies and AC = GT, AT = CG; TIM2, transversion model with variable base frequencies and AC = AT, CG = GT; TN, like HKY but unequal purine/pyrimidine rates (Tamura & Nei, 1993); TNe, like TN but equal base frequencies. Codon substitution rates: MGK, model non-synonymous/synonymous (dn/ds) rate ratio (Muse & Gaut, 1994) with additional transition/transversion (ts/tv) rate ratio; SCHN05, empirical codon model (Schneider *et al.*, 2005). Base frequencies: +F, empirical base frequencies; +FQ, equal base frequencies. Codon frequencies: +F3X4, unequal nucleotide frequencies and unequal nucleotide frequencies over three codon positions. Rate heterogeneity across sites: +G4, discrete Gamma model (Yang, 1994) with four categories; +I, proportion of invariable sites. Non-standard model parameters are indicated in curly brackets.

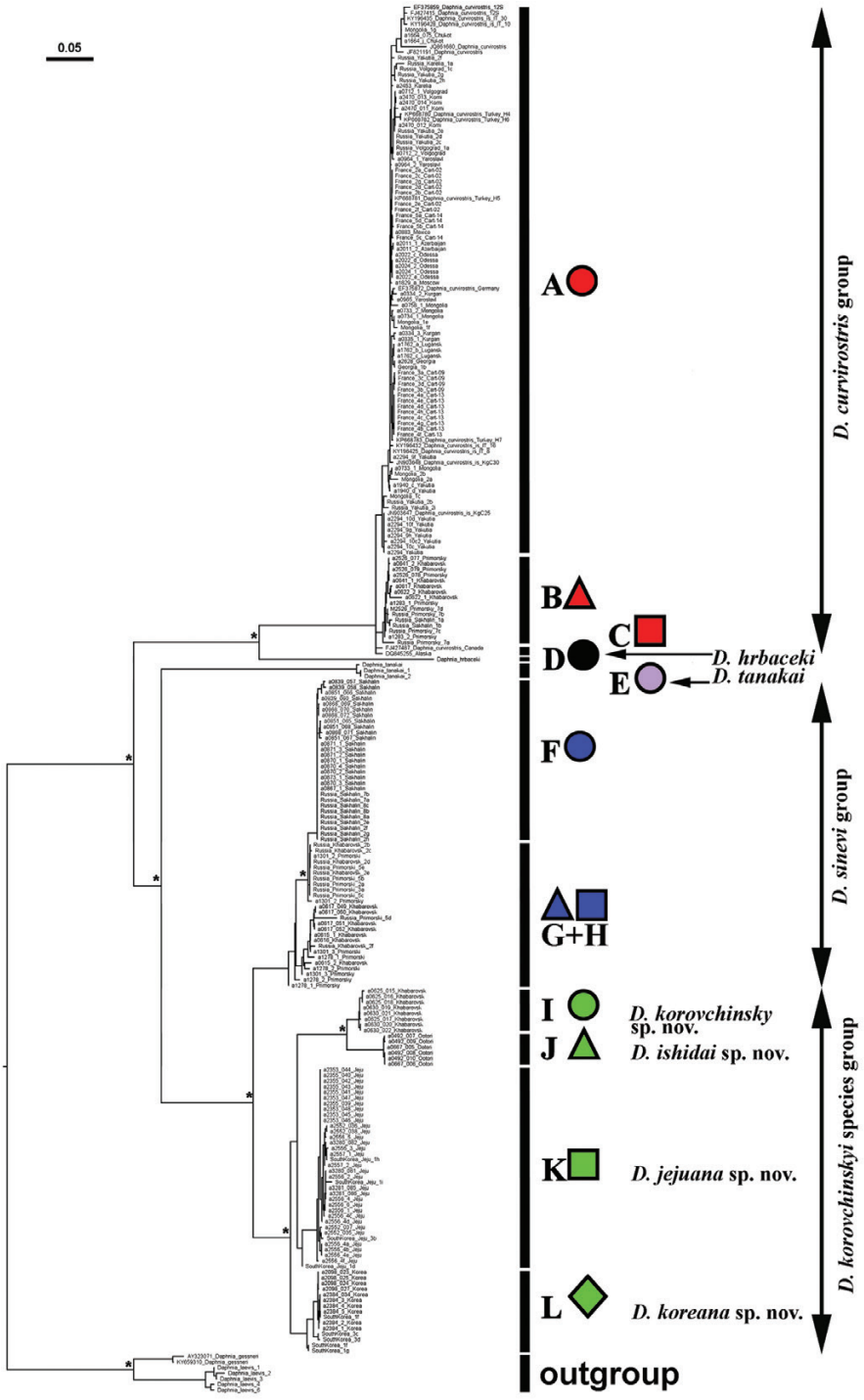

Figure 19. Maximum likelihood tree based on all available unlinked data on the mitochondrial *COI*, *12S* and *ND2* and nuclear *HSP90* genes by W-IQ-TREE algorithm with 1000 replicas of UFboot2. *Branches with support > 0.75. All symbols are the same as those of Kotov & Taylor (2019).

The galled network of three mitochondrial and three nuclear loci showed that there was a high level of uncertainty (frequency of hybridization) within subclade A (which was expected owing to the absence of reproductive isolation within this subclade) see Supporting Information (Fig. S2). But more interesting was the position of subclade J (*D. ishidai*), represented by a single montane population. It had a mitogenome

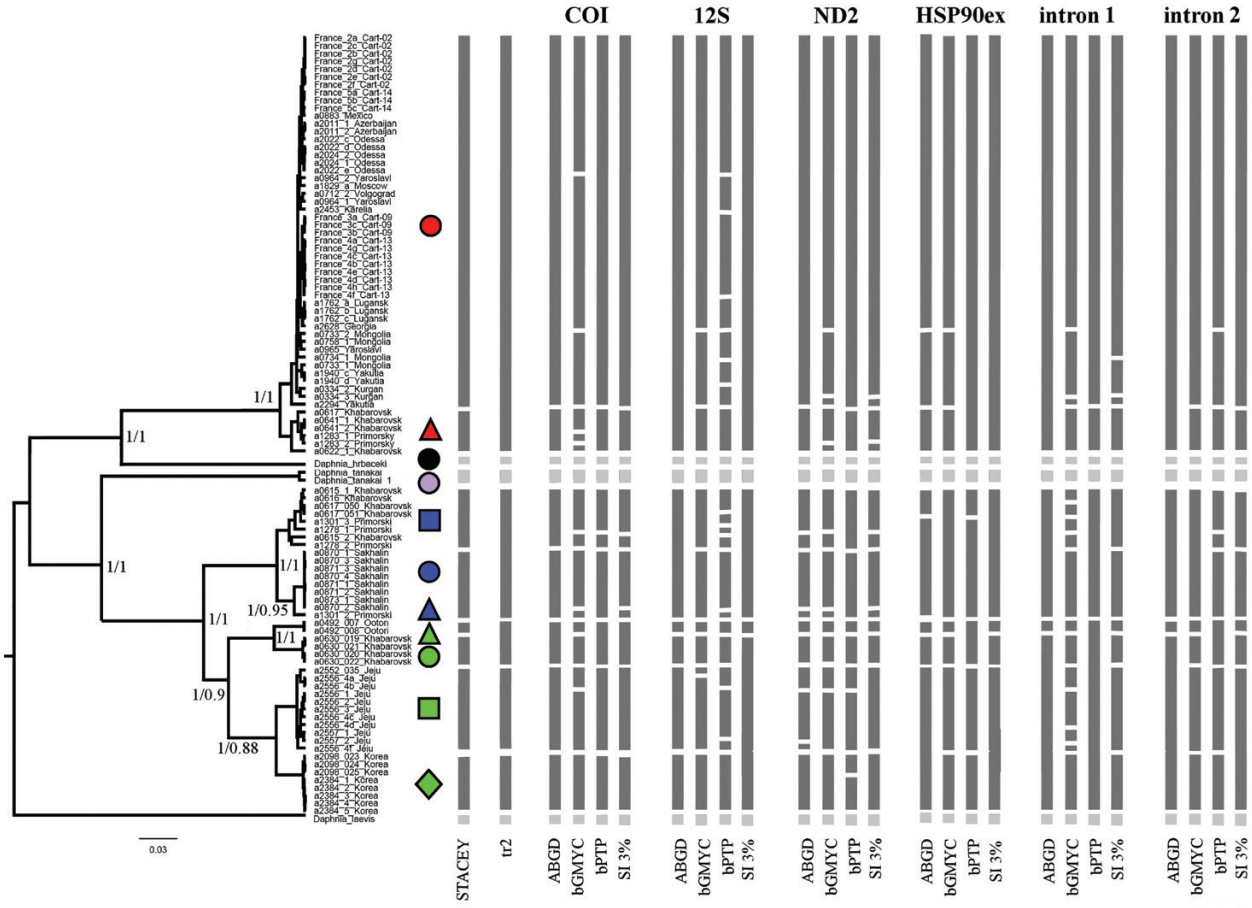

Figure 20. Bayesian information (BI) tree for *Daphnia curvirostris* group based on all genetic data available. Clades with support > 60% are represented. Support values: BI (posterior probability)/maximum likelihood (ultrafast bootstrap).

related to subclade I (*D. korovchinskyi*) from the continent, but its nuclear genome was related to subclade E (*D. tanakai*) from Japan. Such a situation could be explained either by invasion of the Japanese mitochondrial lineage to the continent or by a hybrid origin of population J.

We analysed the haplotype and nucleotide diversity of nine independent subclades present from the eastern Palaearctic (subclades C, D and G were excluded because they were absent from the region and/or insufficiently represented for adequate analysis). All populations had the high genetic diversity that is characteristic of *Daphnia* (Bekker *et al.*, 2018). The G+C rate in protein-coding loci was > 40% and significantly smaller in other loci, as in other animals (Li & Du, 2014). Results of the neutrality tests for the studied loci could suggest different directionalities of the demographic processes in different lineages (Table 3). For example, we could assume a demographic expansion of clade A based on $F_S << 0$ and $R_2 > 0$, which was understandable, because colonization of such a large area would be related to rapid population growth and intensive dispersal. For clade K, we could assume a bottleneck effect based on $F_S >> 0$ and $R_2 > 0$, which is generally characteristic for island endemics.

Owing to a high haplotype polymorphism at the *COI* locus of the *D. curvirostris* complex, the haplotype networks were constructed separately for the 'widely distributed' clade 1 (subclades A and B, *D. curvirostris* group; Fig. 21, top panel) and the 'Far Eastern' group of clades 4 and 5 (subclades F–L, *D. sinevi* and *D. korovchinskyi* groups; Fig. 21, bottom panel). The 'widely distributed group' was clearly subdivided into regional subgroups of populations: western European, northern European, western European, 'Central Asian' and 'Far Eastern' ones (the last corresponded to clade B), separated by only one to three mutations. Exclusions from this rule (arrows) could be explained by human-mediated inter-regional invasions. A Mexican population belonging to the 'eastern European' group apparently appeared after a human-mediated introduction from Europe (Kotov & Taylor, 2019). The eastern European haplotypes in France and Mongolia (arrows) might also have appeared as a result of human-mediated invasions.

Table 3. Polymorphism of genes studied here

Clade	$N_{sequences}$	G+C	N_{sites}	S	h	H_d	π	k	F_S	R_2
12S (mitochondrion, ribosomal DNA)										
A	15	0.342	571	7	6	0.762	0.0037	2.095	–0.697	0.138
B	4	0.343	571	4	2	0.500	0.0035	2.000	2.197	0.433
E	3	0.318	570	0	1	–	–	–	–	–
F	11	0.334	568	5	5	0.836	0.0039	2.218	–0.155	0.212
H	4	0.338	568	2	2	0.667	0.0023	1.333	1.530	0.333
I	6	0.335	569	3	2	0.600	0.0031	1.800	2.759	0.300
J	3	0.331	568	1	2	0.667	0.0012	0.666	0.201	0.471
K	17	0.323	566	7	3	0.404	0.0018	1.015	1.091	0.203
L	9	0.332	566	0	1	–	–	–	–	–
COI (mitochondrion, coding)										
A	57	0.417	657	51	29	0.953	0.0106	6.992	–10.68	0.066
B	10	0.419	657	17	8	0.933	0.0072	4.711	–1.211	0.142
F	20	0.437	657	16	11	0.805	0.0051	3.332	–3.397	0.096
H	10	0.425	657	27	7	0.933	0.0122	8.022	0.364	0.128
I	7	0.369	657	5	5	0.857	0.0022	1.428	–2.311	0.140
J	6	0.370	657	1	2	0.333	0.0005	0.333	–0.003	0.373
K	26	0.423	657	18	9	0.791	0.0081	5.323	0.977	0.141
L	10	0.417	657	6	4	0.644	0.0038	2.533	1.135	0.189
ND2 (mitochondrion, coding)										
A	49	0.394	930	72	29	0.959	0.0095	8.822	–9.046	0.056
B	7	0.385	930	57	6	0.952	0.0210	19.52	1.293	0.178
E	3	0.348	930	15	3	1.000	0.0108	10.00	1.139	0.425
F	8	0.366	930	0	1	–	–	–	–	–
H	8	0.368	930	64	8	1.000	0.0235	21.82	–0.780	0.129
I	4	0.353	926	4	2	0.667	0.0029	2.667	2.719	0.333
J	2	0.339	930	3	2	1.000	0.0032	3.000	1.099	0.500
K	12	0.337	930	16	4	0.636	0.0064	5.924	4.314	0.171
L	8	0.347	930	0	1	–	–	–	–	–
HSP90 (nuclear, coding exon)										
A	8	0.469	654	17	8	1	0.0087	5.678	–3.548	0.106
B	2	0.475	654	0	1	–	–	–	–	–
E	2	0.443	654	2	2	1	0.0031	2.000	0.6932	0.500
F	5	0.457	654	0	1	–	–	–	–	–
H	3	0.456	654	10	3	1	0.0102	6.666	0.7032	0.339
I	2	0.457	654	4	2	1	0.0061	4.000	1.3863	0.500
J	1	0.460	654	0	1	–	–	–	–	–
K	11	0.458	654	12	8	0.945	0.0077	5.054	–1.432	0.198
L	5	0.460	654	2	2	0.600	0.0018	1.200	1.687	0.300
Intron 1 (nuclear, non-coding intron)										
A	8	0.244	64	5	5	0.786	0.0268	1.714	–1.495	0.137
B	2	0.250	64	0	1	–	–	–	–	–
E	2	0.303	61	1	2	1.000	0.0164	1.000	0.001	0.500
F	5	0.308	65	0	1	–	–	–	–	–
H	3	0.291	63	4	2	0.667	0.0423	2.667	2.022	0.471
I	2	0.308	65	2	2	1.000	0.0308	2.000	0.693	0.500
J	1	0.313	64	0	1	–	–	–	–	–
K	11	0.287	62	5	4	0.600	0.0317	1.964	0.726	0.187
L	5	0.271	62	1	2	0.400	0.0065	0.400	0.090	0.400
Intron 2 (nuclear, non-coding intron)										
A	8	0.309	81	14	8	1.000	0.0644	5.214	–3.791	0.150
B	2	0.309	81	0	1	–	–	–	–	–
E	2	0.328	61	0	1	–	–	–	–	–

Table 3. Continued

Clade	$N_{sequences}$	G+C	N_{sites}	S	h	H_d	π	k	F_S	R_2
F	5	0.303	66	0	1	–	–	–	–	–
H	3	0.313	64	2	2	0.667	0.0208	1.333	1.061	0.471
I	2	0.343	67	0	1	–	–	–	–	–
J	1	0.348	66	0	1	–	–	–	–	–
K	11	0.341	67	4	5	0.873	0.0271	1.818	–0.618	0.227
L	5	0.352	67	2	2	0.400	0.0119	0.800	1.040	0.400

Abbreviations: F_S, Fu's neutrality statistic (Fu, 1997); G+C, guanine–cytosine content; h, number of haplotypes; H_d, haplotype diversity; k, average number of nucleotide differences; $N_{sequences}$, number of sequences; N_{sites}, total number of sites (excluding sites with gaps/missing data); π, nucleotide diversity per site; R_2, Ramos-Onsins and Rozas R_2 statistic (Ramos-Onsins & Rozas, 2002); S, number of segregating (polymorphic) sites.

A higher diversity was characteristic of the 'Far Eastern' group of haplotypes having a distinct regional structure. The islands had specific groups of haplotypes corresponding to the subclades and taxa described above: *D. ishidai* (subclade J) in Honshu, *D. jejuana* (subclade K) in Jeju and an undescribed *D. sinevi*-like taxon (subclade F) in Sakhalin. Regional groups of haplotypes were separated by numerous mutations (> 20), with two exceptions: the J and I groups of haplotypes differed in a single mutation only; and the I and H groups differed in seven mutations. In general, the continental portion of the Far East was more diverse haplotypically than the islands, which could be regarded as a sign that it was a centre of dispersal for this species group (Sanmartin *et al.*, 2001).

Results of the DEC and the BayArea reconstructions are presented in the Supporting Information (Fig. S3). They were basically similar, perhaps indicating evidence of the adequateness of reconstruction. Most probably, the majority of recent geographical clades of the *D. curvirostris* complex resulted from vicariance events. It is necessary to keep in mind that the DEC algorithm favours vicariance explanations, but vicariance is possible in this case: European and Asian populations are separated by mountains, and the islands (Sakhalin, Honshu, Jeju) are isolated by the ocean. At the same time, a dispersion model is characteristic of the European portion of the 'widely distributed' group of haplotypes (subclade A). Interpretation of the separation of the Mexican population as a vicariance event is apparently wrong, because it is a confirmed case of human-mediated invasion.

Results from a test of the molecular clock using the ML method are presented in Table 4. All loci supported the possibility of a molecular clock, although keeping in mind the minimal log-likelihood values, their contribution to the molecular clock was not so obvious. We recalculated 'simple' genetic *p*-distances to the time of divergence using separate 'fast' and 'slow' clocks.

Even 'fast' molecular clock estimates of the age of the *D. curvirostris* complex yielded times of 24–26 Mya, in the mid-Miocene. With the exception of the young I–J pair, all groups and taxa differentiated during pre-Pleistocene times (Table 5). The relaxed molecular clock suggested a Cretaceous origin of the complex and its main branches (*D. curvirostris* group vs. all others), a Late Cretaceous separation of *D. tanakai*, a Palaeogene separation of the *D. sinevi* and *D. korovchinskyi* species groups and a Neogene species differentiation of *D. sinevi* and *D. korovchinskyi*.

DISCUSSION

SPECIES DELIMITATION: MORPHOLOGICAL VS. MOLECULAR METHODS AND CYBERTAXONOMY VS. 'TRADITIONAL TAXONOMY'

Each cybertaxonomic species delimitation method recognizes five main clades within the *D. curvirostris* complex, in accordance with our subdivision of the tree based on the phylogenies from a few loci (Kotov & Taylor, 2019) and the morphology-based delimitations. However, different cybertaxonomic methods suggest a significantly different number of provisionary species within the *D. curvirostris* complex.

Remarkably, even the simplest distance methods reveal strong differentiation among the population groups in the *D. curvirostris* complex. In general, the SI3% and ABGD results reveal a less complicated taxonomic structure (and are more realistic according to our 'subjective' opinions). Our data also confirm earlier proposals (Srivathsan & Meier, 2012) that some corrected distances (i.e. Kimura-2-parameter) might be less appropriate than uncorrected *p*-distances for the delimitation of closely related species (e.g. the non-protein-coding sequence loci in the present study). Even for the *COI* locus, often used in DNA barcoding, 'historical tradition' seems to remain the main justification for using Kimura-2-parameter (Collins

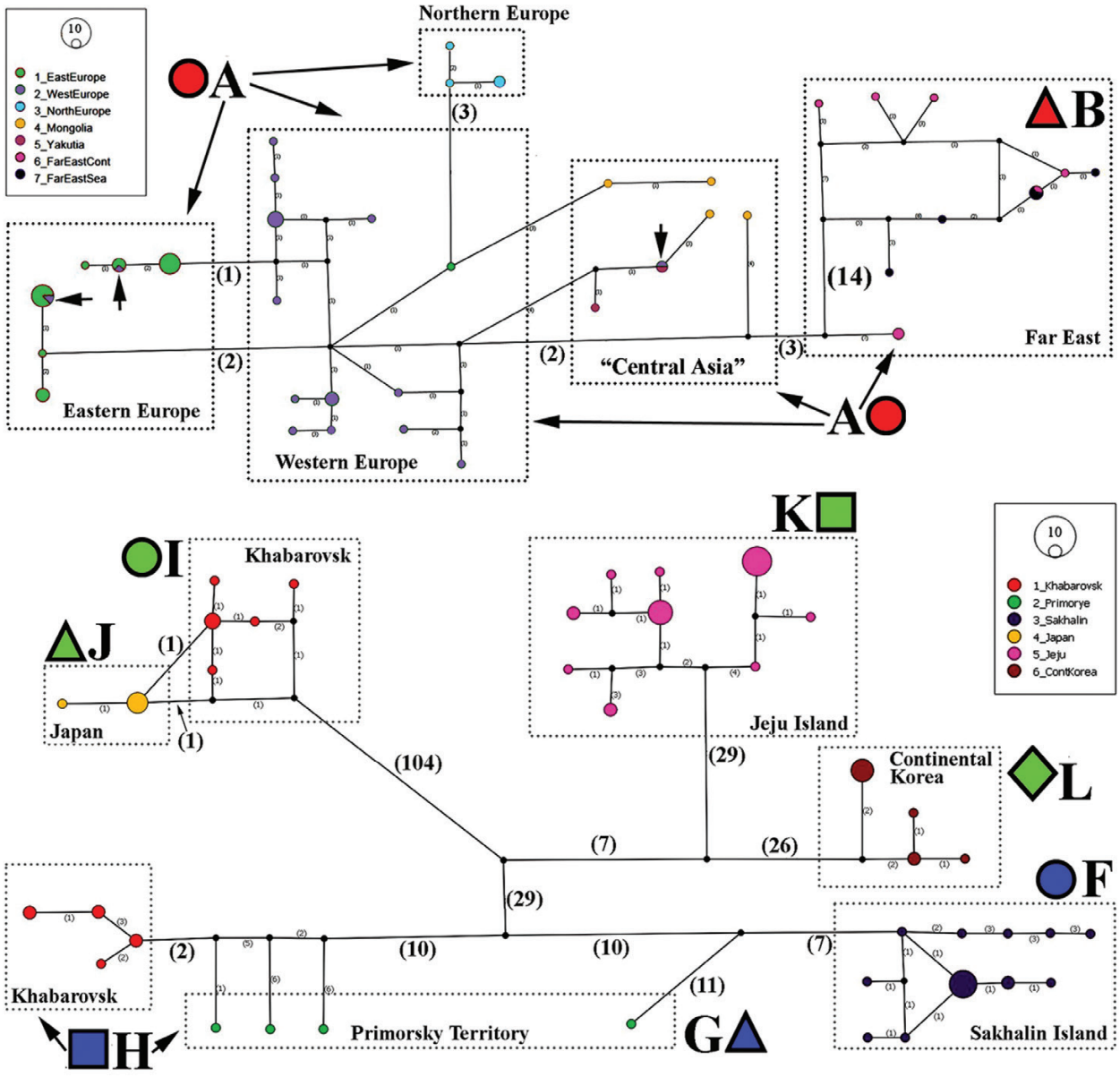

Figure 21. Median-joining networks for the 'widely distributed' group of clades A and B (top panel) and the Far Eastern group of clades F–L (bottom panel).

et al., 2012). In contrast, the bGMYC and bPTP reveal a higher potential taxonomic diversity within the *D. curvirostris* complex compared with previous approaches, because the coalescent models frequently overestimate the taxonomic complexity (Talavera *et al.*, 2013).

Advantages and disadvantages of different cybertaxonomic methods have been discussed intensively in the recent literature (Hebert *et al.*, 2003; Lohse, 2009; Reid & Carstens, 2012; Collins & Cruickshank, 2013; Zhang *et al.*, 2013; Fujisawa *et al.*, 2016; Vitecek *et al.*, 2017). Each species delimitation approach has some defects, and a universal cybertaxonomic method remains elusive (perhaps impossible). Again, a combination of different methods might be the most useful, and morphological methods could be included in such a combination. In general, in our work we follow a careful strategy for species delimitation based on genetic data (Carstens *et al.*, 2013), and the main criterion for the independent species status for a subclade recognized by the phylogenetic methods is the presence of morphological characters differentiating one subclade from another.

Table 4. Results from a test of molecular clock using the maximum likelihood method

Locus	Substitution model	Test for molecular clock: with clock (log-likelihood)	Test for molecular clock: without clock (log-likelihood)	Null
12S (all)	T92+G	–2401.39	–2324.66	Rejected
COI (first + second + third)	T92+G+I	–4403.74	–4074.95	Rejected
ND2 (first + second + third)	TN93+G+I	–7763.64	–7637.09	Rejected
HSP90 exon (first + second + third)	TN93+G	–1911.79	–1852.25	Rejected
Intron 1	T92	–432.33	–411.86	Not rejected
Intron 2	T92	–559.08	–501.48	Rejected

The null hypothesis of equal evolutionary rate throughout the tree (at a 5% significance level) was tested. Models: TN93 (Tamura & Nei, 1993) and T92 (Tamura, 1992). Non-uniformity of evolutionary rates among sites may be modelled by using a discrete Gamma distribution (+G) with five rate categories and by assuming that a certain fraction of sites is evolutionarily invariable (+I).

Table 5. Genetic distances between phylogroups of *Daphnia curvirostris* and divergence time based on data for the *COI* locus

	A	B	F	G	H	I	J	K	L
A	–	4.75	24.12	24.87	23.25	27.87	27.75	23.75	26
B	0.038	–	23.01	23.62	22.25	28.62	28.37	22.51	23.62
F	0.193	0.184	–	3.25	6.01	28.5	28.5	13.5	14.75
G	0.199	0.189	0.026	–	4.51	29.75	29.62	13.5	15.02
H	0.186	0.178	0.048	0.036	–	27.62	27.5	12.87	14.01
I	0.223	0.229	0.228	0.238	0.221	–	0.25	27.02	26.62
J	0.222	0.227	0.228	0.237	0.220	0.002	–	27.05	26.62
K	0.190	0.180	0.108	0.108	0.103	0.216	0.216	–	10.75
L	0.208	0.189	0.118	0.120	0.112	0.213	0.213	0.086	–

Below the diagonal are estimates of evolutionary divergence over sequence pairs between groups. Above the diagonal is time of divergence, in millions of years ago, with 'fast clock' from Schwentner *et al.* (2013).

Importantly, we find diagnostic characters for all four subclades having the status of independent phylogenetic lineages in our genetic analysis. Frequently, the limitations of morphology-based taxonomy are discussed (Hebert *et al.*, 2003), but recent results that combine morphological and molecular data in the Cladocera unambigously confirm the usefulness of morphology. The *D. curvirostris* complex is now the taxonomically best-studied group in the genus *Daphnia*. Global approaches with morphological data are still unusual for this genus (Kotov, 2015). Ultimately, morphology-based taxonomy does have a lower limit of resolution, but the *D. curvirostris* complex and many other cladoceran groups appear to exceed this limit.

The morphological differences among *Daphnia* taxa concern small-scale characters, and such differences are mostly found by well-trained taxonomists. We are certain that morphological taxonomy still has independent value. Attempts 'to abandon the benefits of morphological studies in favor of a limited molecular identification system, would ultimately impede our understanding of biodiversity' (Will & Rubinoff, 2004).

NOTES ON MORPHOLOGICAL EVOLUTION IN THE *D. CURVIROSTRIS* COMPLEX

Cladocera is an old group (Kotov & Korovchinsky, 2006; Van Damme & Kotov, 2016) and the genus *Daphnia* is also old, a proposal initially supported by authors using molecular clocks (Adamowicz *et al.*, 2009). Later, the age of *Daphnia* was confirmed by the direct findings of fossil daphniid ephippia (Kotov & Taylor, 2011; Van Damme & Kotov, 2016). Species groups differentiated at various geological times and passed through complicated evolutionary histories (Cornetti *et al.*, 2019). We can thus expect some cases of convergent morphological evolution among different groups of Cladocera. We alluded to morphological convergence between the *D. curvirostris* complex and other complexes of the subgenus *Daphnia s.s.* Diagnostic morphological characters of the Far Eastern taxa (discriminating them from other members of the *D. curvirostris* complex) inform about tendencies in daphniid morphological evolution: (1) a strong projection is present on the posterior head

margin (*D. curvirostis*, *D. tanakai* and *D. ishidai* lack this projection); (2) antenna I is located ventrally to this margin (in contrast to *D. tanakai* with antenna I located on the margin); and (3) a low crest is present on the anterodorsal portion of head in some taxa (*D. korovchinskyi* and *D. koreana*), and as a result the compound eye does not occupy the anteriormost portion of the head (in contrast to all other taxa). Remarkably, these characters are analogous to those discriminating *Daphnia galeata* G. O. Sars, 1864 from other species of the *D. longispina–galeata* group (Glagolev, 1986). Male *D. ishidai* have a denticulated stiff seta on limb II. Again, the same character has evolved in males of the *D. longispina–galeata* complex, i.e. in *D. galeata s.s.* (Glagolev, 1986).

All four taxa described here from East Asia have a smaller size and the first (proximal-most) abdominal process shorter compared with *D. curvirotris s.s*. These characters of Far Eastern daphniids might be paedomorphic, saying something about the general direction of the evolution of this group. In general, smaller species of *Daphnia* are more characteristic for large water bodies of northern Eurasia, whereas temporary waters are occupied by larger species from *Daphnia* subgenus *Ctenodaphnia* Dybowski & Grochowski, 1895, *D.* (*Daphnia*) *pulex* Leydig, 1860 and *D.* (*D.*) *obtusa* Kurz, 1874 groups. The *D. curvirostris* group seems to be an exception to this general rule, because some of its species from temporary waters are also small in size, and it is not clear how these small pond *Daphnia* deal with invertebrate predation.

As with the *D. longispina* complex and the *D. pulex* complex, juveniles of some members of the *D. curvirostris* complex have neck teeth, whereas others lack these. Juracka *et al.* (2010) summarized information on the neck teeth in different groups of *Daphnia s.s.* and concluded that the ability to form the neck teeth could be a synapomorphy of the subgenus instead of a product of convergent evolution, as suggested before (Colbourne *et al.*, 1997; Kotov *et al.*, 2006). We hypothesize that the presence of the '*curvirostris*' type of neck teeth is a synapomorphy of the *D. curvirostris* group. Remarkably, species from large lakes (*D. tanakai* and *D. ishidai*) lack the neck teeth, wheresa some taxa from small (usually temporary) water bodies are able to form them. This phenomenon needs further study, particularly regarding the different predation regimens in ponds and lakes.

Morphological convergence among species complexes of *Daphnia* might facilitate the identification of diagnostic characters in groups with a confused taxonomy. Predominantly, such characters concern the ephippium and male characters (Popova *et al.*, 2016).

PHYLOGEOGRAPHY

The *D. curvirostris* complex has a broad longitudinal range across Eurasia, but its latitudinal range is not wide: it includes 'northern Europe and Asia south of Norway-Moscow-Middle Baikal and Primorie (Hrbácek et al., 1978; Glagolev, 1986) and the far north-west of Canada (Hebert 1995)' (Benzie, 2005: p. 140). Subclade C is present in the Beringian region (Chukotka and Alaska), where its populations are rare (present study). Along most of this range, only a single member of the *D. curvirostris* group is detected. In the Far East, the complex reaches peak diversity. A disproportionate distribution of species richness is found in many Holarctic taxa, and such patterns are a reflection of the history of biodiversity formation (Sanmartin *et al.*, 2001). Phylogeographical methods are helpful for revealing the relationships between populations from different geographical locations (Huson & Bryant, 2006; Gutierrez-Garcia & Vazquez-Dominguez, 2011), and these methods are applied here.

Differences between networks in the number of mutations separating the geographical groups of haplotypes (corresponding well to the subclades from our trees) are consistent with networks of differing ages. Previously, Kotov & Taylor (2019) analysed a median-joining *ND2* haplotype network for subclades A–C and concluded that there was reduced extinction during the Pleistocene glacial cycles for the eastern Palaearctic. However, if the *ND2* phylogeographical pattern of subclade A corresponds well to a rapid recolonization of the wide Palaearctic range from a single (possibly Last Glacial Maximum) western Palaearctic refugium, the pattern of clades B and C is also consistent with a series of relictual pre-Pleistocene haplotypes. Our top network in Figure 21 represents the *COI* haplotypes from subclades A and B. Given that *ND2* is less conservative in comparison to *COI* (Zhang *et al.*, 2016; Brennan *et al.*, 2017), our *COI* network is less collapsed, although it could be derived from the *ND2* tree by Kotov & Taylor (2019). We observe a deeper regional haplotype differentiation in the *COI* network (more recent events) instead of the star-like shapes in the *ND2* network related to its rapid expansion post-Last Glacial Maximum. Note that similar results were obtained for the *D. longispina* complex (Zuykova *et al.*, 2018a).

Subclades H–L were not analysed by Kotov & Taylor (2019). Our *COI* network demonstrates a pronounced diferentiation of several regional subclades that are strongly isolated from each other (with two exclusions; see the Results section). Apparently, this is an old pattern, with the subclades H–L representing the remains of a large past haplotype diversity. Given that the chance of ten simultaneous mutations is minimal, we need to conclude that numerous

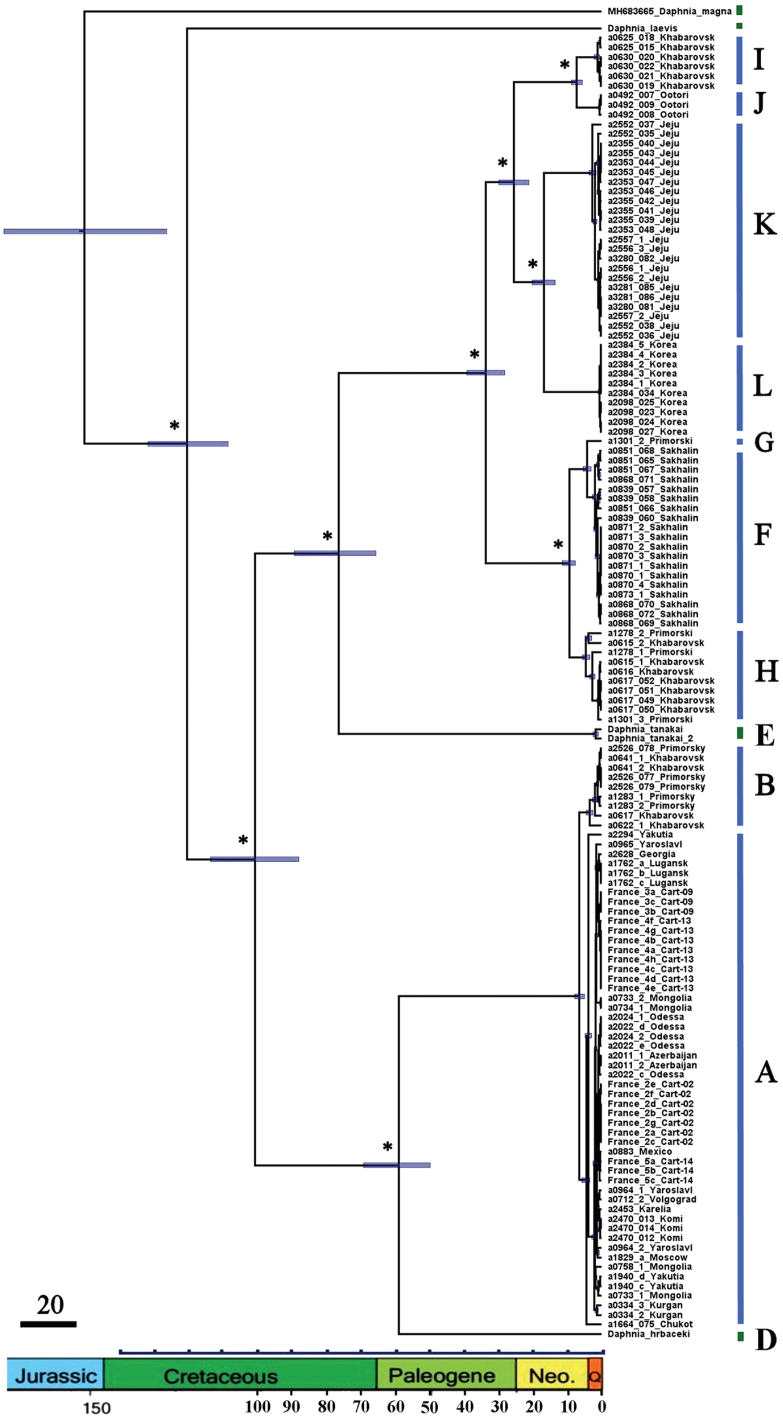

Figure 22. Phylogenetic analyses of the mitochondrial dataset with relaxed molecular clock estimates based on fossil calibration points (Kotov & Taylor, 2011). The bars depict the 95% highest probability density interval of the estimated divergence times. The scale is in millions of years ago. *Posterior probability > 0.95 (support values for constrained taxa are not shown).

haplotypes 'intermediate' between recent haplotype groups existed in the past. But they are now absent, because the group passed through a mass extinction, in which hundreds of 'intermediate' haplotypes and their congeners will have become extinct. We cannot estimate the timing of this large extinction from our

network, but it could be during the Pleistocene or pre-Pleistocene.

We can try to estimate roughly the time of this extinction using molecular clocks, but two different approaches ('fast clock', Table 5; and 'slow clock', Fig. 22) to the reconstruction of the chronology of *D. curvirostris* complex evolutionary history give significantly different clade ages (twofold). The first approach (a mechanistic translation of the mutation rates to the clade divergence time) is based on a strict molecular clock. Such approaches are rarely realistic (Schwartz & Maresca, 2006; Ho, 2008). It is known that the mutation rate, even for mitochondrial genes, varies among animals; it is ~0.8–2.4%/Myr for the *COI* locus within crustaceans (Knowlton & Weigt, 1998; Schubart *et al.*, 1998; Schwentner *et al.*, 2013). Obviously, the accuracy of such analysis is low, keeping in mind such differences and the observed mitochondrial variation in Cladocera (Belyaeva & Taylor, 2009; Bekker *et al.*, 2018). The effectiveness of the second approach (a relaxed molecular clock with palaeontological calibration) depends on the completeness of the fossil record for a group.

Traditionally, the 'simple' method based on the nucleotide substitution rates gives a 'fast' molecular clock, with younger times of phylogroup divergence. One hypothesis for rapid rates in the mitogenome of aquatic crustaceans involves mutagenic habitats (Hebert *et al.*, 2002; Loeza-Quintana *et al.*, 2019). The observed high polymorphism of cladocerans could also be explained, in part, by their complicated life cycle, namely, the recruitment of older, 'extinct' haplotypes from the egg bank.

The main argument against 'ultra-fast' evolution of the cladocerans is their incomplete fossil record. It is known that slow molecular clocks are common in the best-studied organisms. Hominids have a minimal speciation time of ~12–15 Mya (Moorjani *et al.*, 2016), but they have a detailed fossil record, and each new record increases the age. In contrast, many cladoceran fossils are know from the Caenozoic, but we have a limited set of Mesozoic records (Smirnov, 1992a; Kotov & Korovchinsky, 2006; Van Damme & Kotov, 2016). A single Mesozoic finding of *Daphnia* ephippia belonging to two 'recent' subgenera (Kotov & Taylor, 2011) strongly modified our ideas on the ages of daphniid taxa (Van Damme & Kotov, 2016). Biogeographical calibrations for invertebrate taxa are also characterized by uncertainty. Even for molluscs with many fossil records, different approaches for phylogeographical reconstructions give differences of two orders of magnitude in the estimations of phylogenetic lineage ages (Bolotov *et al.*, 2016).

Geological calibrations might be possible within the *D. curvirostris* complex, but the geological history of the eastern margin of Asia is complicated (Barnes, 2003; Kirillova, 2003; Yin, 2010). At ~500 Mya, the Palaeo-Pacific oceanic plate began to be subducted beneath the continental margin of the South China Block, which formed Proto-Japan, which has been located on the convergent margin of East Asia (Wakita, 2013) ever since. Since the Early Mesozoic, the eastern margin of Asia has been subjected to accretionary growth, including the formation of the Cretaceous volcanic belts and a mid-Caenozoic opening of the Sea of Japan that separated Japan and Sakhalin as an archipelago (Maruyama *et al.*, 1997; Yin, 2010). The timings of such events are somewhat different among authors, with proposals for the time of opening of the Sea of Japan varying from the Miocene (Maruyama *et al.*, 1997) to the Oligocene or even the Late Eocene (Kano *et al.*, 2007). Given that world sea level dropped several times during the Pleistocene glaciation cycles, the exit straits of the Sea of Japan were partly or fully dried and closed, and the Sea of Japan was represented from time to time by a large inland lake (Park *et al.*, 2000). Jeju Island was formed only ~2 Mya by volcanic activity (Park *et al.*, 2000), but the youngest part of this island was part of the land, not sea, at least during some previous periods in the Pleistocene.

Most probably, the common ancestor of the *D. sinevi* and *D. korovchinskyi* groups (subclades E–L) lived at the eastern margin of Asia. Even a 'fast' molecular clock suggests the time of differentiation for the *D. curvirostris* complex to be 24–26 Mya, with separation of the *D. sinevi–D. korovchinskyi* cluster at ~12–28 Mya. Both dates are correspond roughly to the earlier stages of formation of the Sea of Japan. Taxon differentiation within the latter cluster took place at 1–20 Mya, mainly during a pre-Pleistocene (Tertiary?) time. At the same time, the differentiation was probably associated with the mass extinction of intermediate haplotypes (as suggested by the network pattern). Therefore, even accepting the 'fast' clock dates, members of the *D. sinevi* and *D. korovchinskyi* group are likely to be 'Tertiary relicts', but they are biogeographical, not phylogenetic, relicts *sensu* Grandcolas *et al.* (2014), not being an earlier derived lineage of the *D. curvirostris* complex. *Daphnia tanakai* (of Japan) is a case where both phylogenetic relict and biogeographical relict status seems likely.

However, the 'fast' clock suggests that all the *D. curvirostris* complex differentiation had already taken place during the Neogene. This is somewhat dubious keeping in mind that fossil ephippia of the subgenus *Daphnia s.s.* are known from the Jurassic–Cretaceaous boundary (Kotov & Taylor, 2011) and that the *D. curvirostris* complex is an earlier derived lineage of the *D. longispina* cluster, one of two main clusters within the subgenus *Daphnia s.s.* (Adamowicz *et al.*, 2009). We can regard the entire *D. curvirostris* complex as a phylogenetic relict *sensu* Grandcolas

et al. (2014), and it is presumably old; its Mesozoic 'Laurasian' differentiation, suggested by a 'slow' clock, seems to be a more preferable version in comparison to a young Neogene differentiation.

A 'slow' clock is consistent with differentiation of all of the Far Eastern supergroup (subclades H–L) and its two main groups (*D. sinevi* and *D. korovchinskyi*) at the earlier stages of formation of the Sea of Japan (~40–20 Mya). A Neogene differentiation and mass extinction of the main lineages also appears to have occurred (with Quaternary intraspecific diversification). Remarkably, both clocks support the Tertiary age of the mass cladoceran extinction predicted by Korovchinsky (2006); the *D. curvirostris* complex might be part of this event. Recently, a Tertiary diversification of freshwater animals was demonstrated for some fishes of Japan (Tominaga *et al.*, 2016; Watanabe *et al.*, 2017). During the Tertiary, the region became favourable for freshwater animals owing to a wet monsoonal climate (Zhisheng *et al.*, 2001; in contrast to an otherwise global climate aridification at the time). Strong Tertiary geological and climatic changes at the continental margin of Asia might also have promoted geogaphical speciation.

The haplotype diversities within each species of the *D. sinevi* and *D. korovchinskyi* groups are of a Quaternary origin, even following a 'slow' clock. Such recent diversification is consistent with the existence of numerous haplotypes with one or two mutations in difference between them. A Quaternary diversification was demonstrated previously in the region for other species groups of *Daphnia s.s.* (Ishida & Taylor, 2007a, b). It is obvious that the Tertiary biogeographical patterns in the temperate zone were strongly altered during the Pleistocene glacial oscillations (Hewitt, 2000).

Ishida & Taylor (2007a) demonstrated that the Far East was a source for the dispersal across the eastern Palaearctic for some daphniids, and Japan was regarded as an important area for refugal survival and subsequent dispersal. Sampling in nearby regions to Japan (Sakhalin, Korea) reveals additional biogeographical complexity. For example, some mitochondrial lineages have colonized Japan from more northern regions (Kotov *et al.*, 2016; Bekker *et al.*, 2018).

In the case of the *D. korovchinskyi* complex, a recent differentiation of subclades I and J could be explained by a colonization of Japan from the continent, with a subsequent hybridization/introgression involving the Japanese endemic, *D. tanakai* (see Supporting Information, Fig. S2). Earlier hybridization was demonstrated for another pair of daphniids in Japan, *D. galeata* and *Daphnia dentifera* Forbes, 1893, but it was not associated with speciation (Ishida *et al.*, 2011). The *D. curvirostris* complex has an older evolutionary history than the *D. galeata* complex, with potentially hybridizing lineages being more differentiated (morphologically and genetically). Genomic-scale analyses are needed to assess the role of hybridization further.

Endemics: high risk of extinction

Empirical studies have often shown that relicts are at particular risk of extinction (Grandcolas *et al.*, 2014; Grandcolas & Trewick, 2016). There is a chance that locally distributed East Asian freshwater relicts are endangered, because of: (1) a general tendency for the eutrophication of water bodies owing to human activity; and (2) the introduction of invasive species in the plankton, as was recently demonstrated for Holarctic *D. galeata* invading euthrophied water reservoirs in Australia (see Karabanov, *et al.*, 2018). The pace of introduction of exotic freshwater species is increasing from year to year (Benzie, 2005). For example, North American *Daphnia ambigua* Scourfield, 1947 and *Daphnia pulicaria* Forbes, 1893 have successfully invaded Japan (Tanaka & Shigaki, 1987; Urabe *et al.*, 2003) owing to human activity.

The subclades H and I of the *D. sinevi* group are usual taxa, whereas subclade G is present in a single locality. Four taxa forming the *D. korovchinsky* species group have local ranges, and *D. ishidai* and *D. koreana* are found in a single water body each. *Daphnia koreana* is an endangered species that needs protection, and the chance of its full extinction in South Korea is already high. We can know what is threatened or lost by anthropogenic activity within each freshwater animal group only after gaining a basic understanding of its local diversity. Such knowledge is urgently needed for other cladocerans.

ACKNOWLEDGEMENTS

Many thanks to two anonymous reviewers of this manuscript, E. V. Bragina, J. F. Cart, Y. V. Deart, Y. R. Galimov, D. M. Glazov, S. Ishida, S. Nandini, A. Petrusek, E. V. Popova, D. E. Shcherbakov, A. Y. Sinev, P. A. Sorokin and D. D. Vasjukov for samples of *Daphnia* and to M. A. Gololobova, H. G. Jeong, S. A. Ivanov, A. I. Klimovsky, N. M. Korovchinsky and M. A. Kotova for assistance during sampling in Russia and Korea. Korean specimens were collected with the support of a grant from the National Institute of Biological Resources (NIBR), funded by the Ministry of Environment (MOE) of the Republic of Korea (NIBR201601201). This study was supported by the Russian Science Foundation (grant no. 18-14-00325).

REFERENCES

Adamowicz SJ, **Petrusek A**, **Colbourne JK**, **Hebert PDN**, **Witt JDS. 2009.** The scale of divergence: a phylogenetic appraisal of intercontinental allopatric speciation in a passively dispersed freshwater zooplankton genus. *Molecular Phylogenetics and Evolution* **50:** 423–436.

Alonso M. 1991. *Review of Iberian Cladocera with remarks on ecology and biogeography*. Dordrecht: Springer.

Arenas M. 2015. Trends in substitution models of molecular evolution. *Frontiers in Genetics* **6:** 319.

Baas Becking LGM. 1934. *Geobiologie of inleiding tot de Milieukunde*. Den Haag: W. P. van Stockum & Zoon.

Barley AJ, **Thomson RC. 2016.** Assessing the performance of DNA barcoding using posterior predictive simulations. *Molecular Ecology* **25:** 1944–1957.

Barnes GL. 2003. Origins of the Japanese islands: the new "big picture". *Nichibunken Japan Review* **15:** 3–50.

Bekker EI, **Karabanov DP**, **Galimov YR**, **Haag CR**, **Neretina TV**, **Kotov AA. 2018.** Phylogeography of *Daphnia magna* Straus (Crustacea: Cladocera) in northern Eurasia: evidence for a deep longitudinal split between mitochondrial lineages. *PLoS ONE* **13:** e0194045.

Bekker EI, **Karabanov DP**, **Galimov YR**, **Kotov AA. 2016.** DNA barcoding reveals high cryptic diversity in the north Eurasian *Moina* species (Crustacea: Cladocera). *PLoS ONE* **11:** e0161737.

Bekker EI, **Kotov AA**, **Taylor DJ. 2012.** A revision of the subgenus *Eurycercus* (*Eurycercus*) Baird, 1843 emend. nov. (Cladocera: Eurycercidae) in the Holarctic with the description of a new species from Alaska. *Zootaxa* **3206:** 1–40.

Belyaeva M, **Taylor DJ. 2009.** Cryptic species within the *Chydorus sphaericus* species complex (Crustacea: Cladocera) revealed by molecular markers and sexual stage morphology. *Molecular Phylogenetics and Evolution* **50:** 534–546.

Benzie JAH. 2005. *The genus* Daphnia *(including Daphniopsis): Anomopoda: Daphniidae*. Ghent: Kenobi Productions.

Berg LS. 1962. *The division of the Palaearctic and the Amur region into zoogeographic regions on the basis of the distribution of freshwater fishes*. Moscow: Izdatelstvo AN SSSR.

Bolotov IN, **Vikhrev IV**, **Bespalaya YV**, **Gofarov MY**, **Kondakov AV**, **Konopleva ES**, **Bolotov NN**, **Lyubas AA. 2016.** Multi-locus fossil-calibrated phylogeny, biogeography and a subgeneric revision of the Margaritiferidae (Mollusca: Bivalvia: Unionoida). *Molecular Phylogenetics and Evolution* **103:** 104–121.

Boratyn GM, **Camacho C**, **Cooper PS**, **Coulouris G**, **Fong A**, **Ma N**, **Madden TL**, **Matten WT**, **McGinnis SD**, **Merezhuk Y**, **Raytselis Y**, **Sayers EW**, **Tao T**, **Ye J**, **Zaretskaya I. 2013.** BLAST: a more efficient report with usability improvements. *Nucleic Acids Research* **41:** W29–W33.

Bouckaert R, **Heled J**, **Kühnert D**, **Vaughan T**, **Wu C-H**, **Xie D**, **Suchard MA**, **Rambaut A**, **Drummond AJ. 2014.** BEAST2: a software platform for Bayesian evolutionary analysis. *PLoS Computational Biology* **10:** e1003537.

Brehm V. 1955. Süsswasserfauna und Tiergeographie. *Osterreichische Zoologische Zeitschrift* **6:** 250–269.

Brennan IG, **Bauer AM**, **Van Tri N**, **Wang Y-Y**, **Wang W-Z**, **Zhang Y-P**, **Murphy RW. 2017.** Barcoding utility in a mega-diverse, cross-continental genus: keeping pace with *Cyrtodactylus* geckos. *Scientific Reports* **7:** 5592.

Brooks JL. 1957. *The systematics of North American* Daphnia. New Haven: Connecticut Academy of Arts & Sciences.

Carstens BC, **Pelletier TA**, **Reid NM**, **Satler JD. 2013.** How to fail at species delimitation. *Molecular Ecology* **22:** 4369–4383.

de Carvalho MR, **Bockmann FA**, **Amorim DS**, **Brandão CRF**, **de Vivo M**, **de Figueiredo JL**, **Britski HA**, **de Pinna MCC**, **Menezes NA**, **Marques FPL**, **Papavero N**, **Cancello EM**, **Crisci JV**, **McEachran JD**, **Schelly RC**, **Lundberg JG**, **Gill AC**, **Britz R**, **Wheeler QD**, **Stiassny MLJ**, **Parenti LR**, **Page LM**, **Wheeler WC**, **Faivovich J**, **Vari RP**, **Grande L**, **Humphries CJ**, **DeSalle R**, **Ebach MC**, **Nelson GJ. 2007.** Taxonomic impediment or impediment to taxonomy? A commentary on systematics and the cybertaxonomic-automation paradigm. *Evolutionary Biology* **34:** 140–143.

de Carvalho MR, **Ebach MC. 2009.** Death of the specialist, rise of the machinist. *History and Philosophy of the Life Sciences* **31:** 461–463.

Chen SZ. 1991. On three new species of *Chydorus* from China (Crustacea: Diplostraca: Chydoridae). *Acta Zootaxonomica Sinica* **16:** 398–402.

Chernomor O, **von Haeseler A**, **Minh BQ. 2016.** Terrace aware data structure for phylogenomic inference from supermatrices. *Systematic Biology* **65:** 997–1008.

Chiang SC, **Du NS. 1979.** *Crustacea: freshwater Cladocera*. Beijing: Science Press.

Colbourne JK, **Hebert PD. 1996.** The systematics of North American *Daphnia* (Crustacea: Anomopoda): a molecular phylogenetic approach. *Philosophical Transactions of the Royal Society B: Biological Sciences* **351:** 349–360.

Colbourne JK, **Hebert PDN**, **Taylor DJ. 1997.** *Evolutionary origins of phenotypic diversity in Daphnia*. Cambridge: Cambridge University Press.

Collins RA, **Boykin LM**, **Cruickshank RH**, **Armstrong KF. 2012.** Barcoding's next top model. An evaluation of nucleotide substitution models for specimen identification. *Methods in Ecology and Evolution* **3:** 457–465.

Collins RA, **Cruickshank RH. 2013.** The seven deadly sins of DNA barcoding. *Molecular Ecology Resources* **13:** 969–975.

Cornetti L, **Fields PD**, **Van Damme K**, **Ebert D. 2019.** A fossil-calibrated phylogenomic analysis of *Daphnia* and the Daphniidae. *Molecular Phylogenetics and Evolution* **137:** 250–262.

Cristescu MEA, **Hebert PDN. 2002.** Phylogeny and adaptive radiation in the Onychopoda (Crustacea, Cladocera): evidence from multiple gene sequences. *Journal of Evolutionary Biology* **15:** 838–849.

Dabert M, **Witalinski W**, **Kazmierski A**, **Olszanowski Z**, **Dabert J. 2010.** Molecular phylogeny of acariform mites (Acari, Arachnida): strong conflict between phylogenetic

signal and long-branch attraction artifacts. *Molecular Phylogenetics and Evolution* **56:** 222–241.

Darwin C. 1882. On the dispersal of freshwater bivalves. *Nature* **25:** 529–530.

Degnan JH, **Rosenberg NA. 2009.** Gene tree discordance, phylogenetic inference and the multispecies coalescent. *Trends in Ecology & Evolution* **24:** 332–340.

Drummond AJ, **Ho SYW**, **Phillips MJ**, **Rambaut A. 2006.** Relaxed phylogenetics and dating with confidence. *PLoS Biology* **4:** e88.

Drummond AJ, **Suchard MA**, **Xie D**, **Rambaut A. 2012.** Bayesian phylogenetics with BEAUti and the BEAST 1.7. *Molecular Biology and Evolution* **29:** 1969–1973.

Dumont HJ. 2000. Endemism in the Ponto-Caspian fauna, with special emphasis on the Onychopoda. *Advances in Ecological Research* **31:** 181–196.

Echave J, **Spielman SJ**, **Wilke CO. 2016.** Causes of evolutionary rate variation among protein sites. *Nature Reviews, Genetics* **17:** 109–121.

Eskov KY. 1984. *Continental drift and problems of historical biogeography*. Moscow: Nauka.

Felsenstein J. 1981. Evolutionary trees from DNA sequences: a maximum likelihood approach. *Journal of Molecular Evolution* **17:** 368–376.

Fisher-Reid MC, **Wiens JJ. 2011.** What are the consequences of combining nuclear and mitochondrial data for phylogenetic analysis? Lessons from *Plethodon* salamanders and 13 other vertebrate clades. *BMC Evolutionary Biology* **11:** 300.

Forró L, **Korovchinsky NM**, **Kotov AA**, **Petrusek A. 2008.** Global diversity of cladocerans (Cladocera; Crustacea) in freshwater. *Hydrobiologia* **595:** 177–184.

Frey DG. 1973. Comparative morphology and biology of three species of *Eurycercus* (Chydoridae, Cladocera) with a description of *Eurycercus macrocanthus* sp. nov. *Internationale Revue der Gesamten Hydrobiologie und Hydrographie* **58:** 221–267.

Frey DG. 1982. Questions concerning cosmopolitanism in Cladocera. *Archiv für Hydrobiologie* **93:** 484–502.

Frey DG. 1987. *The non-cosmopolitanism of chydorid Cladocera: implications for biogeography and evolution*. Rotterdam: A. A. Balkema.

Frey DG. 1991. The species of *Pleuroxus* and of three related genera (Anomopoda, Chydoridae) in southern Australia and New Zealand. *Records of the Australian Museum* **43:** 291–372.

Fu YX. 1997. Statistical tests of neutrality of mutations against population growth, hitchhiking and background selection. *Genetics* **147:** 915–925.

Fujisawa T, **Aswad A**, **Barraclough TG. 2016.** A rapid and scalable method for multilocus species delimitation using Bayesian model comparison and rooted triplets. *Systematic Biology* **65:** 759–771.

Fujisawa T, **Barraclough TG. 2013.** Delimiting species using single-locus data and the Generalized Mixed Yule Coalescent approach: a revised method and evaluation on simulated data sets. *Systematic Biology* **62:** 707–724.

Garrigan D, **Lewontin R**, **Wakeley J. 2010.** Measuring the sensitivity of single-locus "neutrality tests" using a direct perturbation approach. *Molecular Biology and Evolution* **27:** 73–89.

Geller J, **Meyer C**, **Parker M**, **Hawk H. 2013.** Redesign of PCR primers for mitochondrial cytochrome *c* oxidase subunit I for marine invertebrates and application in all-taxa biotic surveys. *Molecular Ecology Resources* **13:** 851–861.

Gernhard T. 2008. The conditioned reconstructed process. *Journal of Theoretical Biology* **253:** 769–778.

Glagolev SM. 1986. *Morphology, systematics and geographic distribution of the cladoceran genus* Daphnia *from Eurasia*. Dissertatsia kandidata biologicheskich nauk, Dissertation, Institute of Evolutionary Morphology and Ecology of Animals of the Academy of Sciences of USSR.

Grandcolas P, **Nattier R**, **Trewick S. 2014.** Relict species: a relict concept? *Trends in Ecology & Evolution* **29:** 655–663.

Grandcolas P, **Trewick S. 2016.** What is the meaning of extreme phylogenetic diversity? The case of phylogenetic relict species. *Biodiversity Conservation and Phylogenetic Systematics* **14:** 99–115.

Gutierrez-Garcia TA, **Vazquez-Dominguez E. 2011.** Comparative phylogeography: designing studies while surviving the process. *BioScience* **61:** 857–868.

Hailer F, **Kutschera VE**, **Hallström BM**, **Klassert D**, **Fain SR**, **Leonard JA**, **Arnason U**, **Janke A. 2012.** Nuclear genomic sequences reveal that polar bears are an old and distinct bear lineage. *Science* **336:** 344–347.

Hasegawa M, **Kishino H**, **Yano T-A. 1985.** Dating of the human-ape splitting by a molecular clock of mitochondrial DNA. *Journal of Molecular Evolution* **22:** 160–174.

Hebert PDN, **Cywinska A**, **Ball SL**, **deWaard JR. 2003.** Biological identifications through DNA barcodes. *Proceedings of the Royal Society B: Biological Sciences* **270:** 313–321.

Hebert PDN, **Remigio EA**, **Colbourne JK**, **Taylor DJ**, **Wilson CC. 2002.** Accelerated molecular evolution in halophilic crustaceans. *Evolution* **56:** 909–926.

Hebert PDN, **Stoeckle MY**, **Zemlak TS**, **Francis CM. 2004.** Identification of birds through DNA barcodes. *PLoS Biology* **2:** e312.

Heled J, **Drummond AJ. 2010.** Bayesian inference of species trees from multilocus data. *Molecular Biology and Evolution* **27:** 570–580.

Hewitt G. 2000. The genetic legacy of the Quaternary ice ages. *Nature* **405:** 907–913.

Hillis DM. 1987. Molecular versus morphological approaches to systematics. *Annual Review of Ecology and Systematics* **18:** 23–42.

Hrbáček J, Kořínek V, Frey DJ. 1978. Cladocera. In: J. Illies, ed. *Limnofauna Europaea*, 2nd edn. Stuttgart, New York: Gustav Fischer Verlag, Swets and Zeitlinger B.V. Amsterdam, 189–195.

Ho S. 2008. The molecular clock and estimating species divergence. *Nature Education* **1:** 168.

Huson DH, **Bryant D. 2006.** Application of phylogenetic networks in evolutionary studies. *Molecular Biology and Evolution* **23:** 254–267.

Huson DH, **Rupp R**, **Berry V**, **Gambette P**, **Paul C. 2009.** Computing galled networks from real data. *Bioinformatics* **25:** 85–93.

Huson DH, **Scornavacca C. 2012.** Dendroscope 3: an interactive tool for rooted phylogenetic trees and networks. *Systematic Biology* **61:** 1061–1067.

Ishida S, **Kotov AA**, **Taylor DJ. 2006.** A new divergent lineage of *Daphnia* (Cladocera: Anomopoda) and its morphological and genetical differentiation from *Daphnia curvirostris* Eylmann, 1887. *Zoological Journal of the Linnean Society* **146:** 385–405.

Ishida S, **Takahashi A**, **Matsushima N**, **Yokoyama J**, **Makino W**, **Urabe J**, **Kawata M. 2011.** The long-term consequences of hybridization between the two *Daphnia* species, *D. galeata* and *D. dentifera*, in mature habitats. *BMC Evolutionary Biology* **11:** 209.

Ishida S, **Taylor DJ. 2007a.** Mature habitats associated with genetic divergence despite strong dispersal ability in an arthropod. *BMC Evolutionary Biology* **7:** 52.

Ishida S, **Taylor DJ. 2007b.** Quaternary diversification in a sexual Holarctic zooplankter, *Daphnia galeata*. *Molecular Ecology* **16:** 569–582.

Ishikawa C. 1895a. Phyllopod Crustacea of Japan. *Daphnia morsei*. *Zoological Magazine, Tokyo* **7:** 137–142.

Ishikawa C. 1895b. Phyllopod Crustacea of Japan. *Daphnia whitmani*. *Zoological Magazine, Tokyo* **7:** 147–154.

Ishikawa C. 1896a. Phyllopod Crustacea of Japan. (VIII) *Daphnia mitsukuri*, n. sp. *Zoological Magazine, Tokyo* **8:** 55–57.

Ishikawa C. 1896b. Phyllopod Crustacea of Japan. *Moina paradoxa*, Weismann var. *japonica*. *Zoological Magazine, Tokyo* **7:** 7–12.

Ishikawa C. 1896c. Phyllopod Crustacea of Japan. *Moina weismani* n. sp. *Zoological Magazine, Tokyo* **7:** 1–6.

Jeong H, **Kotov AA**, **Lee W. 2014.** Checklist of the freshwater Cladocera (Crustacea: Branchiopoda) of South Korea. *Proceedings of the Biological Society of Washington* **127:** 216–228.

Ji G-H, **Xiang X-F**, **Chen S-Z**, **Yu G-L**, **Kotov AA**, **Dumont HJ. 2015.** Annotated checklist of Chinese Cladocera (Crustacea: Branchiopoda). Part II. Order Anomopoda (families Macrotrichidae, Eurycercidae and Chydoridae). *Zootaxa* **4044:** 241–269.

Jones G. 2017. Algorithmic improvements to species delimitation and phylogeny estimation under the multispecies coalescent. *Journal of Mathematical Biology* **74:** 447–467.

Juracka PJ, **Korinek V**, **Petrusek A. 2010.** A new Central European species of the *Daphnia curvirostris* complex, *Daphnia hrbaceki* sp. nov. (Cladocera, Anomopoda, Daphniidae). *Zootaxa* **2718:** 1–22.

Kalyaanamoorthy S, **Minh BQ**, **Wong TKF**, **von Haeseler A**, **Jermiin LS. 2017.** ModelFinder: fast model selection for accurate phylogenetic estimates. *Nature Methods* **14:** 587–589.

Kano K, **Uto K**, **Ohguchi T. 2007.** Stratigraphic review of Eocene to Oligocene successions along the eastern Japan Sea: implication for early opening of the Japan Sea. *Journal of Asian Earth Sciences* **30:** 20–32.

Karabanov DP, **Bekker EI**, **Shiel RJ**, **Kotov AA. 2018.** Invasion of a Holarctic planktonic cladoceran *Daphnia galeata* Sars (Crustacea: Cladocera) in the Lower Lakes of South Australia. *Zootaxa* **4402:** 136–148.

Katoh K, **Standley DM. 2016.** A simple method to control over-alignment in the MAFFT multiple sequence alignment program. *Bioinformatics* **32:** 1933–1942.

Kirillova GL. 2003. Cretaceous tectonics and geological environments in East Russia. *Journal of Asian Earth Sciences* **21:** 967–977.

Knowlton N, **Weigt LA. 1998.** New dates and new rates for divergence across the Isthmus of Panama. *Proceedings of the Royal Society B: Biological Sciences* **265:** 2257–2263.

Korovchinsky NM. 1996. How many species of Cladocera are there? *Hydrobiologia* **321:** 191–204.

Korovchinsky NM. 2000. Redescription of *Diaphanosoma dubium* Manuilova, 1964 (Branchiopoda: Ctenopoda: Sididae), and description of a new, related species. *Hydrobiologia* **441:** 73–92.

Korovchinsky NM. 2004. *Cladocerans of the order Ctenopoda of the world fauna (morphology, systematics, ecology, biogeography)*. Moscow: KMK Press.

Korovchinsky NM. 2006. The Cladocera (Crustacea: Branchiopoda) as a relict group. *Zoological Journal of the Linnean Society* **147:** 109–124.

Korovchinsky NM. 2009. The genus *Leptodora* Lilljeborg (Crustacea: Branchiopoda: Cladocera) is not monotypic: description of a new species from the Amur River basin (Far East of Russia). *Zootaxa* **2120:** 39–52.

Korovchinsky NM. 2010. A taxonomic revision of *Pseudosida szalayi* Daday, 1898 (Crustacea: Cladocera: Sididae) over its Asian range, with focus on the northernmost populations first recorded from the Amur River basin (Far East of Russia). *Zootaxa* **2345:** 1–18.

Korovchinsky NM. 2013. Cladocera (Crustacea: Branchiopoda) of South East Asia: history of exploration, taxon richness and notes on zoogeography. *Journal of Limnology* **72:** e7.

Kosakovsky Pond SL, **Posada D**, **Gravenor MB**, **Woelk CH**, **Frost SDW. 2006.** Automated phylogenetic detection of recombination using a genetic algorithm. *Molecular Biology and Evolution* **23:** 1891–1901.

Kotov AA. 2015. A critical review of the current taxonomy of the genus *Daphnia* O. F. Müller, 1785 (Anomopoda, Cladocera). *Zootaxa* **3911:** 184–200.

Kotov AA, **Gololobova MA. 2016.** Traditional taxonomy: quo vadis? *Integrative Zoology* **11:** 500–505.

Kotov AA, **Ishida S**, **Taylor DJ. 2006.** A new species in the *Daphnia curvirostris* (Crustacea: Cladocera) complex from the eastern Palearctic with molecular phylogenetic evidence for the independent origin of neckteeth. *Journal of Plankton Research* **28:** 1067–1079.

Kotov AA, **Ishida S**, **Taylor DJ. 2009.** Revision of the genus *Bosmina* Baird, 1845 (Cladocera: Bosminidae), based on evidence from male morphological characters and molecular phylogenies. *Zoological Journal of the Linnean Society* **156:** 1–51.

Kotov AA, **Jeong HGI**, **Lee W. 2012.** Cladocera (Crustacea: Branchiopoda) of the south-east of the Korean Peninsula, with twenty new records for Korea. *Zootaxa* **3368:** 50–90.

Kotov AA, **Karabanov DP**, **Bekker EI**, **Neretina TV**, **Taylor DJ. 2016.** Phylogeography of the *Chydorus*

sphaericus group (Cladocera: Chydoridae) in the northern Palearctic. *PLoS ONE* **11:** e0168711.

Kotov AA, **Korovchinsky NM. 2006.** First record of fossil Mesozoic Ctenopoda (Crustacea, Cladocera). *Zoological Journal of the Linnean Society* **146:** 269–274.

Kotov AA, **Korovchinsky NM**, **Sinev AY**, **Smirnov NN. 2011a.** Cladocera (Crustacea, Branchiopoda) of the Zeya basin (Amurskaya Area, Russian Federation). 3. Systematic-faunistic and zoogeographic analysis. *Zoologichesky Zhurnal* **90:** 402–411.

Kotov AA, **Sinev AY**, **Korovchinsky NM**, **Smirnov NN**, **Bekker EI**, **Sheveleva NG. 2011b.** Cladocera (Crustacea, Branchiopoda) of the Zeya basin (Amurskaya Area, Russian Federation). 1. New taxa for fauna of Russia. *Zoologichesky Zhurnal* **90:** 131–142.

Kotov AA, **Taylor DJ. 2010.** A new African lineage of the *Daphnia obtusa* group (Cladocera: Daphniidae) disrupts continental vicariance patterns. *Journal of Plankton Research* **32:** 937–949.

Kotov AA, **Taylor DJ. 2011.** Mesozoic fossils (145 Mya) suggest the antiquity of the subgenera of *Daphnia* and their coevolution with chaoborid predators. *BMC Evolutionary Biology* **11:** 129.

Kotov AA, **Taylor DJ. 2019.** Contrasting endemism in pond-dwelling cyclic parthenogens: the *Daphnia curvirostris* species group (Crustacea: Cladocera). *Scientific Reports* **9:** 6812.

Kumar S, **Stecher G**, **Li M**, **Knyaz C**, **Tamura K. 2018.** MEGA X: molecular evolutionary genetics analysis across computing platforms. *Molecular Biology and Evolution* **35:** 1547–1549.

Lakatos C, **Urabe J**, **Makino W. 2015.** Cryptic diversity of Japanese *Diaphanosoma* (Crustacea: Cladocera) revealed by morphological and molecular assessments. *Inland Waters* **5:** 253–262.

Landis MJ, **Matzke NJ**, **Moore BR**, **Huelsenbeck JP. 2013.** Bayesian analysis of biogeography when the number of areas is large. *Systematic Biology* **62:** 789–804.

Leigh JW, **Bryant D**, **Nakagawa S. 2015.** PopART: full-feature software for haplotype network construction. *Methods in Ecology and Evolution* **6:** 1110–1116.

Li X-Q, **Du D. 2014.** Variation, evolution, and correlation analysis of C+G content and genome or chromosome size in different kingdoms and phyla. *PLoS ONE* **9:** e88339.

Liu P, **Xu L**, **Xu S-L**, **Martínez A**, **Chen H**, **Cheng D**, **Dumont HJ**, **Han B-P**, **Fontaneto D. 2018.** Species and hybrids in the genus *Diaphanosoma* Fischer, 1850 (Crustacea: Branchiopoda: Cladocera). *Molecular Phylogenetics and Evolution* **118:** 369–378.

Loeza-Quintana T, **Carr CM**, **Khan T**, **Bhatt YA**, **Lyon SP**, **Hebert PDN**, **Adamowicz SJ. 2019.** Recalibrating the molecular clock for Arctic marine invertebrates based on DNA barcodes. *Genome* **62:** 200–216.

Lohse K. 2009. Can mtDNA barcodes be used to delimit species? A response to Pons *et al*. (2006). *Systematic Biology* **58:** 439–442.

Ma X, **Petrusek A**, **Wolinska J**, **Hu W**, **Yin M. 2019.** Lineage diversity and reproductive modes of the *Daphnia pulex* group in Chinese lakes and reservoirs. *Molecular Phylogenetics and Evolution* **130:** 424–433.

Manujlova EF. 1964. *The cladocerans of fauna of the USSR*. Moscow: Nauka.

Maruyama S, **Isozaki Y**, **Kimura G**, **Terabayashi M. 1997.** Paleogeographic maps of the Japanese islands: plate tectonic synthesis from 750 Ma to the present. *The Island Arc* **6:** 121–142.

Matzke NJ. 2013. Probabilistic historical biogeography: new models for founder-event speciation, imperfect detection, and fossils allow improved accuracy and model-testing. *Frontiers of Biogeography* **5:** 242–248.

Matzke NJ. 2014. Model selection in historical biogeography reveals that founder-event speciation is a crucial process in island clades. *Systematic Biology* **63:** 951–970.

Meier R, **Shiyang K**, **Vaidya G**, **Ng PKL. 2006.** DNA barcoding and taxonomy in Diptera: a tale of high intraspecific variability and low identification success. *Systematic Biology* **55:** 715–728.

Messing J. 1983. New M13 vectors for cloning. *Methods in Enzymology* **101:** 20–78.

Millette KL, **Xu S**, **Witt JDS**, **Cristescu ME. 2011.** Pleistocene-driven diversification in freshwater zooplankton: genetic patterns of refugial isolation and postglacial recolonization in *Leptodora kindtii* (Crustacea, Cladocera). *Limnology and Oceanography* **56:** 1725–1736.

Minh BQ, **Nguyen MAT**, **von Haeseler A. 2013.** Ultrafast approximation for phylogenetic bootstrap. *Molecular Biology and Evolution* **30:** 1188–1195.

Moorjani P, **Amorim CEG**, **Arndt PF**, **Przeworski M. 2016.** Variation in the molecular clock of primates. *Proceedings of the National Academy of Sciences of the United States of America* **113:** 10607–10612.

Murrell B, **Wertheim JO**, **Moola S**, **Weighill T**, **Scheffler K**, **Kosakovsky Pond SL. 2012.** Detecting individual sites subject to episodic diversifying selection. *PLoS Genetics* **8:** e1002764.

Muse SV, **Gaut BS. 1994.** A likelihood approach for comparing synonymous and nonsynonymous nucleotide substitution rates, with application to the chloroplast genome. *Molecular Biology and Evolution* **11:** 715–724.

Nei M, **Kumar S. 2000.** *Molecular evolution and phylogenetics*. New York: Oxford University Press.

Nguyen L-T, **Schmidt HA**, **von Haeseler A**, **Minh BQ. 2015.** IQ-TREE: a fast and effective stochastic algorithm for estimating maximum-likelihood phylogenies. *Molecular Biology and Evolution* **32:** 268–274.

Ni Y, **Ma X**, **Hu W**, **Blair D**, **Yin M. 2019.** New lineages and old species: lineage diversity and regional distribution of *Moina* (Crustacea: Cladocera) in China. *Molecular Phylogenetics and Evolution* **134:** 87–98.

Nikolsky GV. 1956. *Fishes of the Amur river basin. Results of the Amur ichthyological expedition 1944–1949*. Moscow: AN Academy of Sciences of USSR.

Okonechnikov K, **Golosova O**, **Fursov M. 2012.** Unipro UGENE: a unified bioinformatics toolkit. *Bioinformatics* **28:** 1166–1167.

Park S-C, **Yoo D-G**, **Lee C-W**, **Lee E-I. 2000.** Last glacial sea-level changes and paleogeography of the Korea (Tsushima) Strait. *Geo-Marine Letters* **20:** 64–71.

Perlwitz MD, **Burks C**, **Waterman MS. 1988.** Pattern analysis of the genetic code. *Advances in Applied Mathematics* **9:** 7–21.

Petrusek A, **Hobaek A**, **Nilssen JP**, **Skage M**, **Cerny M**, **Brede N**, **Schwenk K. 2008.** A taxonomic reappraisal of the European *Daphnia longispina* complex (Crustacea, Cladocera, Anomopoda). *Zoologica Scripta* **37:** 507–519.

Pons J, **Barraclough TG**, **Gomez-Zurita J**, **Cardoso A**, **Duran DP**, **Hazell S**, **Kamoun S**, **Sumlin WD**, **Vogler AP. 2006.** Sequence-based species delimitation for the DNA taxonomy of undescribed insects. *Systematic Biology* **55:** 595–609.

Popova EV, **Petrusek A**, **Kořínek V**, **Mergeay J**, **Bekker EI**, **Karabanov DP**, **Galimov YR**, **Neretina TV**, **Taylor DJ**, **Kotov AA. 2016.** Revision of the Old World *Daphnia* (*Ctenodaphnia*) *similis* group (Cladocera: Daphniidae). *Zootaxa* **4161:** 1–40.

Poppe SA, **Richard J. 1890.** Note sur divers Entomostraces du Japan et de la Chine (*Leptodora*). *Bulletin de la Société Zoologique de France* **15:** 73–78.

Posada D, **Buckley TR. 2004.** Model selection and model averaging in phylogenetics: advantages of Akaike information criterion and Bayesian approaches over likelihood ratio tests. *Systematic Biology* **53:** 793–808.

Puillandre N, **Lambert A**, **Brouillet S**, **Achaz G. 2012.** ABGD, automatic barcode gap discovery for primary species delimitation. *Molecular Ecology* **21:** 1864–1877.

Rambaut A, **Drummond AJ**, **Xie D**, **Baele G**, **Suchard MA. 2018.** Posterior summarization in Bayesian phylogenetics using Tracer 1.7. *Systematic Biology* **67:** 901–904.

Ramírez-Soriano A, **Ramos-Onsins SE**, **Rozas J**, **Calafell F**, **Navarro A. 2008.** Statistical power analysis of neutrality tests under demographic expansions, contractions and bottlenecks with recombination. *Genetics* **179:** 555–567.

Ramos-Onsins SE, **Rozas J. 2002.** Statistical properties of new neutrality tests against population growth. *Molecular Biology and Evolution* **19:** 2092–2100.

Rannala B, **Yang Z. 2003.** Bayes estimation of species divergence times and ancestral population sizes using DNA sequences from multiple loci. *Genetics* **164:** 1645–1656.

Reid NM, **Carstens BC. 2012.** Phylogenetic estimation error can decrease the accuracy of species delimitation: a Bayesian implementation of the general mixed Yule-coalescent model. *BMC Evolutionary Biology* **12:** 196.

Rozas J, **Ferrer-Mata A**, **Sanchez-DelBarrio JC**, **Guirao-Rico S**, **Librado P**, **Ramos-Onsins SE**, **Sanchez-Gracia A. 2017.** DnaSP 6: DNA sequence polymorphism analysis of large data sets. *Molecular Biology and Evolution* **34:** 3299–3302.

Sanmartin I, **Enghoff H**, **Ronquist F. 2001.** Patterns of animal dispersal, vicariance and diversification in the Holarctic. *Biological Journal of the Linnean Society* **73:** 345–390.

Schneider A, **Cannarozzi GM**, **Gonnet GH. 2005.** Empirical codon substitution matrix. *BMC Bioinformatics* **6:** 134.

Schubart CD, **Diesel R**, **Hedges SB. 1998.** Rapid evolution to terrestrial life in Jamaican crabs. *Nature* **393:** 363–365.

Schwartz JH, **Maresca B. 2006.** Do molecular clocks run at all? A critique of molecular systematics. *Biological Theory* **1:** 357–371.

Schwentner M, **Clavier S**, **Fritsch M**, **Olesen J**, **Padhye S**, **Timms BV**, **Richter S. 2013.** *Cyclestheria hislopi* (Crustacea: Branchiopoda): a group of morphologically cryptic species with origins in the Cretaceous. *Molecular Phylogenetics and Evolution* **66:** 800–810.

Scornavacca C, **Zickmann F**, **Huson DH. 2011.** Tanglegrams for rooted phylogenetic trees and networks. *Bioinformatics* **27:** i248–i256.

Sinev AY, **Alonso M**, **Sheveleva NG. 2009.** New species of *Alona* from south-east Russia and Mongolia related to *Alona salina* Alonso, 1996 (Cladocera: Anomopoda: Chydoridae). *Zootaxa* **2326:** 1–23.

Smirnov NN. 1992a. Mesozoic Anomopoda (Crustacea) from Mongolia. *Zoological Journal of the Linnean Society* **104:** 97–116.

Smirnov NN. 1992b. *The Macrothricidae of the world*. The Hague: SPB Academic Publishing.

Smirnov NN. 1996. *Cladocera: the Chydorinae and Sayciinae (Chydoridae) of the world*. Amsterdam: SPB Academic Publishing.

Smirnov NN, **Sheveleva NG. 2010.** *Chydorus irinae* sp. n. (Anomopoda, Chydoridae, Chydorinae) from the Tom' River (the Amur basin, Russia). *Zoologichesky Zhurnal* **89:** 635–638.

So M, **Ohtsuki H**, **Makino W**, **Ishida S**, **Kumagai H**, **Yamaki KG**, **Urabe J. 2015.** Invasion and molecular evolution of *Daphnia pulex* in Japan. *Limnology and Oceanography* **60:** 1129–1138.

Srivathsan A, **Meier R. 2012.** On the inappropriate use of Kimura-2-parameter (K2P) divergences in the DNA-barcoding literature. *Cladistics* **28:** 190–194.

Suchard MA, **Lemey P**, **Baele G**, **Ayres DL**, **Drummond AJ**, **Rambaut A. 2018.** Bayesian phylogenetic and phylodynamic data integration using BEAST 1.10. *Virus Evolution* **4:** vey016.

Sweet AD, **Boyd BM**, **Allen JM**, **Villa SM**, **Valim MP**, **Rivera-Parra JL**, **Wilson RE**, **Johnson KP. 2018.** Integrating phylogenomic and population genomic patterns in avian lice provides a more complete picture of parasite evolution. *Evolution* **72:** 95–112.

Talavera G, **Dincă V**, **Vila R**, **Paradis E. 2013.** Factors affecting species delimitations with the GMYC model: insights from a butterfly survey. *Methods in Ecology and Evolution* **4:** 1101–1110.

Tamura K. 1992. Estimation of the number of nucleotide substitutions when there are strong transition-transversion and G+C-content biases. *Molecular Biology and Evolution* **9:** 678–687.

Tamura K, **Nei M. 1993.** Estimation of the number of nucleotide substitutions in the control region of mitochondrial DNA in humans and chimpanzees. *Molecular Biology and Evolution* **10:** 512–526.

Tanaka S. 1994. Notes on the Cladocera of Japan – 1. *Memoirs of the Faculty of Education Toyama University. Series B. Natural Sciences* **45:** 75–80.

Tanaka S. 1996. Notes on the Cladocera of Japan – 3. Family Daphniidae Straus, 1820 – 1. Key to the genera of Daphniidae and on the genus *Daphnia*. *Memoirs of the Faculty of Education Toyama University. Series B. Natural Sciences* **48:** 37–42.

Tanaka S. 1997. Notes on the Cladocera of Japan – 4. Family Daphniidae Straus, 1820 – 2. Genus *Daphnia*, subgenus *Daphnia*. *Memoirs of the Faculty of Education Toyama University. Series B. Natural Sciences* **49:** 55–66.

Tanaka S, **Shigaki S. 1987.** *Daphnia obtusa* Kurz, 1874 emend. Scourfleld, 1942 (Cladocera: Daphniidae) in Japan. *Japanese Journal of Limnology* **48:** 111–115.

Tanaka S, **Tominaga H. 1986.** *Daphnia curvirostris* Eylmann in Japanese high mountain waters (Cladocera: Daphniidae). *Hydrobiologia* **137:** 33–43.

Tian XY. 2004. Freshwater Cladocera with new generic and species records for Shandong Province and 23 new records for North China. *Shandong Science* **17:** 22–25.

Tokishita S-I, **Shibuya H**, **Kobayashi T**, **Sakamoto M**, **Ha J-Y**, **Yokobori S-I**, **Yamagata H**, **Hanazato T. 2017.** Diversification of mitochondrial genome of *Daphnia galeata* (Cladocera, Crustacea): comparison with phylogenetic consideration of the complete sequences of clones isolated from five lakes in Japan. *Gene* **611:** 38–46.

Tominaga K, **Nakajima J**, **Watanabe K. 2016.** Cryptic divergence and phylogeography of the pike gudgeon *Pseudogobio esocinus* (Teleostei: Cyprinidae): a comprehensive case of freshwater phylogeography in Japan. *Ichthyological Research* **63:** 79–93.

Trifinopoulos J, **Nguyen L-T**, **von Haeseler A**, **Minh BQ. 2016.** W-IQ-TREE: a fast online phylogenetic tool for maximum likelihood analysis. *Nucleic Acids Research* **44:** 232–235.

Uéno M. 1927. The freshwater Branchiopoda of Japan – I. *Memoirs of the College of Science, Kyoto Imperial University. Series B* **2:** 259–311.

Uéno M. 1934. Freshwater Branchiopoda of Japan. IV. Genus *Daphnia* of Japan 2. Local races of Japanese *Daphnia*. *Memoirs of the College of Science, Kyoto Imperial University. Series B* **9:** 321–342.

Uéno M. 1937. Order Branchiopoda (class Crustacea). *Fauna Nipponica* **9:** 1–135.

Uéno M. 1972. *Daphnia* of Hokkaido and their habitat-lakes. *Konan Women's College Research* **8:** 65–102.

Urabe J, **Ishida S**, **Nishimoto M**, **Weider LJ. 2003.** *Daphnia pulicaria*, a zooplankton species that suddenly appeared in 1999 in the offshore zone of Lake Biwa. *Limnology* **4:** 35–41.

Vaidya G, **Lohman DJ**, **Meier R. 2011.** SequenceMatrix: concatenation software for the fast assembly of multi-gene datasets with character set and codon information. *Cladistics* **27:** 171–180.

Van Damme K, **Kotov AA. 2016.** The fossil record of the Cladocera (Crustacea: Branchiopoda): evidence and hypotheses. *Earth-Science Reviews* **163:** 162–189.

Van Damme K, **Sinev AY**, **Dumont HJ. 2011.** Separation of *Anthalona* gen. n. from *Alona* Baird, 1843 (Branchiopoda: Cladocera: Anomopoda): morphology and evolution of scraping stenothermic alonines. *Zootaxa* **2875:** 1–64.

Vitecek S, **Kucinic M**, **Previsic A**, **Zivic I**, **Stojanovic K**, **Keresztes L**, **Balint M**, **Hoppeler F**, **Waringer J**, **Graf W**, **Pauls SU. 2017.** Integrative taxonomy by molecular species delimitation: multi-locus data corroborate a new species of Balkan Drusinae micro-endemics. *BMC Evolutionary Biology* **17:** 129.

Wakita K. 2013. Geology and tectonics of Japanese islands: a review – the key to understanding the geology of Asia. *Journal of Asian Earth Sciences* **72:** 75–87.

Wallace AR. 1876. *The geographical distribution of animals*. New York: Harper and brothers.

Warren DL, **Geneva AJ**, **Lanfear R. 2017.** RWTY (R We There Yet): an R package for examining convergence of Bayesian phylogenetic analyses. *Molecular Biology and Evolution* **34:** 1016–1020.

Watanabe K, **Tominaga K**, **Nakajima J**, **Kakioka R**, **Tabata R. 2017.** *Japanese freshwater fishes: biogeography and cryptic diversity*. Tokyo: Springer.

Weaver S, **Shank SD**, **Spielman SJ**, **Li M**, **Muse SV**, **Kosakovsky Pond SL. 2018.** Datamonkey 2.0: a modern web application for characterizing selective and other evolutionary processes. *Molecular Biology and Evolution* **35:** 773–777.

Wei W, **Giebler S**, **Wolinska J**, **Ma X**, **Yang Z**, **Hu W**, **Yin M. 2015.** Genetic structure of *Daphnia galeata* populations in eastern China. *PLoS ONE* **10:** e0120168.

Wiens J. 2004. The role of morphological data in phylogeny reconstruction. *Systematic Biology* **53:** 653–661.

Will KW, **Rubinoff D. 2004.** Myth of the molecule: DNA barcodes for species cannot replace morphology for identification and classification. *Cladistics* **20:** 47–55.

Xiang X-F, **Ji G-H**, **Chen S-Z**, **Yu G-L**, **Xu L**, **Han B-P**, **Kotov AA**, **Dumont HJ. 2015.** Annotated checklist of Chinese Cladocera (Crustacea: Branchiopoda). Part I. Haplopoda, Ctenopoda, Onychopoda and Anomopoda (families Daphniidae, Moinidae, Bosminidae, Ilyocryptidae). *Zootaxa* **3904:** 1–27.

Xu L, **Han B-P**, **Van Damme K**, **Vierstraete A**, **Vanfleteren JR**, **Dumont HJ. 2011.** Biogeography and evolution of the Holarctic zooplankton genus *Leptodora* (Crustacea: Branchiopoda: Haplopoda). *Journal of Biogeography* **38:** 359–370.

Xu M, **Zhang HJ**, **Deng DG**, **Wang WP**, **Zhang XL**, **Zha LS. 2014.** Phylogenetic relationship and taxonomic status of four *Daphnia* species based on *16S* rDNA and *COI* sequence. *Acta Hydrobiologica Sinica* **38:** 1040–1043.

Xu S, **Hebert PDN**, **Kotov AA**, **Cristescu ME. 2009.** The noncosmopolitanism paradigm of freshwater zooplankton: insights from the global phylogeography of the predatory cladoceran *Polyphemus pediculus* (Linnaeus, 1761) (Crustacea, Onychopoda). *Molecular Ecology* **18:** 5161–5179.

Yang L, **Tan Z**, **Wang D**, **Xue L**, **Guan M-X**, **Huang T**, **Li R. 2014.** Species identification through mitochondrial rRNA genetic analysis. *Scientific Reports* **4:** 4089.

Yang Z. 1994. Maximum likelihood phylogenetic estimation from DNA sequences with variable rates over sites:

approximate methods. *Journal of Molecular Evolution* **39:** 306–314.

Yin A. 2010. Cenozoic tectonic evolution of Asia: a preliminary synthesis. *Tectonophysics* **488:** 293–325.

Yoon SM. 2010. Arthropoda: Branchiopoda: Anostraca, Notostraca, Spinicaudata, Laevicaudata, Ctenopoda, Anomopoda, Haplopoda Branchiopods. *Invertebrate Fauna of Korea* **21:** 1–156.

Yu Y, **Harris AJ**, **Blair C**, **He X. 2015.** RASP (Reconstruct Ancestral State in Phylogenies): a tool for historical biogeography. *Molecular Phylogenetics and Evolution* **87:** 46–49.

Zhang D, **Yan L**, **Zhang M**, **Chu H**, **Cao J**, **Li K**, **Hu D**, **Pape T. 2016.** Phylogenetic inference of calyptrates, with the first mitogenomes for Gasterophilinae (Diptera: Oestridae) and Paramacronychiinae (Diptera: Sarcophagidae). *International Journal of Biological Sciences* **12:** 489–504.

Zhang J, **Kapli P**, **Pavlidis P**, **Stamatakis A. 2013.** A general species delimitation method with applications to phylogenetic placements. *Bioinformatics* **29:** 2869–2876.

Zhisheng A, **Kutzbach JE**, **Prell WL**, **Porter SC. 2001.** Evolution of Asian monsoons and phased uplift of the Himalaya–Tibetan plateau since Late Miocene times. *Nature* **411:** 62–66.

Zuykova EI, **Simonov EP**, **Bochkarev NA**, **Abramov SA**, **Sheveleva NG**, **Kotov AA. 2018a.** Contrasting phylogeographic patterns and demographic history in closely related species of *Daphnia longispina* group (Crustacea: Cladocera) with focus on north-eastern Eurasia. *PLoS ONE* **13:** e0207347.

Zuykova EI, **Simonov EP**, **Bochkarev NA**, **Taylor DJ**, **Kotov AA. 2018b.** Resolution of the *Daphnia umbra* problem (Crustacea: Cladocera) using an integrated taxonomic approach. *Zoological Journal of the Linnean Society* **50:** 969–998.

SUPPORTING INFORMATION

Additional Supporting Information may be found in the online version of this article at the publisher's web-site:

Appendix S1. Complete list of sequences obtained in the frame of this study with information on specimen IDs and locality provided for each individual.

Figure S1. Tanglegram for mitochondrial (left) and nuclear (right) phylogenetic networks for the *Daphnia curvirostris* species complex.

Figure S2. Galled network (a generalization of galled trees) of three mitochondrial and three nuclear loci. Digits show posterior probability for mitochondrial (first) and nuclear (second) trees.

Figure S3. Phylogeographical reconstruction for the *Daphnia curvirostris* species complex with topology of unrooted tree; only phylogroups discussed here are represented. Left, dispersal–extinction–cladogenesis (DEC) reconstruction, with probable vicariant events marked by a green arrow and dispersal events by a red arrow. Right, BayArea reconstruction.